stratified flows

2 turbulence and mixing in stratified flow

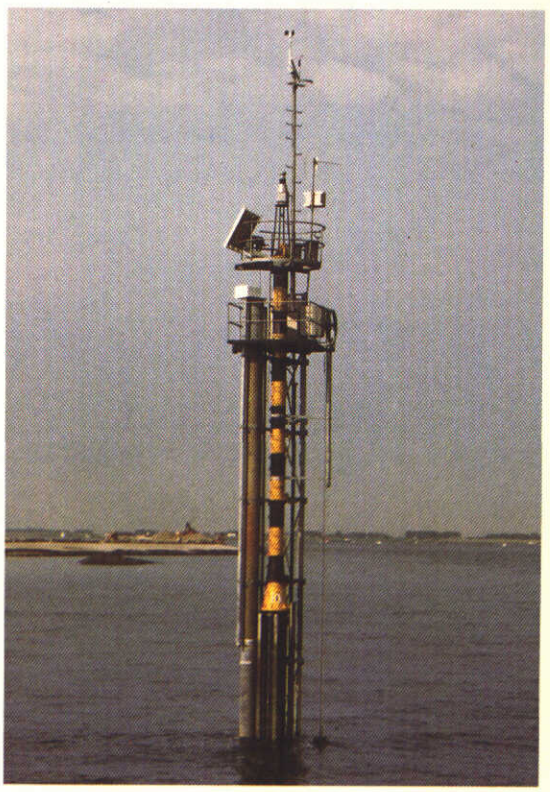

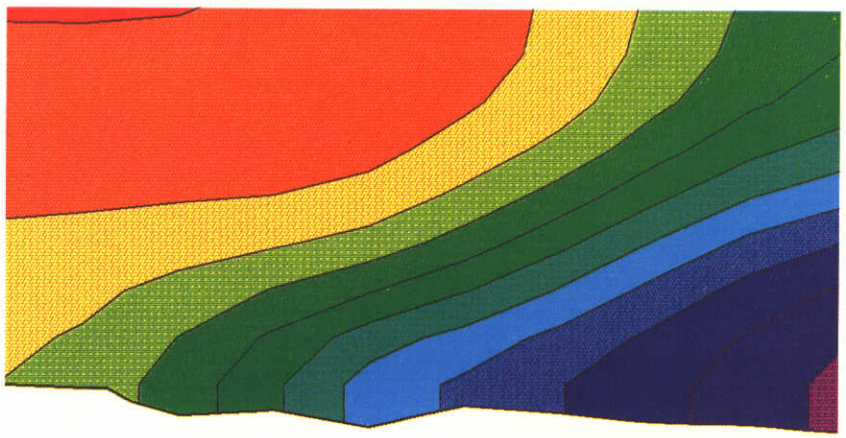

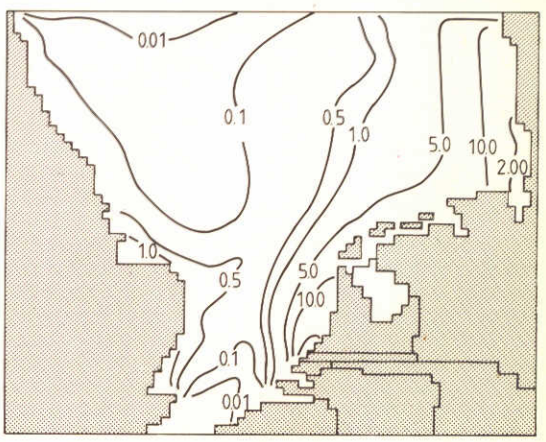

rijkswaterstaat
delft hydraulics

2 turbulence and mixing in stratified flow

report on literature survey

R 880/S 667

November 1986

CONTENTS

CONTENTS (continued)

Notation

A : dimensionless parameter, defined by Eq. 2.11

a_1, a_2 : upper layer depth and lower layer depth (see Fig. 3.1)

C : Chezy coefficient

C_1, C_2 : dimensionless constants, defined in Table 4.1

C_D : modelling constant, defined by Eq. 5.2

c_e, c_s, c_τ : modelling constants, defined by Eqs. 3.15 and 3.16

c_μ : modelling constant, defined by Eq. 5.1

D : depth integrated dissipation of turbulent energy

$Diff(k)$: diffusive transport terms (Eq. 5.4)

d : thickness of intermediate layer

d_L : thickness of intermediate layer after billow collapse

E_D : estuary number, defined by Eq. 3.1

E^* : dimensionless ratio, defined by Eq. 4.21

F_z : turbulent flux of mass in vertical direction

F_0, F_Δ : densimetric Froude numbers, defined by Eqs. 2.13 and 2.3

$F_0(Ri), F_1(Ri)$: damping functions, defined by Eqs. 6.8 and 6.11

$F(u_i'u_j', \ )$: functional relationship between $\overline{u_i'u_j'}$ and other second-order correlations (Eq. 5.5)

G : buoyancy destruction of turbulent energy

$G_o(Ri)$: damping function, defined by Eq. 6.8

g : gravitational acceleration

h : waterdepth

h_o : depth at mouth of estuary

h_1, h_2 : thickness of upper and lower layer

K_t : eddy diffusivity

K_{to} : eddy diffusivity for neutral conditions

k : turbulent kinetic energy (Eq. 4.12)

k_b, k_i : bottom shear coefficient and interfacial shear coefficient, defined by Eqs. 3.10 and 2.15

L : length scale of turbulence

L' : characteristic length of considered mass of fluid (Eq. 4.1)

L_b, L_k, L_R, L_t : buoyancy-, Kolmogorov-, Ozmidov- and turbulence scale of turbulence, given by Eqs. 4.2, 4.8, 4.6 and 4.7

Notation (continued)

L_m, L_n : master length scale of turbulence, length scale of turbulence for neutral conditions (see Section 6.1)

L_i : length of arrested salt wedge (Section 2), length of zone with salinity intrusion (Section 3)

N : Brunt-Väisälä frequency, defined by Eq. 4.3

P : production of turbulent energy

q_{riv} : river flow rate per unit width

Rf : flux Richardson number, defined by Eq. 4.16

Rf_c : maximum (critical) Rf-value, i.e maximum mixing efficiency

Ri : gradient Richardson number, defined by Eq. 4.14

Ri_o : overall Rischardson number, defined by Eq 3.18

Ri^* : layer Richardson number, defined by Eq. 2.1

Ri_e^*, Ri_L^* : equilibrium value of Ri^* for internal mixing (Section 4.3), Ri^*-value for $d = d_L$

T_b, T_e, T_L : time needed for growth and collapse of billows, for amplitude of most unstable internal wave to increase by a factor e, for fresh water to flow over entire length of salt wedge

T_{disp} : dispersive transport, defined by Eq. 2.19

t : time

U : velocity scale of turbulence

U' : characteristic velocity of considered mass of fluid (Eq. 4.1)

u : velocity component in x-direction

u_{riv} : river velocity, i.e river flow rate over cross section

$\hat{u}_{i.o}$: amplitude of profile averaged tidal velocity at mouth of estuary

u_* : shear velocity

$u_{*.b}, u_{*.s}$: bottom shear velocity; $u_{*.b} = (\tau_b/\rho)^{\frac{1}{2}}$, where τ_b is bottom shear stress; surface shear velocity; $u_{*.s} = (\tau_s/\rho)$, where τ_s is surface shear stress

$u_{m.e}, u_{m.f}$: extreme values of u during ebb tide, during flood tide

u_1, u_2 : velocity of upper and lower layer

V : measure for potential energy of stratification, defined by Eq. 3.3

v : velocity component in y-direction

Notation (continued)

w : velocity component in z-direction

w_1, w_2 : entrainment rates, defined by Eq. 3.14 and Fig. 3.1

x : horizontal coordinate in main flow direction

y : horizontal coordinate in transverse direction

z : vertical coordinate ($z = 0$: bottom; $z = h$: water surface)

α : efficiency of conversion from kinetic to potential energy (Section 3); damping factor depending on Ri (Appendix B)

β : ratio between total production rate of turbulent energy and that due to bottom shear

γ : ratio between ε and $u_*^3 h^{-1}$

Δu : difference between mean velocities of upper and lower layer

$\Delta\rho$: difference in density between lower layer and upper layer (Section 2), between sea water and river water (Section 3)

ε : dissipation of turbulent energy per unit mass of fluid and per unit time

κ : von Karmann constant

ν : kinematic viscosity

ν_t : eddy viscosity

ν_{to} : eddy viscosity for neutral conditions

ρ : density

ρ_o : density of either sea water or river water

ρ_1, ρ_2 : density of upper layer and lower layer

ρ : density averaged from $z = z$ to $z = h$

σ_t : turbulent Prandtl number, $\sigma_t = \nu_t K_t^{-1}$

σ_{to} : turbulent Prandtl number for neutral conditions

τ : turbulent shear stress

τ_b, τ_i : bottom shear stress, interfacial shear stress

τ_{ex}, τ_{in} : fraction of τ which is related to bottom shear stress (an internal effect), same related to longitudinal density gradient (an internal effect)

superscripts

$\bar{}$: time mean value

$'$: turbulent fluctuation

$=$: depth averaged value of time mean value

Introduction

1.1 Objective of study

This report presents the findings of a literature survey on turbulence and vertical turbulent transfer of momentum and mass in stratified tidal flows. The objective of the study was to review the literature on the subject from the perspective of salinity intrusion in estuaries.

In its meeting of December 6, 1985 the Working Group "Inhomogeneous Flows" decided to have the literature survey performed. It was intended as an update of part of a previous literature survey on the subject (Breusers, 1974). Both the previous and the present literature survey were performed within the framework of T.O.W., a long term research programme executed by Rijkswaterstaat (Ministry of Transport and Public Works) and the Delft Hydraulics Laboratory . The present study was made by Dr. G. Abraham.

The 1974 study included reviews on internal waves and on the modelling of turbulence. Reviews on these subjects will be presented at the Symposium on Physical Processes in Estuaries, September 1986, to be organized by Rijkswaterstaat and the Delft Hydraulics Laboratory. Therefore internal waves are not included in the present update. Turbulence modelling is dealt with only in sofar as needed to show the implications of the effect of stratification on turbulence for the different types of turbulence models.

1.2 Regimes of estuarine turbulence

In tidal estuaries the longitudinal density gradient has a significant effect on the variation of the velocity over the depth. This is due to the fact that the hydrostatic pressure at distance z from the bed is given by

$$p = \overline{\rho}\, g(h-z) \tag{1.1}$$

and therefore, after partial differentiation in the longitudinal direction

$$\frac{1}{\rho}\frac{\partial p}{\partial x} = g\frac{\partial h}{\partial x} + \frac{1}{\rho}\frac{1}{2} g\, h \frac{\partial \overline{\rho}}{\partial x} + \frac{1}{\rho} g(\frac{1}{2} h - z)\frac{\partial \overline{\rho}}{\partial x} \tag{1.2}$$

where x: horizontal coordinate in main flow direction

z: vertical coordinate, positive when directed upward and measured from bottom

p: pressure

g: gravitational acceleration

h: waterdepth

$\bar{\rho}$: density averaged from z = z to z = h

ρ: (reference) density of either sea water or river water, which are about equal.

Per unit mass of fluid, Eq. 1.2 gives the force in the horizontal direction due to a variation of the pressure in this direction. The first term on the right hand side of Eq. 1.2 is constant over the depth. Further, when the vertical variation of $\partial\bar{\rho}/\partial x$ is small, the second term on the right hand side is about constant over the depth and, while varying over the depth, depth-averaged the third term is about zero. Therefore, the first and second term on the right hand side of Eq. 1.2 represent forces (per unit mass of fluid) which cause the depth-averaged tidal flow. The third term represents forces, which cause the gravitational circulation. As the sign of $\partial\bar{\rho}/\partial x$ does not change with time, throughout the tidal cycle the third term represents a seaward force at the water surface (z = h) and a land-inward force at the bottom (z = 0).

For the Rotterdam Waterway Fig. 2.3 shows the effect of the forces represented by the third term on the right hand side of Eq. 1.2 on the variation of the velocity over the depth. On the ebb tide (7 hr) the variation of the velocity over the depth is large, on the flood tide it is small to zero (13 - 15 hr), while density induced exchange flows occur at low water slack (10 - 11 hr).

The production of turbulent energy is given by the product of the turbulent shear stress and the vertical gradient of the horizontal velocity. On the ebb tide the vertical gradient of this velocity is large. Hence, on the ebb tide the production of turbulent energy is large. On the flood tide the vertical gradient of the velocity is small, and so is the production of turbulent energy. This means that on the ebb tide and flood tide different terms are dominant in the conservation equation for turbulent energy.

In addition, in stratified flows distinction has to be made between what Turner (1973, Section 4.3) calls "internal mixing processes", i.e. the energy for the mixing is supplied from within the region where the mixing occurs (e.g. the interface) and "external mixing processes", meaning that in this case the energy for the mixing is supplied from a region (the solid boundaries) external to the region where the mixing occurs (the interior of the fluid).

At tidal slack the bottom shear stress is small, while it must go through zero as its direction changes from the ebb tide to the flood tide. Hence, at tidal slack conditions are favourable for internal mixing to occur. On the (maximum) ebb tide and flood tide the bottom shear stress is large, and external mixing is likely to occur.

Summarizing, the following regimes of turbulence can be distinguished in connection with salinity intrusion into estuaries

- around tidal slack mixing tends to be an internal proces
- on the (maximum) ebb tide mixing tends to be an external process, while production of turbulent energy tends to be large
- on the (maximum) flood tide mixing tends to be an external process, while production of turbulent energy tends to be small.

1.3 Subjects included in review

In a classification of estuaries on stratification the arrested salt wedge and the well mixed estuary are at the extreme ends of the spectrum. For the arrested salt wedge estuary mixing - if any - is primarily an internal process, while in a well mixed estuary it is primarily an external process. Chapters 2 and 3 deal with the arrested salt wedge and the well mixed estuary respectively.

Chapter 2 deals with the arrested salt wedge and the role of internal mixing therein. For this two-layer stratified flow the internal mixing leads to the development of an intermediate layer, induced by Kelvin-Helmholtz instability. This layer has a stabilizing effect. Once its thickness exceeds a limiting value, it eliminates further instability of internal waves. Then it also

suppresses turbulence. The time scale for the development of the intermediate layer is such that around tidal slack these internal effects occur in a sufficiently stratified tidal estuary.

The main issue of Chapter 3 is to illustrate that it is in essence boundary-generated turbulence which controls the stratification of a tidal estuary by external mixing. To this end experimental information on the overall efficiency of the conversion from boundary-generated turbulent kinetic energy to potential energy is collected. On this basis an energy balance is given and a criterion for well mixed conditions is derived. Part of the underlying information on the efficiency of the conversion is obtained from parameterization studies on boundary induced entrainment in two-layer stratified flow. Reviews on this subject, which are available in the literature, are summarized.

The length scale of turbulence is controled by the external boundaries of the flow. In addition in stratified flows density stratification acts as an internal control.

Chapter 4 deals with the effects of stable density stratifications on turbulence. It does so on a local level, expressing these effects in terms of local parameters, i.e. parameters which describe the flow and turbulence at a specific location within the flow. It presents a length scale classification of turbulence in stratified conditions, expressed in local parameters. It presents experimental support for this classification. It explains that for the ebb tide regime and for the flood tide regime, distinguished at the end of Section 1.2, different local parameters have to be used to describe the effects of density stratification on turbulence.

Turbulence modelling is described briefly in Chapter 5. Is distinguishes turbulence models which require the length scale of turbulence (the mixing length) as an empirical input from those which contain a partial differential equation to determine the length scale. In the former group of models damping functions are used to express the effect of stratification on the length scale. These damping functions are expressed in local stability parameters such as the gradient Richardson number. The latter group of turbulence models - referred to as higher order turbulence models - give the length scale of

turbulence as a function of time and spatial coordinates, not as a function of local stability parameters. Therefore, the above damping functions cannot be derived from the higher order turbulence models.

Chapter 6 deals with the combined effects of the external boundaries and the density stratification on turbulence. It deals with the effect of these factors on the mixing length and the related damping functions. In particular it shows the difficulties involved in finding damping functions appropriate for the different regimes distinguished at the end of Section 1.2. For reasons explained at the end of the preceding paragraph these damping functions cannot be derived from higher order turbulence models.

A summary of the findings of the study and some recommendations for further study in the new DHL tidal flume are given in Chapter 7.

2 Arrested salt wedge

2.1 Stabilizing intermediate layer

The arrested salt wedge is a sub-critical stratified flow which may be treated as a two-layer flow without mixing at or through the interface (Schijf and Schönfeld, 1953). This is because in sub-critical stratified flows there is the tendency towards the development of a stabilizing intermediate layer. Its development may be looked upon as being initiated by unstable internal waves at an originally sharp interface. The unstable waves can generate mixing as a consequence of which an intermediate layer is formed. The thickness of the intermediate layer can increase with time until all internal waves become stable. This happens when the thickness of the intermediate layer is a small fraction of the total depth of both layers (Abraham et al, 1979).

The limiting thickness of the intermediate layer can be derived from linear instability theory, which studies the behaviour of a periodic small disturbance (e.g. an internal wave) superimposed upon a background flow. It indicates under which circumstances the disturbance is stable or unstable. The conditions of stability and instability are given as a function of the wave length of the disturbance and characteristics of the background flow by means of neutral stability curves which separate the zones of stable and unstable solutions.

For the background flow represented in Fig. 2.1, Miles (1961) and Howard (1961) showed that for inviscid background flow a sufficient condition for stability of small amplitude internal waves of all wave lengths is that the gradient Richardson number be everywhere larger than 1/4. This criterion leads to stability if (Thorpe (1971), Hazel (1972)) (see also Fig. 2.2).

$$Ri^* = \frac{\frac{\Delta\rho}{\rho}\, g\, d}{(u_1 - u_2)^2} \geq \frac{1}{4} \qquad (2.1)$$

where h_1, h_2 : thickness of upper and lower layer

u_1, u_2 : velocity of upper and lower layer

ρ_1, ρ_2 : density of upper and lower layer

$\Delta\rho$: difference in density between lower and upper layer

ρ : density of either upper layer or lower layer (ρ_1 - ρ_2)

d : thickness of intermediate layer

g : gravitational acceleration

Ri* : layer Richardson number, defined by Eq. 2.1

For sub-critical stratified flows

$$\frac{u_1^2}{\frac{\Delta\rho}{\rho} g h_1} + \frac{u_2^2}{\frac{\Delta\rho}{\rho} g h_2} \leq 1 \qquad (2.2)$$

and hence

$$F_\Delta = \frac{(u_2 - u_1)^2}{\frac{\Delta\rho}{\rho} g (h_1 + h_2)} < 1 \qquad (2.3)$$

where F_Δ: densimetric Froude number, defined by Eq. 2.3.

Eqs. 2.1 and 2.3 imply that starting from zero, the thickness of the intermediate layer has to increase to less than $(h_1 + h_2)/4$, in order to make internal waves of all wave length stable.

Table 2.1 summarizes growth rates of the most unstable wave, calculated by Miles and Howard (1964), the most unstable wave being defined as the first to become unstable for $Ri^* < \frac{1}{4}$. Its wave length is about 7.5 d.The calculated growth rate, T_e^{-1}, decreases with increasing Ri^* to become zero for $Ri^* = \frac{1}{4}$, the lowest value with stability of internal waves of all wave lengths.

Turbulent kinetic energy is produced when internal waves become unstable (see Section 2.2). Hence, turbulence will not be able to receive energy from or to lose energy to the mean flow, once internal waves of all wave lengths become stable. Hence, under this condition turbulent intensity must decay owing to the steady drain of turbulent energy by viscous dissipation, and neither mixing due to unstable internal waves nor turbulent mixing occurs when the condition of Eq. 2.1 is satisfied. For $Ri^* \sim 0.32$ the decay of turbulence intensity was observed in experiments performed by Chu and Baddour (1984).

Table 2.1 T_e as function of Ri^* for background flow of Fig. 2.1 (Miles and Howard, 1964); T_e: time needed for amplitude of most unstable wave to increase by factor e

Ri^*	T_e
0.05	$5\ d\ \lvert u_1 - u_2 \rvert^{-1}$
0.15	$10\ d\ \lvert u_1 - u_2 \rvert^{-1}$
0.20	$20\ d\ \lvert u_1 - u_2 \rvert^{-1}$
0.25	∞

The above description of the formation of the intermediate layer is a schematized one. It actually is associated with Kelvin-Helmholz instabilities, which are described in the following section.

2.2 Kelvin-Helmholz instability

For $Ri^* > 0$, in the internal layer the internal waves lose their stability first in the region of the wave crests and troughs, and thereby produce turbulent kinetic energy (Turner, 1973, Section 4.3.3). This energy comes from the internal waves, and so provides a mechanism for limiting their amplitude. This instability, and its subsequent development in a stably stratified shear flow, is generally known as Kelvin-Helmholtz instability. Its wave length and growth rate are in reasonable agreement with the theoretical predictions of the preceding section (Turner, 1973, Section 4.3.3). Its development is associated with the formation and eventually the collapse of billows (Thorpe (1973a), Maxworthy and Browand (1975), Sherman et al (1978)).

Corcos (1979) has investigated theoretically the initial stages of Kelvin-Helmholz billow growth from unstable waves to concentrated vortices which

repeatedly orbit and pair, finding billow heights of order $(u_1 - u_2)^2 \, \Delta\rho^{-1} \, g^{-1}$ in a time or order 10 $|u_1 - u_2| \, \Delta\rho^{-1} \rho \, g^{-1}$. The final stage of mixing and collapse occurs in a time of the order 20 $|u_1 - u_2| \, \Delta\rho^{-1} \rho \, g^{-1}$ (Thorpe, 1973a). Therefore, following Imberger and Spigel (1980), for the background flow of Fig. 2.1, a time scale for billowing may be defined as

$$T_b = 20 \, \frac{|u_1 - u_2|}{\frac{\Delta\rho}{\rho} \, g} \tag{2.4}$$

where T_b: time needed for growth and collapse of billows.

In accordance with experiments performed by Thorpe (1973b), Koop and Browand (1979), Gartrell (1980) and Chu and Baddour (1984) the corresponding thickness of the stabilizing intermediate layer satisfies

$$Ri_L^* = \frac{\frac{\Delta\rho}{\rho} \, g \, d_L}{(u_1 - u_2)^2} \approx 0.32 \tag{2.5}$$

where d_L : thickness of intermediate layer after billow collapse

Ri_L^*: corresponding layer Richardson number, defined by Eq. 2.5.

$Ri_L^* \approx 0.32$ is slightly higher than the minimum value of Ri^* required for stability of small amplitude internal waves (Section 2.1). It is for $Ri_L^* \approx 0.32$ that Chu and Baddour (1984) found the turbulence to decay in the intermediate layer. Corcos and Hopfinger (1976) refer to $Ri_L^* \approx 0.32$ as the experimental criterion for the halt of the intermediate layer growth and the beginning of its relaminarization (see also Hopfinger, 1985). Gartrell (1980) found the intermediate layer to collapse to nearly laminar flow for $Ri_L^* \approx 0.3$.

The relaminarization takes place since $Ri_L^* \approx 0.32$ is larger than the equilibrium Richardson number Ri_e^*, the significance of which is elaborated upon in Section 4.3.

2.3 Formation of intermediate layer

The fresh water needs a certain time to flow over the entire length of an arrested salt wedge ($u_2 \sim 0$)

$$T_L \sim \frac{L_i}{|u_1 - u_2|} \tag{2.6}$$

where T_L: time needed for fresh water to flow over entire length of arrested salt wedge

L_i: length of arrested salt wedge

An intermediate layer is formed when

$$T_e \ll T_L \qquad T_b \ll T_L \tag{2.7}$$

From Table 2.1

$$T_e = 20 \frac{d}{|u_1 - u_2|} \qquad \text{for } R_i^* \leq 0.2 \tag{2.8}$$

Eqs. 2.1, 2.2, 2.3, 2.4, 2.6 and 2.8 imply

$$\frac{T_e}{T_L} < 5 \frac{(h_1 + h_2)}{L_i} \tag{2.9}$$

and

$$\frac{T_b}{T_L} < 20 \frac{(h_1 + h_2)}{L_i} \tag{2.10}$$

For a schematized estuary with constant cross-section (Schijf and Schönfeld, 1953)

$$L_i = \frac{1}{4} \frac{(h_1 + h_2)}{k_i} A \tag{2.11}$$

with

$$A = \frac{1}{5} F_o^{-1} - 2 + 3 F_o^{1/3} - \frac{6}{5} F_o^{2/3} \qquad (2.12)$$

$$F_o = \frac{u_{riv}^2}{\frac{\Delta\rho}{\rho} g (h_1 + h_2)} \qquad (2.13)$$

$$u_{riv} = \frac{q_{riv}}{(h_1 + h_2)} \qquad (2.14)$$

and

$$k_i = \frac{\tau_i}{\rho(u_1 - u_2)^2} \qquad (2.15)$$

where F_o : densimetric Froude number, defined by Eq. 2.13
A : dimensionless parameter, defined by Eq. 2.11
u_{riv}: river velocity
q_{riv}: river flow rate per unit width
τ_i : interfacial shear stress
k_i : interfacial shear coefficient

For field conditions (Abraham et al, 1979)

$$k_i = 4\ 10^{-4} \qquad (2.16)$$

Table 2.2 gives $L_i(h_1+h_2)^{-1}$ as a function of $F_o^{\frac{1}{2}}$. The conditions of Eq. 2.7 are satisfied for $F_o^{\frac{1}{2}} \leq 0.6$. This means that for the arrested salt wedge there is sufficient time available for the stabilizing intermediate layer to be formed. By itself, this prevents further internal mixing.

Table 2.2 Length of arrested salt wedge
$k_i = 4\ 10^{-4}$ (Schijf and Schönfeld, 1953)

$F_o^{\frac{1}{2}}$	$L_i(h_1+h_2)^{-1}$
0.1	11.620
0.2	2430
0.3	828
0.4	328
0.5	134
0.6	52
0.7	17
0.8	4.1
0.9	0.4
1.0	0

2.4 Application to conditions of tidal slack

At tidal slack tidal velocity and boundary shear stress are small, and little turbulent energy is supplied from the solid boundaries. Then the vertical exchange of momentum is small. This leads to a pronounced effect of the longitudinal density gradient on the variation of the longitudinal velocity over the depth.

At tidal slack conditions are favourable for internal mixing to occur. Whether or not by then a stabilizing intermediate layer occurs depends on whether or not the time needed for its establishment, T_b, is a small fraction of the tidal period.

At tidal slack the flow is density induced, and may be approximated as being of the lock exchange flow type (Schijf and Schönfeld, 1953). This implies

$$\frac{(u_1-u_2)^2}{\frac{\Delta\rho}{\rho} g (h_1+h_2)} = 1 \qquad (2.17)$$

and with Eq. 2.4

$$\frac{T_b}{T} = 20 \frac{(h_1+h_2)}{(u_1-u_2)\ T} \qquad (2.18)$$

where T : duration of tidal cycle.

For sufficiently stratified estuaries, Eq. 2.18 implies $T_b << T$, meaning that around tidal slack vertical mixing is weak, since a stabilizing intermediate layer is formed. This condition applies to the Rotterdam Waterway Estuary, with close to its mouth around low water slack $(h_1+h_2) \approx 10$ m and $|u_1-u_2| \approx 1.0$ m s-1 (Fig. 2.3). These parameter values imply $T_b/T \approx 10^{-2}$.

For a station close to the mouth of the Rotterdam Waterway Estuary, the top part of Fig. 2.3 (after Stigter and Siemons, 1967) gives the variation of velocity and salinity over the depth throughout the tidal cycle, 11 hrs about coinciding with low water slack. By then an intermediate layer can be recognized, with a gradient Richardson number (defined by Eq. 4.14) of the order 0.3, at the relative depth with zero velocity.

The bottom part of Fig. 2.3 gives the dispersive transport of salt into the estuary. It is defined as

$$T_{disp} = h \overline{(u-\bar{u})\ (s-\bar{s})} \qquad (2.19)$$

where T_{disp} : dispersive transport, defined by Eq. 2.19
h : depth
s : salinity
$\bar{}$: depth mean value of parameter

The dispersive transport is the salt transport into the estuary through a reference plane moving at velocity $\bar{u}$. Salt would not penetrate further into the estuary from its mouth than the tidal excursion length, if the dispersive

transport were zero. If so, salt water which enters into the estuary from the sea on the flood tide, will return to the sea before the end of the following ebb tide. This is because, when moving at velocity $\bar{u}$, the river flow makes the seaward displacement on the ebb tide larger than the land inward displacement on the flood tide.

Fig. 2.3 shows that for the considered station close to the mouth of the Rotterdam Waterway Estuary a significant fraction of the total (time integrated) dispersive transport occurs around low water slack and that salinity intrusion through that station is primarily due to low water slack flow conditions. For stations further upstream in the zone of salt intrusion, the dispersive transport occurs on the ebb tide and around high water slack (Karelse, 1976).

That for the Rotterdam Waterway salinity intrusion through the station close to its mouth is primarily due to the dispersive transport around low water slack makes it important to include the slack tide internal mixing properly in salinity intrusion studies for that estuary. In general this applies to estuaries above a given level of stratification. Abraham (1980) presents a criterion to determine when for a given estuary the slack tide internal mixing is a factor to be considered.

2.5 Final remark

Treating the arrested salt wedge as a two-layer stratified flow requires experimental information on the magnitude of the interfacial shear stress coefficient k_i, defined bij Eq. 2.13. For various sub-critical stratified flows experimental information on the magnitude of this coefficient can be derived from the 1974 literature survey (Breusers, 1974) and from Abraham et al (1979). Within the framework of the present study the literature has not been scanned for further experimental data.

3 On stratification of estuaries

3.1 Dimensional arguments

In estuaries stratification is induced by the differential advection, which the gravitational circulation is associated with. Where sufficient turbulent energy is supplied by the tidal current, the whole water column tends to remain well mixed. The buoyancy flux into the estuary is proportional to the product of the river flow per unit width and the density difference between sea water and river water. The energy input by the tidal current per unit area and per unit time is proportional to the product of the bottom shear and the tidal velocity, i.e. to the tidal velocity cubed. Therefore, the ratio of the energy available and needed for mixing is proportional to the parameter E_D, defined as

$$E_D = \frac{1}{\pi} \frac{\hat{u}_{1,0}^3}{\frac{\Delta\rho}{\rho_o} g h_o u_{riv}} \qquad (3.1)$$

where E_D : estuary number, introduced by Thatcher and Harleman (1981)
$\hat{u}_{1,0}$: amplitude of profile averaged tidal velocity at mouth of estuary
u_{riv} : river velocity, i.e. river flow rate over cross-sectional area
h_o : depth at mouth of estuary
$\Delta\rho$: difference in density between sea water and river water
ρ_o : density of either sea water or river water, which are about equal
g : gravitational circulation.

From Harleman and Ippen (1967) the following classification on the estuary number can be derived for prismatic channels:

well mixed conditions	$E_D > 8$	
partly mixed conditions	$8 > E_D > 0.2$	(3.2)
stratified conditons for	$0.2 > E_D$	

This classification about coincides with the one given by Fischer et al (1979, p. 243).

3.2 Energy considerations

The following energy considerations, which are derived from van Aken (1986), serve to substantiate the classification of the preceeding section and to emphasize the effect of external mixing on the stratification of an estuary. They are limited to well mixed conditions to avoid averaging of non-linear parameters over the depth of the estuary. They provide a criterion for the estuary to be well mixed. Application of this criterion requires quantitative information on the efficiency of the conversion from turbulent kinetic energy to potential energy.

3.2.1 Criterion for well mixed conditions

The potential energy of stratification may be related to the parameter V, defined as

$$V = \int_0^h (\rho - \bar{\bar{\rho}})\, g\, (h-z)\, dz \qquad (3.3)$$

where : ρ: density
h: water depth
z: vertical coordinate (z=0 at bottom, z=h at water surface)
V: measure for potential energy of stratification (V=0 for well mixed conditions, V>0 for stable stratification), and

where an double overbar refers to the depth mean value of the parameter underneath.

The temporal change of V is related with that of ρ and $\bar{\bar{\rho}}$. From the conservation equation for mass

$$\frac{\partial \rho}{\partial t} = - \frac{\partial}{\partial z} F_z - u \frac{\partial \rho}{\partial x} - w \frac{\partial \rho}{\partial z} \qquad (3.4)$$

where F_z: turbulent flux of mass in vertical direction

u,w: velocity components in x-direction and z-direction

x: longitudinal coordinate, landinward positive (x=0 at mouth of estuary)

t: time

For well mixed conditions ($\partial\rho/\partial x - \partial\bar{\rho}/\partial x$; $u\,\partial\rho/\partial x \gg w\,\partial\rho/\partial z$) eq. 3.4 reduces to

$$\frac{\partial\rho}{\partial t} = -\frac{\partial}{\partial z} F_z - u\frac{\partial\bar{\rho}}{\partial x}, \qquad \frac{\partial\bar{\rho}}{\partial t} = \bar{u}\frac{\partial\bar{\rho}}{\partial x} \tag{3.5}$$

The conservation equation for turbulent energy relates F_z with the production and dissipation of turbulent energy (Eq. 4.11, Section 4.3). In tidal estuaries the variation with time of the turbulent kinetic energy within a control volume dxdz is primarily due to the production and dissipation, and not caused by the net inflow through the boundaries. Therefore, for well mixed conditions, substituting Eqs. 3.5 and 4.11 into Eqs. 3.3 gives

$$\frac{\partial\langle V\rangle}{\partial t} = -\langle(P - D)\rangle - \langle g\frac{\partial\bar{\rho}}{\partial x}\int_o^h (u - \bar{u})\,(h-z)\,dz\rangle \tag{3.6}$$

with

$$P = \int_o^h \tau\frac{\partial u}{\partial z}\,dz \qquad D = \int_o^h \varepsilon dz$$

where P: depth integrated production of turbulent energy

D: depth integrated dissipation of turbulent energy

τ: turbulent shear stress

ε: dissipation of turbulent energy per unit mass of fluid and per unit time, and

where pointed brackets refer to time mean values, obtained by averaging over a tidal cycle.

Eq. 3.5 illustrates that in estuaries stratification is induced by differen-

tial edvection, i.e. the variation of $u\ \partial\rho/\partial x$ over the depth.

For sufficiently well mixed estuaries to neglect the effect of $\partial\bar{\rho}/\partial x$ on the variation of the velocity over the depth, calculations with linear velocity profiles and with a variety of step and parabolic profiles indicate that a reasonable estimate for the magnitude of the integral term in Eq. 3.5 is (van Aken, 1986)

$$<\int_0^h (u-\bar{u})\ (h-z)\ dz> = 0.1\ |\bar{u}_{riv}|h^2 \qquad (3.7)$$

Substituting Eq 3.7 into Eq. 3.6 gives the following criterion for a well mixed estuary to remain well mixed ($\partial V/\partial t < 0$)

$$<(P-D)> \ > \ 0.1\ g\ \frac{\partial\bar{\rho}}{\partial x}\ |\bar{u}_{riv}|h^2 \qquad (3.8)$$

Eq. 3.8 gives a lower limit of $<(P-D)>$, as in its derivation $\partial\bar{\rho}/\partial x$ was assumed not to vary with time.

3.2.2 Efficiency of conversion from kinetic energy to potential energy

Quantitative information on the overall efficiency of the conversion from turbulent kinetic energy to potential energy can be obtained from the field data behind the Simpson-Hunter (1974) stratification parameter for shelf seas. It further can be obtained from the experimental information behind the parameterization of the entrainment for a mixed bottom layer (e.g. Kranenburg, to be published).

The energy supplied by the tidal current plays an important role in the Simpson-Hunter (1974) stratification parameter. This parameter is introduced to distinguish areas in shelf seas where sufficient turbulent energy is supplied by the tidal current to keep the whole water column well mixed from those areas where the stabilizing heat flux at the sea surface in spring and summer is capable of overcoming the mixing by the tidal current. In the underlying energy considerations (P-D) is parameterized as

$$\langle (P-D) \rangle = \alpha \frac{4}{3\pi} k_b \rho \hat{u}_1^3 \qquad (3.9)$$

with

$$\tau_b = k_b \rho \bar{u}^2 = \frac{g}{C^2} \rho \bar{u}^2 \qquad (3.10)$$

where τ_b: bottom shear stress

$\bar{u}$: depth averaged velocity

k_b : bottom shear coefficient

C : Chezy coefficient

α : efficiency of conversion from kinetic to potential energy

The efficiency α satisfies

$$\alpha = (0.3 \text{ to } 2)\ \% \qquad (3.11)$$

Efficiencies of this order were obtained from shelf sea field data by Fearnhead (1975) (1%), Garrett et al (1978) (0,3%), Schumacher et al (1979) (2%) and Simpson and Bowers (1981)(0,4%).

The efficiencies applied in the parameterization of the boundary-induced entrainment of a stratified two-layer flow coincide with the lower limit given by Eq. 3.11. This is elaborated upon in Section 3.3. In addition, Eq. 3.8 gives a lower limit of the energy needed to keep an estuary well mixed. Therefore, in the following text the lower limit given by Eq. 3.11 is applied.

3.2.3 Criterion for well mixed conditions (continued)

In first approximation

$$\frac{\partial \bar{\rho}}{\partial x} = \frac{\Delta \rho}{L_i} \qquad (3.12)$$

where L_i: length of zone with salinity intrusion.

Substituting Eqs. 3.9 and 3.12 into Eq. 3.8 gives as the condition for a well mixed estuary to remain well mixed

$$\frac{\partial V}{\partial t} \leq 0 \text{ if } \quad E_D \geq 0.1\alpha^{-1} \frac{3}{4} \frac{C^2}{g} \frac{h}{L_i} \tag{3.13}$$

Typical values for C and $L_i h^{-1}$ are 60 $m^{\frac{1}{2}}s^{-1}$ and 1000 respectively. Substituting these values into Eq. 3.13 and deriving α from the lower limit of Eq. 3.11 gives $E_D \geq 9$ as the condition for an estuary to remain well mixed. This limiting value is of the same order of magnitude as the limiting value given in the classification after Harleman and Ippen (1967) ($E_D \geq 8$, Eq. 3.2). This agreement is only an order of magnitude one, since $L_i h^{-1}$ varies with q_{riv}. Nevertheless it illustrates that in essence boundary generated turbulence controls the stratification of an estuary.

3.3 Boundary-induced entrainment

In recent years considerable progress has been made in the modelling of boundary-induced entrainment. Reviews on the subject are presented by Sherman et al (1978), Tennekes and Driedonks (1980) and Imberger and Hamblim (1982). A condensed summary of these reviews is given by Kranenburg (1986). Turner (1981) reviews the literature on the subject from the oceanographic point of view.

Kranenburg (1986) deals with the boundary-induced entrainment of a stratified two-layer flow as a two-way process. To this end he defines two effective interfacial transports (entrainment rates) w_1 and w_2 (notation as in Fig. 3.1) so that

$$\begin{aligned} w_2 - w_1 &= \text{mean vertical volume flux through interface} \\ w_2\rho_2 - w_1\rho_1 &= \text{mean vertical mass flux through interface} \end{aligned} \tag{3.14}$$

where w_1, w_2 : entrainment rates, defined by Eq. 3.14 and Fig. 3.1

ρ_1, ρ_2 : density of homogeneous parts of upper and lower layer (see fig. 3.1).

The entrainment rate w_1 represents a transport of fluid from the homogeneous part of the upper layer to the lower layer caused by the bottom-induced turbulence in that layer. The entrainment rate w_2 represents an upward transport caused by the turbulence induced at the free surface.

Disregarding a possible interaction between the two processes causing entrainment into either layer - as found justified for grid-stirred experiments (Turner, 1973, Section 9.1.1) - Kranenburg integrates the conservation equation for turbulent energy (Eq. 4.11) over either layer. Introducing closure assumptions as introduced in the above mentioned reviews, he obtains the following equations.

In the case of entrainment into the turbulent upper layer:

$$\tfrac{1}{2}\left(\frac{\rho_2 - \rho_1}{\rho}\right) g\, a_1 w_2 = \tfrac{1}{2}\, c_e w_2\, \Delta u^2 + \tfrac{1}{2}\, c_\tau u_{*.s}^2 |\Delta u| + \tfrac{1}{2}\, c_s u_{*.s}^3 \qquad (3.15)$$

where a_1 : upper layer depth (see Fig. 3.1)

Δu : difference between mean velocities of upper layer and lower layer

$u_{*.s}$: surface shear stress velocity; $u_{*.s} = (\tau_s/\rho)^{1/2}$, where τ_s is surface shear stress

c_e, c_τ, c_s : modelling constants

and for the case of entrainment into the turbulent lower layer:

$$\tfrac{1}{2}\left(\frac{\rho_2 - \rho_1}{\rho}\right) g\, a_2 w_1 = \tfrac{1}{2}\, c_e w_1 \Delta u^2 + \tfrac{1}{2}\, c_\tau u_{*.b}^2 |\Delta u| + \tfrac{1}{2}\, c_s u_{*.b}^3 \qquad (3.16)$$

where a_2 : lower layer depth (see Fig. 3.1)

$u_{*.b}$: bottom shear stress velocity; $u_{*.b} = (\tau_b/\rho)^{1/2}$ where τ_b is bottom shear stress.

The terms in Eqs. 3.15 and 3.16 represent increase in potential energy caused by buoyancy transport, shear production caused by transport of mass, shear production caused by momentum transport and the net production of turbulent kinetic energy by external shear. A term accounting for storage of turbulent kinetic energy must be added to the left hand side of Eqs. 3.15 and 3.16 in applications to weakly stratified flows (see e.g. Bloss and Harleman, 1980).

Kranenburg gives the following values for the model constants: $c_e = 0.22$, $c_\tau = 0.14$ and $c_3 = 0.17$. These values are derived from laboratory measurements, and for c_s also from field experiments (Fisher et al, 1979, Section 6.3.2).

For $\Delta u = 0$, $c_s = 0.17$ and $C = 60\ m^{\frac{1}{2}}s^{-1}$ (Eq. 3.10), Eq. 3.16 reduces to

$$\tfrac{1}{2}(\rho_2 - \rho_1)g\, a_2 w_1 = 0.0045\, \tau_b u_2 \qquad (3.17)$$

where u_2 : mean velocity of lower layer.

Eq. 3.17 implies $\alpha = 0.45\%$.

Unified presentations of the entrainment rates measured under different conditions are presented by Anwar and Weller (1981), by Alavian (1986) and in the review by Cristodoulou (1986). Their accuracy is limited, however, because experimental results of different flow types are included: stratified flows driven by a surface stress, buoyant overflows over stagnant heavier water, buoyant underflows underneath stagnant lighter water and counterflows.

Christodoulou (1986) distinguishes four different entrainment regimes, depending on the magnitude of the overall Richardson number, defined as

$$Ri_o = \frac{\Delta\rho\, g\, h_1}{\rho \Delta u^2} \qquad \text{or } Ri_o = \frac{\Delta\rho\, g\, h_2}{\rho \Delta u^2} \qquad (3.18)$$

where Ri_o: overall Richardson number, defined by Eq 3.18

h_1, h_2: depth of flowing lager

For supercritical conditions, Christodoulou indicates, mixing takes place through vortex entrainment and a $Ri_o^{-\frac{1}{2}}$ relation holds. For subcritical conditious mixing occurs by cusp entrainment and a $Ri_o^{-3/2}$ relation holds. In the intermediate range of Ri_o the two mechanisms coexist and the entrainment appears to be described by a Ri_o^{-1} relationship. Finally for $Ri_o \to 0$, an asymptotic relation of the form Ri_o^{0} applies, corresponding to mixing in a homogeneous fluid. Inspection of Christodoulou's final graph (his fig. 5) shows that the range of Ri_o-values corresponding to the different regimes varies with the type of flow.

4 Effect of stable stratification on turbulence

4.1 Scales of turbulence, limiting conditions

A buoyancy scale, L_b, can be derived from the condition that inertial forces and buoyancy forces are of the same order, i.e. from

$$\bar{\rho} \frac{(U')^2}{L'} \sim g \frac{\partial \bar{\rho}}{\partial z} L' \tag{4.1}$$

where g : gravitational acceleration
z : vertical coordinate, positive when directed upwards
U': characteristic velocity of considered mass of fluid
L': characteristic length of considered mass of fluid
ρ : density
$\bar{}$: time mean value of parameter.

The length scale L', which satisfies Eq. 4.1 is the buoyancy scale L_b, i.e.

$$L_b = \frac{U'}{N} \tag{4.2}$$

with $$N = \left(-\frac{1}{\rho} g \frac{\partial \bar{\rho}}{\partial z}\right)^{1/2} \tag{4.3}$$

where N : Brunt-Väisälä frequency

L_b represents the largest vertical excursion a mass of fluid can have before converting all its kinetic energy into potential energy

In Eqs. 4.1 and 4.2 the characteristic velocity may be due to either turbulence or internal waves. When entirely due to turbulence, or considering only the effect of turbulence

$$U' = U \qquad L' = L \tag{4.4}$$

with (Tennekes and Lumley, 1972, Sections 3.1 and 3.2)

$$\varepsilon = \frac{U^3}{L} \qquad U^2 = \frac{1}{3}\left(\overline{u'^2} + \overline{v'^2} + \overline{w'^2}\right) \tag{4.5}$$

where U : velocity scale of turbulence
L : length scale of turbulence
u,v,w: velocity component in x-, y- and z-direction
x : horizontal coordinate in main flow direction
y : horizontal coordinate in transverse direction
ε : rate of dissipation of turbulent energy per unit mass of fluid
' : turbulent fluctuation of parameter.

The Ozmidov scale, L_R, is the length scale L, which satisfies Eq. 4.1, deriving U' from Eqs. 4.4 and 4.5 i.e.

$$L_R = (\varepsilon N^{-3})^{1/2} \tag{4.6}$$

It defines the upper limit permissible for the size of overturning turbulent motions. Larger scales of turbulent motion are confined to horizontal movement (Ozmidov, 1965).

The typical vertical distance travelled by particles before either returning towards their equilibrium level or mixing is the turbulence scale, L_t, defined on the basis of the rms ρ' -value as (Ellison, 1957)

$$L_t = \frac{\rho'_{rms}}{\frac{\partial \bar{\rho}}{\partial z}} \tag{4.7}$$

The smallest scales of turbulence are characterized by the Kolmogorov scale, L_k, i.e.

$$L_k = (\nu^3 \varepsilon^{-1})^{1/4} \tag{4.8}$$

where ν : kinematic viscosity

For $L \approx L_k$ viscous and inertial forces are ofthe same order.

A simplified length scale classification of the fluctuating motions in a stratified fluid is shown in Table 4.1. In this table C_1 and C_2 represent dimensionless constants. Experiments, which are described in Section 4.2 show that $C_1 = O(1)$ and $C_2 = O(10)$. The latter value has to be related with the fact that the peak of the normalized dissipation spectrum, related to isotropic turbulence, occurs at $L = 5\ L_k$ (Tennekes und Lumley, 1972. Chapter 8).

Table 4.1 Classification of fluid motion in stratified fluid (after Stillinger et al, 1983)

1	Fully turbulent flow $C_1 L_R > L > C_2 L_k$ Largest scale of the motion $L^* < C_1 L_R$ everywhere in the flow. Behaviour can be described by the statistical laws of nonstratified turbulence. Efficiently mixes scalar fluid properties.
2	Combined turbulent/wave field Scales with $C_1 L_R > L > C_2 L_k$ are still actively turbulent, but the largest scales of the flow $L^* > C_1 L_R$ have insufficient energy to overturn. Wave-like oscillations result. Reduced ability to mix scalars.
3	Internal wave field $C_1 L_R = L = C_2 L_k$ $(L_R L_k^{-1} = C_1^{-1} C_2)$. No overturning occurs and no transport of scalar quantities. Overturning motions cease to exist due to combined effect of buoyancy and viscosity.

As indicated by Rohr et al (1984), in the above classification the scale of turbulent eddies remains unaffected by buoyancy until the largest eddies reach a scale proportional to the Ozmidov scale L_R, after which they can no longer overturn. The next regime in the evolution of turbulence is one marked by a mixture of some scales overturning (the smaller ones farthest removed from buoyancy constaints) while the larger ones have retired in bobbing (wavelike motion) and could perhaps be forming a quasi two-dimensional turbulent field. Finaly, when there if no possible overturning at any scale ($L_R L_k^{-1} = C_1^{-1} C_2$,) the original three-dimensional turbulence is considered extinct, even though wavelike motions may persist for a long time afterwards.

The spectral distributions associated with the above length scale classification are given in Table 4.2, which is primarily derived from Turner (1973, Section 5.2.2). Detailed considerations on spectral distributions of turbulent energy and density fluctuations are given by Bogliano (1959), Lumley (1964) and Weinstock (1978 and 1985). Scheffers (1984) presents spectral distributions, measured at the North Sea under stratified conditions.

Table 4.2 Spectral distributions associated with the length scale classification given in Table 4.1.

1	Large scale wave-like motions and internal wave regime, $L' > C_1 L_R$ When at each length scale L' the largest vertical excursion possible occurs $U' \sim L'$ (Eq. 4.1), $(U')^2 L' \sim (L')^3$, i.e. k^{-3} energy spectrum. Under buoyancy dominated conditions $L_t \sim L'$ (Stillinger et al (1983), Rohr et al (1985)). Therefore $\rho' \sim L'$, $(\rho')^2 L' \sim (L')^3$, i.e. k^{-3} spectrum of density fluctuations.
2	Turbulence regime, $C_1 L_R > L > C_2 L_k$. Turbulent energy is dissipated at scales of the order L_k. Therefore, at scales larger than L_k, $U \sim \varepsilon^{1/3} L^{1/3}$ (Eq. 4.5), $U^2 L \sim L^{5/3}$, i.e. $k^{-5/3}$ turbulent energy spectrum
3	Small scale wave-like motions and internal wave regime, $L' < C_2 L_k$. Considerations which are given for item 1 of this table apply.

4.2 Experimental data

Dickey and Mellor (1980) and Stillinger et al (1983) conducted experiments on decaying grid-generated turbulence in homogeneous and stratified unsheared fluids. Stillinger et al measured all relevant turbulence properties, including turbulent stress, turbulent transport of mass, spectral distribution of turbulent energy and dissipation rate. The measurements of Dickey and Mellor were restricted to turbulent velocity fluctuations. Therefore turbulence modelling is required to derive the scales L_R and L_k from their experiments.

For grid-generated unsheared turbulence, decaying in a homogeneous fluid (Tennekes and Lumley, 1972, pp. 70-73)

$$U^2 \sim x^{-1} \qquad L \sim x^{\frac{1}{2}} \qquad \varepsilon \sim x^{-2} \tag{4.9}$$

where x: distance from grid

Hence, with constant N and ν

$$\frac{L}{L_R} \sim x^{3/2} \qquad \frac{L_R}{L_k} \sim x^{-3/2} \qquad \frac{L}{L_k} \sim \text{constant} \tag{4.10}$$

From the measurements of Stillinger et al (1983) $C_1 = 1.4$, $C_2 = 15,4$ and $C_1^{-1}C_2 = 11$. The constant C_1 is determined from measuring the ratio L/L_R at the estimated distance x, where the growth of L first falls from the curve describing its growth under homogeneous conditions. The constant C_2 is determined from measuring the ratio L_R/L_k at the estimated distance x, where $\overline{w'\rho'}$ first goes to zero. Stillinger et al find the energy spectra for stratified and homogeneous fluid to coincide only in the range of scales satisfying $1.4\ L_R < L < 15.4\ L_k$ (see Fig. 4.1).

Itsweire et al (1986) re-examined the data of Stillinger et al. From their analysis $C_1 = 1.7$, $C_2 = 13\text{-}17$ and $C_1^{-1}C_2 = 8\text{-}10$.

In their stratified experiments on decaying grid-generated turbulence, Dickey and Mellor (1980) found a transition in the energy decay rate. Up to some distance x, the decay rate was in accordance with Eq. 4.9. Beyond this distance it was slowed down and oscillated with time. Dickey and Mellor characterize the transition in the energy decay rate as a transition from a turbulence regime to a coherent internal wave regime. Analyzing the experimental results of Dickey and Mellor, Stillinger et al (1983) indicate that at the transition $1.4\ L_R = L = 15.4\ L_k$ ($C_1^{-1}C_2 = 11$). This implies that all overturning motions have ceased to exist due to the combined effect of buoyancy and viscosity, and only wave-like motions and internal waves remain.

Field measurements on the decay of unsheared turbulence in a stratified fluid have been taken by Gargett et al (1984). They took measurements in Knight Inlet behind the front of an internal wave train generated at a sill. They found the turbulence to decay with increasing distance from the area of generation under the influence of a stable background stratification. In the experiments $L_R L_k^{-1}$ ranged from 4000 to 50. These values are too large to derive information on C_2 from the experimental results.

The turbulent energy spectra presented by Gargett et al coincide with the normalized ones, related to isotropic turbulence, for 0,1 $L_R > L > 10\ L_k$. Only for $L_R L_k^{-1}$ values of 100 and less turbulent fluctuations of velocity in the horizontal direction were found to be larger than those of velocity in the vertical direction. For $L_R > L > 0.1\ L_R$, and relatively small values of $L_R L_k^{-1}$, Gargett et al found a k^{-1} range in the one-dimensional energy spectrum for the vertical velocity components.

Gargett et al (their tables 1 and 3) give measured values of ε, N and the three turbulent velocity component variances of Eq. 4.5. Substituting this information into Eqs. 4.5 and 4.6 gives $C_1 \approx 1$.

Rohr et al (1985) extended the unsheared grid-generated turbulence study reported in Stillinger et al(1983) to a stratified shear flow. Measurements taken close to the grid are in both cases characterized by decaying grid-generated turbulence. Only farther from the grid, and when the gradient Richardson number, Ri, is small enough to allow turbulent growth (see Section 4.3) do the features of the sheared flow distinctively depart from decaying unsheared grid-generated turbulence. It appeared that for large enough Ri-number (larger than 0.2) the shear may only marginally influence the developing flow.

For the two decaying shear cases studied, where Ri ≈ 0,36, Rohr et al (1985) found $C_1 \approx 2.2$ and $C_2 \approx 17.6$, $C_1^{-1} C_2 \approx 8$, using the same procedure as Stellinger et al (1983).

4.3 Limiting conditions based on Richardson number

4.3.1 Shear flow; turbulence in local equilibrium

For a stable stratification, neglecting the effect of diffusive transport, the turbulent energy balance can be written as

$$\frac{dk}{dt} = \overline{u'w'} \frac{\partial \bar{u}}{\partial z} - \frac{g}{\rho} \overline{w'\rho'} - \varepsilon \qquad (4.11)$$

with

$$k = \tfrac{1}{2} \left(\overline{u'^2} + \overline{v'^2} + \overline{w'^2}\right) \tag{4.12}$$

where k: turbulent kinetic energy

t: time

Coefficients for turbulent exchange of momentum and mass are defined as:

$$\overline{u'w'} = \nu_t \frac{\partial \bar{u}}{\partial z} \qquad \overline{w'\rho'} = - K_t \frac{\partial \bar{\rho}}{\partial z} \tag{4.13}$$

where ν_t : eddy viscosity

K_t : eddy diffusivity

For turbulence in conditions of local equilibrium (dk/dt = 0 and no diffusive transport in Eq. 4.11) Eqs 4.11 and 4.13 imply

$$\varepsilon = \nu_t \left(\frac{\partial \bar{u}}{\partial z}\right)^2 \left(1 - \frac{Ri}{\sigma_t}\right) \qquad Ri = - \frac{g}{\bar{\rho}} \frac{\partial \bar{\rho}/\partial z}{(\partial \bar{u}/\partial z)^2} \tag{4.14}$$

where Ri: gradient Richardson number, defined by Eq 4.14

σ_t: turbulent Prandtl number, $\sigma_t = \nu_t K_t^{-1}$

The gradient Richardson number is a measure of the relative importance of the stabilizing buoyancy and destabilizing shear.

Eq 4.14 leads to the existence criterion of turbulence (see e.g. Monin, 1959)

$$Ri < Ri_{cr} = \sigma_t \tag{4.15}$$

Of more direct physical significance is the flux Richardson number Rf, defined as the ratio of the rate of removal of turbulent energy by buoyancy forces to its production by shear. For turbulence in conditions of local equilibrium Rf represents the mixing efficiency, i.e the efficiency of the conversion from kinetic turbulent energy to potential energy. For local equilibrium, in terms of Rf the limiting conditions can be expressed as

$$Rf = \frac{g\,\overline{\rho' w'}}{\bar{\rho}\,\overline{u'w'}\,\frac{\partial \bar{u}}{\partial z}} = \frac{Ri}{\sigma_t} < Rf_{cr} \qquad (4.16)$$

where Rf: flux Richardson number, defined by Eq 4.16.

For turbulence ($\varepsilon \neq 0$) in conditions of local equilibrium $Rf_{cr} < 1$, since for these conditions

$$Rf = 1 - \frac{\varepsilon}{\overline{u'w'}\,\frac{\partial \bar{u}}{\partial z}} \qquad (4.17)$$

In accordance with Table 4.1 internal wavelike motions occur when $L \geq C_1 L_R$. Under these circumstances Rf=o. Therefore, deriving the value of C_1 from the experiments listed in Section 4.2, the conditions with internal wavelike motion are characterized by

$$L \geq (1 \text{ to } 2)\, L_R \qquad Rf=o \qquad (4.18)$$

Further

$$L^2 = \overline{u'w'}\,(\frac{\partial \bar{u}}{\partial z})^{-2} \qquad (4.19)$$

Substituting Eqs. 4.3, 4.6, 4.17 and 4.19 into Eq 4.18 gives

$$Ri \geq 1 \text{ to } 2.5 \qquad (4.20)$$

Hence, internal wavelike motions occur when the conditions represented by Eq 4.20 are satisfied. This finding is compatible with experimental observations by Kondo et al (1978), Komori et al (1983, p.20) and West et al (1986, p. 175).

4.3.2 Equilibrium Richardson number for internal mixing

Turner (1973, Sections 10.2.1 and 10.2.2, and 1981, Section 8.4.1) introduces a critical equilibrium Richardson number Ri_e^* of the order 0.1 which applies to conditions as found in the stabilizing intermediate layer of an arrested salt wedge, with Ri^* defined by Eq 2.1. This equilibrium Richardson number applies to a deep region of stable fluid, having linear profiles of both density and velocity through it, when there in a constant momentum flux and buoyancy flux through the region, sustained by small scale turbulent motions. The above conditions imply that there is also a constant rate of turbulent energy supply through the region. A further contition is that only internal length scales (e.g. L_R) are relevant, not external length scales (e.g. overall depth or distance from the boundaries).

Turbulence can be maintained in the above equilibrium state only when the rate of turbulent energy supply exactly matches the internally regulated gradients ($Ri^* = Ri_e^*$). For a given fixed energy supply, if $Ri^* < Ri_e^*$, the shear will dominate and mixing reduces the density gradient. Since σ_t is a weak function of Ri for $Ri < 0.1$ (Fig. 6.7) and the supply of turbulent energy is fixed, the reduction of the density gradient is associated with a reduction of the mixing efficiency Rf. When $Ri^* > Ri_e^*$ the density gradient is the dominant factor and turbulence is suppressed. This is also associated with a reduction of the mixing efficiency Rf. Consequently Rf has a maximum value for $Ri^* = Ri_e^*$. This is illustrated by Fig. 4.2, which is derived form Turner (1981).

Fig 4.3 shows a comparison of Rf versus Ri^* given by Linden (1979) on the basis of various experiments, in which external length scales are irrelevant. Fig. 4.3 confirmes that Ri_e^* is of the order 0.1.

$Ri_e^* = 0.1$ is smaller than $Ri_L^* = 0.32$ (Eq 2.5) This explains the relaminarization referred to in Section 2.2 (see Fig 4.2).

Rohr et al (1984) performed measurements on grid-generated turbulence like the ones made by Stellinger et al (1983) (Section 4.2). For both sets of measurements, made for conditions in which external length scales are irrelevant,

they found a relationship between Rf and Ri^*, which agrees with the one given by Linden (1978). The absolute numerical agreement is somewhat fortuitous, however, as Rohr et al used a rather arbitrary definition of Ri^*. Rohr et al found a peak Rf value of 20%, ie a peak value of the same order as given by Linden (Fig 4.3). Rohr et al argue that is the experiments which they analyzed this peak value occurs when the overturning eddies have the largest size allowed by buoyancy.

According to McEwan (1983) for large Ri^*-values mixing events are infrequent and limited in volume. Therefore, while molecular diffusivity may be insignificant in the mixing events themselves, averaged over the whole volume of the layer with linear profiles of density and velocity the dissipation rate ε may include a large component of laminar viscous dissipation which contributes nothing to the vertical mixing. On this basis, McEwan relates the mixing efficiency to the dissipation in the mixing events only. Doing so, he relates the mixing efficiency only to a fraction of ε. Because of Eq. 4.17, this means that he finds higher mixing efficiencies than given by Linden (1979). Making the above distinction in the analysis of measurments which he performed, McEwan found a mixing efficiency of the order 0.26 (based on the energy dissipation in the mixing events themselves) which in first approximation is independent of Ri^* for $Ri^* \leq 0.4$, the range of Ri^*-values covered in the experiments.

The above limiting Rf values apply for conditions of local equilibrium, i.e when the effect of diffusive transport and variations with time may be neglected in the turbulent energy balance (Eq 4.11). For $E^* > 0.5$, Gartrell (1980) found experimentally that Rf_{cr} becomes larger with increasing values of the parameter E^*, defined by the relationship

$$E^* = \frac{\overline{\frac{\partial w'k'}{\partial z}}}{\overline{u'w'}\,\frac{\partial \bar{u}}{\partial z}} \qquad (4.21)$$

where E^* : dimensionless ratio, defined by Eq 4.21.

The increase of Rf is apparently due to the fact that in Gartrell's experiments part of the mixing is induced by the turbulent transport of turbulent energy, when $E^* > 0.5$.

4.4 Summary

This chapter gives the effect of stable density stratification on turbulence. It does so in terms of the Ozmidov length scale of turbulence, L_R and the Kolmogorov length scale of turbulence, L_k (Tables 4.1 and 4.2). Overturning turbulent motions cannot be maintained and internal wavelike motions result when the length scale of the largest overturning motions exceeds the Ozmidov length scale. This was shown to be equivalent to the gradient Richardson number, Ri, being in the order 1 to 2.5. Overturning turbulent motions cease to exist because of the combined effect of buoyancy and viscosity when the parameter $L_R\ L_k^{-1}$ is smaller than the dimensionless parameter $C_1^{-1}\ C_2$. From experiments $C_1^{-1}\ C_2$ was found to be of the order ten.

The effect of density stratification on turbulence can be related to the gradient Richardson number, Ri, provided that the local production of turbulence energy is an important factor in the turbulent energy balance. If not, the effect of stratification on turbulence has to be related to the parameter E^*, defined by Eq 4.21. This means that different dimensionsless parameters have to be used to describe the effect of a stable stratification for the ebb tide and flood tide regime of turbulence, distinguished at the end of section 1.2.

5 On turbulence modelling

5.1 Introduction

This chapter lists the main characteristics of some turbulence models. This information is used in the following chapter to show the implications of including the effect of stratification in turbulence modelling.

Various reviews on turbulence modelling are available in the literature (Mellor and Yamada (1974), Reynolds (1976), Saffman (1977), Rodi (1980)). Reviews including applications to stratified flows are given by Mellor and Yamada (1982) and Rodi (1985). Among the most advanced applications in three-dimensional salinity intrusion modelling is the application of the algebraic stress/flux relations by Oey et al (1985) in their study of the salinity intrusion in the Hudson-Raritan Estuary.

In turbulence modelling the following distinction is being made:

(1) Zero-equation models : models using only partial differential equations (pde's) for the mean velocity and mean concentration field, and no turbulence pde's; in stead they use empirical expressions for mixing length, eddy viscosity and eddy diffusivity
(2) One-equation models : models involving an additional pde relating to the turbulent velocity scale
(3) Two-equation models : models involving additional pde's relating the turbulent velocity scale and the length scale of turbulence
(4) Stress-equation models : models involving pde's for all components of the turbulence stress tensor, and
(5) Large-eddy simulations : computations of the three-dimensional time-dependent large-eddy structure and a low-level model for the small-scale turbulence.

Large-eddy simulations are serving mainly to help assess the lower level models. For this reason large-eddy simulations are not discussed further in this review.

The applications to stratified flows listed by Mellor and Yamada (1982) and Rodi (1985) primarily deal with two-equation models and algebraic stress-equation models.

5.2 Zero-equation models

Zero-equation mdels are essentially based on equations like Eq 4.13. According to Boussinesq's eddy viscosity concept, the eddy viscosity ν_t is treated as a scalar quantity, though, from theoretical arguments (Hinze , 1975, pp 23-25) it may be concluded that the eddy viscosity is a tensor of second or higher order. This is not too important, however, for two-dimensional salinity intrusion modelling (one dimension being the vertical one), as in this type of modelling it is sufficient to reproduce the vertical turbulent transport of momentum and mass.

5.3 One-equation models

In addition to Eq 4.13, the one-equation models are based on the equations

$$\nu_t = c_\mu k^{\frac{1}{2}} L \qquad K_t = \sigma_t^{-1} \nu_t \tag{5.1}$$

and

$$\varepsilon = C_D k^{3/2} L^{-1} \tag{5.2}$$

where ν_t : eddy viscosity
K_t : eddy difusivity
σ_t : turbulent Prandtl number
k : turbulent kinetic energy
ε : dissipation rate of turbulent energy per unit mass of fluid
L : length scale of turbulence
c_μ, C_D : modelling constants.

Eqs. 5.1 and 5.2 express ν_t, K_t and ε in k and L. Hence, the turbulent transport of momentum and mass can be derived from the conservation equation of turbulent kinetic energy, which contains k and ε, and from a specification of the variation of L in the considered flow.

In its complete form, in addition to the turbulent transport of momentum and mass (double correlations between turbulent fluctuations), the conservation

equation for turbulent energy contains triple correlations between turbulent fluctuations (see e.g. Rodi (1980), Eq. 2.34). Hence, when applying the above procedure, the triple correlations contained in the conservation equation for turbulent energy must be modelled, i.e. expressed in the double correlations. For the modelling procedures involved, the reader is referred to the literature on the subject (e.g. Rodi (1980), Section 2.5).

5.4 Two-equation models

Combining Eqs. 5.1 and 5.2 gives

$$\nu_t = c_\mu k^2 \varepsilon^{-1} \qquad K_t = \sigma_t^{-1} \nu_t \tag{5.3}$$

Eq. 5.3 expresses ν_t and K_t in k and ε. Hence the turbulent transports of momentum and mass can be derived from the conservation equation for turbulent energy, k, and the conservation equation for dissipation, ε, provided that the triple correlations contained in these transport equations are modelled (see e.g. Rodi (1980), Section 2.6).

The conservation equation for dissipation may be looked upon as a pde for the length scale of turbulence. Other versions of this pde are given by e.g. Mellor and Yamada (1982).

5.5 Stress-equation models

Solving the conservation equations for the stress-tensor $\overline{u_i' u_j'}$ and for the mass flux vector $\overline{u_i' \rho'}$ should be the correct way to get around the limitations of the eddy viscosity concept, underlying the models mentioned in the preceeding sections. But owing to the occurrence of higher-order correlations in these transport equations modelling assumptions concerning these higher-order correlations are to be introduced.

Rodi (1985) concludes that stress-equation models involve quite a large number of differential equations, the solution of which is not a trivial task and may also be expensive. He further observes that at present stress-equation models have their largest practical significance as starting point for the develop-

ment of two-equation models using non-isotropic algebraic stress/flux relations (see also Rodi (1980), Section 2.7).

5.6 Two-equation models using algebraic stress/flux relations

The conservation equation for turbulent energy may be written as

$$\frac{\partial k}{\partial t} + \bar{u}_i \frac{\partial k}{\partial x_i} - \text{Diff}(k) = P + G - \varepsilon \qquad (5.4)$$

where P : production by turbulent shear
G : buoyant destruction
Diff(k) : diffusive transport terms

The transport equations for the stress-tensor are of the type (Rodi (1980), Section 2.7.c)

$$\frac{\partial \overline{u_i'u_j'}}{\partial t} + \bar{u}_i \frac{\partial \overline{u_i'u_j'}}{\partial x_i} - \text{Diff}(\overline{u_i'u_j'}) = F(u_i'u_j', \quad) \qquad (5.5)$$

where

$F(u_i'u_j', \quad)$: functional relationship between $\overline{u_i'u_j'}$ and other second-order correlations.

The critical assumption in the derivation of the algebraic stress/flux relations is the assumption

$$\frac{\partial \overline{u'_i u'_j}}{\partial t} + \bar{u}_i \frac{\partial \overline{u'_i u'_j}}{\partial x_i} - \text{Diff}(\overline{u'_i u'_j}) = \frac{\overline{u'_i u'_j}}{k}\left[\frac{\partial k}{\partial t} + \bar{u}_i \frac{\partial k}{\partial x_i} - \text{Diff}(k)\right] \qquad (5.6)$$

which implies that the temporal and spatial change of $\overline{u_i'u_j'}/k$ is small compared with the change of $\overline{u_i'u_j'}$ itself (Rodi, 1976).

When the assumption of Eq. 5.6 is satisfied, substituting Eqs. 5.4 and 5.6 into Eq. 5.5 allows the latter differential equation to be reduced to an algebraic equation, as the substitution yields

$$\frac{\overline{u_i'u_j'}}{k}(P+G-\varepsilon) = F(\overline{u_i'u_j'}, \quad) \qquad (5.7)$$

The parameters k, ε, P and G can be derived from two-equation turbulence models. Therefore, Eq. 5.7 is reduced to an algebraic equation when the higher-order correlations contained in the functional relationship F are modelled as is done in the stress-equation models. Reducing differential equations to algebraic functions of k and ε is the strength of the above prodedure. This is elaborated upon further in the following chapter.

6 Effect of stable stratification on length scales of turbulence

6.1 Effect of geometry and stratification on length scales of turbulence

In homogeneous, unstratified tidal flows the length scale L of the large energy containing eddies is limited to a length L_n which is controlled by the external boundaries (e.g. bed and free surface). This length scale will be referred to as the length scale for neutral conditions.

Stratified flows may exhibit interfacial zones with vertical density gradients, which are substantially larger than elsewhere over the depth. For the time being the interfacial zones are assumed to be sufficiently pronounced to act as internal boundaries. The additional assumption is made that outside the interfacial zones the stratification is sufficiently weak to have no effect on the development of turbulence. Then the length scale L is limited to a length L_m, which is controlled by both external and internal boundaries. This length scale will be referred to as the master length scale for stratified conditions, a terminology derived from Mellor and Yamada (1982).

Generally speaking

$$L_m \leq L_n \tag{6.1}$$

where L_n: length scale of large energy containing eddies for neutral conditions, controlled by external boundaries only

L_m: master length scale for stratified conditions, controlled by both external and internal boundaries, assuming density stratification outside interfacial zones to have no effect on development of turbulence.

Whether or not a master length scale L_m can be distinguished depends on the vertical density gradients outside the interfacial zones.

The Ozmidov length scale L_R (Eq 4.6) is expressed in local parameters (ε and N). Hence, at a local level the Ozmidov scale defines the upper limit

permissible for the size of overturning turbulent motions. Therfore,

$$L = L_m \quad \text{if} \quad L_R >> L_m \qquad\qquad L = C_1 L_R \quad \text{if} \quad L_R << L_m \tag{6.2}$$

where L_R: Ozmidov scale defined by Eq 4.6.

C_1: dimensionless parameter, defined in Table 1.

Further assuming a faired transition between the asymptotic values given by Eq 6.2 (Kranenburg, 1985)

$$\frac{L}{L_m} = f_1\left(\frac{L_R}{L_m}\right) \qquad L = L_m \text{ for } L_R \to \infty \tag{6.3}$$

$$L = C_1 L_R \text{ for } L_R \to 0$$

where f_1: functional relationship, defined by Eq 6.3, represented in Fig 6.1.

From dimensional arguments

$$\nu_t = c_\nu k^{1/2} L \qquad K_t = \frac{c_\nu}{\sigma_t} k^{1/2} L \qquad \varepsilon = C_D \frac{k^{3/2}}{L} \tag{6.4}$$

where ν_t : eddy viscosity

K_t : eddy diffusivity

k : turbulent energy (Eq 4.12)

σ_t : turbulent Prandtl number, $\sigma_t = \nu_t K_t^{-1}$

ε: rate of dissipation of turbulent energy per unit mass of fluid

c_ν, C_D : modelling constants.

For local equilibrium ($dk/dt = 0$ and no diffusive transport in Eq 4.11), substituting Eqs 4.13, 4.14 and 6.4 into the turbulent energy balance (Eq 4.11) gives.

$$\left(\frac{1}{Ri} - \frac{1}{\sigma_t}\right) \frac{g}{\rho} \frac{\partial \bar{\rho}}{\partial z} = \frac{C_D}{c_\nu} \frac{k}{L^2} \tag{6.5}$$

Eqs 4.6, 6.4 and 6.5 into Eq 6.3 gives

$$\frac{L}{L_m} = f_1 \left[C_D^{\frac{1}{2}} \frac{L}{L_m} \left\{ \left(\frac{1}{Ri} - \frac{1}{\sigma_t} \right) \right\}^{3/4} \right] \qquad (6.6)$$

where Ri: gradient Richardson number, defined by Eq 4.14.

Appendix A elaborates upon the significance of the above findings for the Rotterdam Waterway Estuary.

In turbulent motions collisions occur between lumps of fluid. The collisions will influence the momentum of the lumps involved immediately, while the lumps of fluid may retain their identity, e.g. their density. If the lumps are temporarily in a surrounding of different density, buoyancy forces tend to bring them back to their original equilibrium level. The time needed for buoyancy to do so may be small in comparison with the time needed for the lumps to exchange their density with the fluid they are temporarily surrounded by. This means that with increasing stratification vertical exchange of momentum becomes a more efficient process than vertical exchange of mass. Therefore, and because of Eq 6.6

$$\sigma_t = \frac{\nu_t}{K_t} = f\,(Ri) \qquad \frac{L}{L_m} = f\,(Ri) \qquad (6.7)$$

Turner (1973, pp, 149-150) argues that the functional relationship between σ_t an Ri is due not to the suppression of the velocity and density fluctuations themselves, but to a reduction of the mean product $\overline{w'\rho'}$. In the limit of pure internal wave motion, ρ' and w' are 90° out of phase, so this correlation tends to zero. This occurs for Ri-values given by Eq 4.20.

Turbulence models need the master length scale and the functional relationships of Eq 6.7 as input, unless they are capable to produce this information as output.

The following section relates the above input to the damping functions used in zero-equation and one-equation turbulence models. How this input can be provided by higher-order turbulence models is the subject of Section 6.3, in particular Section 6.3.2.

6.2 Zero-equation and one-equation turbulence models

6.2.1 Damping functions to express effect of stratification on scale of turbulence

Because of the considerations of the preceding section, damping functions have to be introduced in all turbulence models which relate the eddy viscosity and the eddy diffusivity with the length scale L.

Applying Prandtl's mixing length hypothesis to stratified flows, it is necessary to include the effect of stratification, both acting as an additional internal boundary and at local level. As an internal boundary it is included by the parameter $L_m L_n^{-1}$, at local level by damping functions F_0 and G_0, i.e.

$$\nu_t = L_n^2 \left(\frac{L_m}{L_n}\right)^2 \left|\frac{\partial \bar{u}}{\partial z}\right| F_0(Ri) \qquad K_t = L_n^2 \left(\frac{L_m}{L_n}\right)^2 \left|\frac{\partial \bar{u}}{\partial z}\right| G_0(Ri) \tag{6.8}$$

where u : velocity in horizontal main flow direction

z : vertical coordinate, positive when directed upwards

$F_0(Ri)$, $G_0(Ri)$: damping functions, defined by Eq 6.8

Except for very pronounced interfacial zones, the distinction between what effect of stratification to include in either the damping functions or in the parameter $L_m L_n^{-1}$ is an arbitrary one. This is an item which is elaborated upon in Section 6.2.2.

Substituting Eq 6.5 into Eq into Eq 6.4 gives

$$\nu_t = c_\nu L^2 \left[\frac{c_\nu}{C_D}\left(1 - \frac{Ri}{\sigma_t}\right)\right]^{\frac{1}{2}} \left|\frac{\partial \bar{u}}{\partial z}\right| \tag{6.9}$$

For homogeneous flow Ri = 0 and $L = L_n$. Therefore, Eq 6.9 gives $C_D = c_\nu^3$, and from Eqs 6.8 and 6.9

$$F_0(Ri) = \left(\frac{L}{L_m}\right)^2 \left(1 - \frac{Ri}{\sigma_t}\right)^{1/2} \qquad G_0(Ri) = \sigma_t^{-1} \left(\frac{L}{L_m}\right)^2 \left(1 - \frac{Ri}{\sigma_t}\right)^{1/2} \qquad (6.10)$$

Hence in order to determine the damping functions the information of Eq 6.7 must be provided as input.

For the one-equation model, which is based on Eq 6.4, the above procedure gives

$$\nu_t = c_\nu k^{1/2} L_n \frac{L_m}{L_n} F_1(Ri) \qquad K_t = \frac{c_\nu}{\sigma_t} k^{1/2} L_n \frac{L_m}{L_n} F_1(Ri) \qquad (6.11)$$

with

$$F_1(Ri) = \frac{L}{L_m} \qquad (6.12)$$

where F_1 (Ri): damping function, defined by Eq 6.11.

Applying the k-L turbulence model to stratified flows the damping function F_1, which is equal to $L\ L_m^{-1}$, and the parameter σ_t have to be specified as functions of Ri.

Hence, determining the damping functions of this model also requires the information of Eq 6.7 as input.

6.2.2 Limitations of damping functions

Introducing the damping functions distinction has been made between the effect of stratification acting as an internal boundary (incorporated in the length scale L_m) and that at local level (incorporated in the damping functions). This distinction seems to some extent an arbitrary one, since the scale of turbulence is such that any eddy covers a considerable height range. Therefore it is by no means obvious that there should be a simple dependence of F_0, G_0 and F_1 on a strictly local parameter as the gradient Richardson number, Ri

(Ellison and Turner, 1960). Therefore, for steady flow Delvigne (1986) relates the damping not to the local stratification, pertaining at the considered location, but to the stratification of a more extended area around it. For the same reason for estuarine tidal flows, throughout the depth, Odd and Rodger (1978) relate the damping functions with the magnitude and relative depth of the local peak Ri value. They do so unless the local Ri values increase continuously from the bed upwards. Only in the latter case, throughout the depth they relate the damping functions with the local Ri values.

In line with the above observations, from a conceptual point of view Mellor and Yamada (1982) deem it incorrect in turbulence modelling to use an equation which describes the small-scale (local) turbulence to determine the master length scale. This they observe in connection with the dissipation transport equations of the k-ε model.

In tidal estuaries the bed shear stress is proportional with the velocity squared. Therefore it is about zero at tidal slack. By then, in partly mixed estuaries the local shear stress is primarily influenced by longitudinal density gradients, and this influence remains large compared to that of the bed shear during a significant part of the tidal cycle (Abraham, 1980). For this part of the tidal cycle $L_m L_n^{-1} \neq 1$, and L_m has to be specified when applying Eqs 6.10 - 6.12. This information on L_m cannot be derived from measurements made in steady atmospheric or laboratory flows, since in these flows longitudinal density gradients tend to be small. These arguments are elaborated upon in appendix B.

For homogeneous tidal flows, neglecting the convective accelerations while subtracting the depth averaged equation of motion from that pertaining at a local level gives

$$\frac{\tau}{\rho} = \int_0^z \frac{\partial (\bar{u} - \bar{\bar{u}})}{\partial t} dz + \frac{1}{\rho} (1 - \frac{z}{h}) \tau_b \qquad (6.13)$$

where τ : turbulent shear stress (positive when decelerating fluid above flowing in positive direction)

τ_b: bottom shear stress

z : vertical coordinate, positive when directed upward, z = 0 corresponds to bottom

h : water depth

$\bar{\bar{u}}$: depth averaged value of $\bar{u}$

For $\tau_b > 0$ and accelerating flow ($\partial\bar{\bar{u}}/\partial t > 0$), the integral of Eq 6.13 is negative for any z, while for decelerating flow it is positive. Further, in homogeneous flow

$$\tau = \bar{\rho} L_n^2 \left(\frac{\partial \bar{u}}{\partial z}\right)^2 \qquad (6.14)$$

Therefore, $\bar{\bar{u}}$ being equal, in accelerating homogeneous flow production of turbulent energy, $\tau\, \partial\bar{u}/\partial z$, tends to be smaller than it is in steady flow, while in decelerating flow it tends to be larger. This has the effect of an hysteresis in the mean flow-turbulence system (Gordon (1975), Mc Lean (1983), Lavelle and Mofjeld (1983)).

The above effect is the most pronounced when $\partial\bar{\bar{u}}/\partial t$ is large compared with $(\tau_b/\bar{\rho})h^{-1}$, i.e. at tidal slack. Therefore, damping functions to be applied at slack tide cannot be derived from steady flow experiments.

Appendix C gives the ratio of the terms at the right hand side of Eq 6.13 for Rotterdan Waterway conditions.

The damping functions (Eqs 6.10 and 6.12) apply for conditions of local equilibrium, i.e. when the effect of diffusive transport and variations with time may be neglected in the turbulent energy balance. It may be expected that these conditons are not satisfied where during the flood tide $\partial\bar{u}/\partial z = 0$. (Fig 2.3). By then it may be expected that the damping functions depend on the parameter E^* (Eq. 4.21), because of the arguments given in Section 4.3 when introducing this parameter.

For stratified tidal flow the above considerations imply that the damping functions vary through the tidal cycle. At slack tide they are to be related to $\partial\bar{\bar{u}}/\partial t$ and L_m with $L_m \neq L_n$, and on the flood tide to E^*.

6.3 Two-equation turbulence models

6.3.1 k-ε model

The necessity to use damping functions does not arise in turbulence models which relate the eddy viscosity and eddy diffusivity to local parameters. For instance, in the k-ε model (Section 5.4)

$$\nu_t = c_\mu \frac{k^2}{\varepsilon} \qquad k_t = \frac{c_\mu}{\sigma_t} \frac{k^2}{\varepsilon} \tag{6.15}$$

For local equilibrium the turbulent energy balance satisfies Eq 4.14. Substituting Eqs 4.13 and 6.15 into Eq 4.14 gives

$$c_\mu = \frac{\overline{u'w'}^2}{k^2} \left[1 - \frac{Ri}{\sigma_t}\right] \tag{6.16}$$

Vertical motions are damped by density stratification. Therefore the ratio $\overline{u'w'}\ k^{-1}$ decreases with increasing Ri. The mixing efficiency $Rf = Ri\ \sigma_t^{-1}$. Hence, from Fig. 4.2 it follows that the term between brackets of Eq 6.16 decreases with increasing Ri for $Ri < Ri_e^*$, while it increases with increasing Ri for $Ri > Ri_e^*$.

Applying the k-ε model to stratified flows, the model constant c_μ and the parameter σ_t have to be specified as functions of Ri. It is not necessary, however, to specify the parameter $L_m\ L_n^{-1}$, as the model uses a partial differential equation related to the turbulence length scale to determine L. This differential equation in itself, however, is a critical issue in turbulence modelling (Mellor and Yamada, 1982).

6.3.2 Algebraic stress/flux relations

For stratified flow under conditions of local equilibrium the procedure of Section 5.6 gives σ_t, $\overline{u'w'}\ k^{-1}$ and c_μ (Eq 6.16) as a function of the flux

Richardson number, i.e. the ratio of the terms P and G contained in Eq 5.7. As $Rf = \sigma_t^{-1} Ri$, these functions can also be expressed in Ri. Using this method distinction has to be made between the surface layer, close to the boundary, and free shear flow, further from the boundary. This is elaborated upon further in Section 6.4.

For stratified free shear flow under conditions of local equilibrium Launder (1975) applied the above method. He used experiments of Webster (1964) to determine the value of model constants. In this way he derived

$$\sigma_t \sigma_{t0}^{-1} = \frac{1 - 2.07\ Rf}{1 - 2.91\ Rf} \tag{6.17}$$

where Rf: flux Richardson number, defined by Eq 4.26

index 0: index referring to neutral conditions ($\partial\rho/\partial z = 0$)

In the experiments of Webster $Rf_c = 2.91^{-1}$. On this basis Smith and Takhar (1979) generalized Eq 6.17 to obtain the expression (see also Smith and Takhar, 1981)

$$\sigma_t \sigma_{t0}^{-1} = \frac{1 - 2\ Rf}{1 - Rf\ Rf_c^{-1}} \tag{6.18}$$

where Rf_c: maximum (critical) Rf value, i.e maximum mixing efficiency.

Ellison (1957) derived an expression for σ_t from the conservation equation for turbulent energy and approximate equations for the turbulent fluctuations of mass and the turbulent transport of mass (see also Turner, 1973, Section 5.2.3). Under the closure assumptions adopted, Ellison obtained the expression

$$\sigma_t \sigma_{t0}^{-1} = \frac{(1 - Rf)^2}{1 - Rf\ Rf_c^{-1}} \tag{6.19}$$

As $Rf < Rf_c \ll 1$, Eq 6.19 about coincides with Eq 6.18.

For the k-ε model the relationship between σ_t, c_μ and Ri can be derived from algebraic stress/flux relations. For instance, Goussebaile and Viollet (1982) introduced the relationship between these parameters, which can be derived from the above work of Launder (1975), into the standard k-ε model to determine the development of the intermediate layer in two-layer stratified flow.

The zero-equation and one-equation turbulence models require σ_t and L as input. The required information on L_m cannot be derived from algebraic stress/flux relations as such. It can be derived from two-equation turbulence models using algebraic stress/flux relations. However, these models contain a pde relating to the turbulence length scale, and therefore give L as a function of time and spatial coordinates, not as a function of Ri or other local parameters.

6.3.3 Turbulent Prandtl number for neutral conditions and critical flux Richardson number

In Eqs 6.18 and 6.19 the turbulent Prandtl number for neutral conditions, σ_{t0}, and the critical flux Richardson number Rf_c have to be specified. There is no unique information on these parameters in the literature.

From atmospheric boundary layer data Mellor and Yamada (1982) give $\sigma_{t0} = 0.74$. Businger et al (1971) $\sigma_{t0} = 0.77$, Pruitt et al (1973) $\sigma_{t0} = 0.88$ and Webb (1970) $\sigma_{t0} = 1.0$. From laboratory data, which are described further in Section 6.5, Mizushina et al (1978) derive $\sigma_{t0} = 0.83$.

On theoretical grounds Ellison (1957) proposes $Rf_c = 0.15$, which has been spupported experimentally in the laboratory (Ellison and Turner, 1960). From field data collected in the Great Ouse estuary during the ebb tide Odd and Rodger (1978) derive $Rf_c = 0.08$. From algebraic stress type turbulence models Arya (1972) derives $Rf_c = 0.12 - 0.25$, Yamada (1975) $Rf_c = 0.18 - 0.27$ and Launder (1975) $Rf_c = 0.31$, depending on the set of empirical model constants introduced into these models. From their laboratory experiments, Mizushina et al (1978) find $Rf_c = 0.07 - 0.20$ (Section 6.5.1, Fig 6.8).

6.4 Wall effect on turbulent pressure field

Turbulence parameters and the effect of stability thereon are significantly different for flows which are influenced by boundaries, and flows which are not. Gibson and Launder (1978) illustrate this effect in Table 6.1, which gives the variation of three dimensionless turbulence parameters under stable conditions. The two flows compared are the lower region of the atmospheric surface layer, close to the ground and a horizontal free shear flow in which a linear vertical profile of mean velocity and density has been established. The experimental data on the atmospheric surface layer are amongst others from Businger et al (1971). The entries for the free shear flow relate to the wind tunnel measurements of Webster (1964) and Young (1975). Both cases are close to local equilibrium. The behaviour summarized is basically and consistently different for the two situations.

Gibson and Launder (1978) relate the above difference with the wall effect on the fluctuating pressure field. That is, the pressure contributes to correlations which appear in the transport equations for Reynolds stress and mass flux, so that turbulent transport processes are affected not only by the stratification but also by the modification of the fluctuating pressure field by the presence of a wall. Gibson and Launder (1978) supported this explanation quantitatively by modelling the pressure-containing correlations which appear in the conservation equation for the Reynolds stress and mass flux. This modelling accounts for both gravitational effects and the fluctuating pressure field by the presence of a wall. The predicted changes were shown to agree with the differences listed in Table 6.1. The model by Gibson and Launder (1978) is an extention of the model by Launder (1975), referred to in Section 6.3.2. The latter model applies to the free shear flow.

In line with the above observations Ueda et al (1981) found the effect of buoyancy on turbulent transport processes in the lower atmosphere to vary with the level of the atmosphere observed. Measurements made in the surface layer, mainly within a few metres adjacent to the ground surface (Webb (1970), Oke (1970), Businger et al (1971) and Pruitt et al (1973)) show a weak dependence of the ratio K_t/K_{to}, where index o refers to neutral conditions, while measurements in the layer form 25 to 200 m (Deardorff, 1967, and Ueda et al, 1981) show a significant effect of increasing stability (Fig 5.2).

Table 6.1 Effects of stable stratification on atmospheric surface layer and free shear flow (after Gibson and Launder, 1978)

Turbulence parameter	Changes produced by increasing Rf from 0 to 0.2	
	Free shear flow	Atmospheric surface layer
$[\overline{w'w'}/\overline{u'u'}]^{1/2}$	decreases by about 30%	increases by about 20%
$\overline{w'\rho'}/\overline{u'\rho'}$	decreases by about 70%	increases rapidly by 50%, then levels out
σ_t^{-1}	decreases by about 50%	initially decreases by 10%, then rises slowly

The two-equation model of Mellor and Yamada (1982), is geared to wall boundary layers. It is this model which Oey et al (1985) apply to the Hudson-Raritan Estuary.

6.5 Experimental data

Presenting experimental data, for reasons given at the end of Section 6.2.2 distinction has to be made between steady flow and tidal flow.

6.5.1 Steady flow

Several studies on the effect of stratification on the development of turbulence in stratified open-channel flow give the dimensionless parameters $\nu_t \nu_{to}^{-1}$ and $K_t K_{to}^{-1}$ as a function of the local gradient Richardson number, Ri. These parameters may not be equated with the damping functions F_o and G_o, however, unless $L_m = L_n$ and stratification and longitudinal density gradients have little effect on $\partial\bar{u}/\partial z$ (Eq 5.8). The above conditions are not satisfied when stratification becomes of some significance. By then unique dependence on Ri occurs only for F_o, G_o and $\sigma_t = F_o G_o^{-1}$, not for $\nu_t \nu_{to}^{-1}$ and $K_t K_{to}^{-1}$.

Mizushina et al(1978), Ueda et al (1981) and Komori et al (1982 and 1983) describe different aspects of the same series of laboratory experiments. Together they present detailed experimental information on the turbulence structure in a stably stratified outer layer in steady open channel flow, under conditions of local equilibrium. This outer layer coincides with the layer of free shear flow distinguished by Gibson and Launder (1978) in Table 6.1. The experiments involved will be referred to as the Mizushina experiments.

Fig. 6.3 gives distributions of the velocity and temperature typical for the Mizushina experiments. In the experiments saturated steam was mildly condensed on the free surface in order to obtain stably stratified flow. This seems to explain the shape of the temperature distributions. For reasons explained in Section 6.4 and presumably because of the typical shape of the temperature distribution, the correlations given in the following text apply to that part of the outer layer where surface effects are neglible, i.e $0.4 < z/h < 0.75$ (Komori et al, 1982).

Measured phase-coherence relationships suggest that in strongly stable conditions ($Ri^* \approx 0.9$) background motion is a wavelike one. This is compatible with Eq. 4.20

For $0.4 < z/h < 0.75$, Fig 6.4 gives correlations of turbulence quantities with local Ri values. The differences with the measurements of Webster (1964) seem due to the fact that in the first position of these measurements there was an appreciable effect of the decaying turbulence of the shear generating grid (Rohr et al, 1985). The same seems to apply to the measurements of Young (1975).

Figs. 6.5, 6.6 and 6.7 give respectively $\nu_t \nu_{to}^{-1}$, $K_t K_{to}^{-1}$ and σ_t^{-1} as function of the local Ri-value. Fig 6.8 presents the information given in Fig 6.7 by comparing the local flux Richardson number with the local Ri-value.

According to Bloss (1985)the outer layer results of the Mizushina experiments may be described by the following emperical relationships, which are plotted in Figs 6.5, 6.6 and 6.7.

$$\nu_t \nu_{to}^{-1} = (1+ 3Ri)^{-1} \qquad K_t K_{to}^{-1} = (1 + 3Ri)^{-3} \qquad \sigma_t \sigma_{to}^{-1} = (1 + 3Ri)^{2} \tag{6.20}$$

Functional relationships of this type were proposed by Rossby and Montgomery (see Kent and Pritchard, 1959) based on the argument that the turbulent kinetic energy per unit mass of fluid for the neutral case should be equal to the sum of turbulent kinetic and potential energy per unit mass of fluid for the stable case.

For the Mizushina experiments $\sigma_{t.0} \approx 0.8$ and $Rf_c \approx 0.1$. (Fig 5.8 with Rf_c ranging from 0.07 to 0.2). The relationship which is obtained by substituting these parameter values into Eq 6.18 (derived by Launder, 1975) and Eq 6.19 (derived by Ellison, 1957) is plotted in Fig 6.7.This figure shows a satisfactory agreement between the above theoretical relationships and the Mizushina experiments. However, in accordance with Eq 4.16 $Rf = \sigma_t^{-1} Ri$. Hence, assuming $\sigma_t^{-1} = Ri^{-n}$, Rf increases with increasing Ri for $n < 1$. Fig 6.7 shows this to apply to Eqs 6.18 and 6.19 over the whole Ri-range of this figure. Hence according to the models of Ellison (1957) and Launder (1975) Rf increases with increasing Ri for Ri up to about 3. Nevertheless, the experiments of Fig 6.7 show a maximum Rf value for $Ri \approx 0.3$ (Fig 6.8).This may imply that the closure assumptions underlying both models may not be applied to the extreme of strong stability. This could well be true for the assumption behind Eq 5.6.

Fig 6.6 illustrates that the outer layer laboratory observations made in the Mizushina experiments coincide with observations made in the outer atmospheric layer by Ueda et al (1981).

Fig 6.9 gives a comparison of the results of the above experiments with those of other investigators. The differences with the measurements of Businger et al (1971) and Pruitt et al (1973) are due to the fact that these measurements were made in the surface layer (Fig 6.2). The explanation of the differences with the mearurements of Webster (1964) is even with Fig 6.4.

The presented experimental data relates to eddy viscosities and eddy diffusivities rather than to turbulence quantities. Information on the effect of

stratification on turbulence quantities is of interest for the development of turbulence models and to determine model constants. It can be derived from the Mizushina experiments (eq Komori et al, 1983) and from the experiments of Webster (1964) and Young (1975) (Fig 6.4). Further it can be obtained from the experiments referred to in Section 4.2, i.e. the experiments of Stillinger et al (1983) (Fig. 4.1), experiments using the same experimental installation (Rohr et al. 1985, Isweire et al 1986) and the field experiments of Gargett et al (1984).

Fig. 6.10, 6.11 and 6.12 give the results of the Mizushina experiments, compared with the experimental data collected in the previous literature survey (Breusers, 1974). The $\nu_t \nu_o^{-1}$ values about coincide (Fig 6.10). The Mizushina experiments tend to give lower $K_t K_{to}^{-1}$ and σ_t^{-1} values (Figs 6.11 and 6.12). For σ_t^{-1} the tendency is about the same as the one represented in Fig 6.9.

6.5.2 Tidal flow

For salinity intrusion into a partially mixed estuary Odd and Rodger (1978) present field data on damping funcions as observed at different instances of time on the ebb tide. Similar data are presented by Knight et al (1980). From their measurements Odd and Rodger derive an empirical expression for $L\ L_n^{-1}$. This parameter is given as a funciton of the local Ri-value, when Ri increases continuously from the bed upwards. If not, they relate $L\ L_n^{-1}$ with the magnitude and relative depth of the local peak Ri-value.

Further field data on the effect of stratification on damping functions are based on tidally averaged parameter values (e.g. Kent and Pritcard, 1959, Bowden and Gilligan,1971). Damping functions obtained from laboratory measurements made at different instances of time on the ebb tide are given by van Rees (1975).

The above data are not conclusive with respect to which damping functions to apply in salinity intrusions modelling using zero-equation or one-equation trubulence models. Nor do they indicate how to relate L_m to L_n at low water slack. (See Section 7.1).

Measurements on turbulence quantities and the effect of stratification thereon are scarce. A summary is given by West et al (1986), who further present the result of exploratory measurements on the subject made by them.

6.6 Final remark

The shear production of turbulent energy in the wall region is caused by organized structure motions which are intermittent random cyclic motions consisting of large eddy inrush into the region near the wall, and ejection of near-wall fluid mass. This is referred to as the bursting process and turbulent energy is mainly produced in these inrush and ejection phases. There is a substantial literature on the subject (e.g. Talmon et al, 1986) which justifies separate review. The effect of density stratification on the bursting process has been studied in the Mizushina experiments (Ogino et al, 1982) and 8 in the field measurements of West et al, 1986. Ogino et al conclude that the characteristics of the inrush and the ejection are well correlated with the local gradient Richardson number.

7 Summary and conclusions

7.1 On salinity intrusion modelling

A turbulence model, used for salinity intrusion modelling, must be capable of reproducing the three regimes of turbulence, distinguished at the end of section 1.2.

For the Rotterdam Waterway a significant fraction of the total time-integrated dispersive transport through a station close to its mouth occurs at low water slack (Fig. 2.3). Therefore salinity intrusion into that estuary is primarily controled by the low water slack flow conditions. That makes it important to reproduce the slack tide internal regime of turbulence, distinguished at the end of section 1.2, properly in salinity intrusion modelling studies for the Rotterdam Waterway in order to obtain a proper representation of the salinity intrusion as such. In general this applies to estuaries, which in accordance with a criterion presented by Abraham (1980) are sufficiently stratified.

When tidal currents are large, turbulent energy is generated at the solid boundaries. In essence, this boundary induced turbulence is the mechanism which controls the stratification of the estuary by external mixing. Therefore, the ebb tide and flood tide external regimes of turbulence, distinguished at the end of Section 1.2, must be included properly in salinity intrusion modelling studies in order to obtain a proper representation of the stratification of the estuary.

In order to satisfy the above requirements the damping functions used in zero-equation and one-equation turbulence models must vary with the regime of turbulence. At tidal slack they have to describe mixing which is primarily internal, to account for the effect of the acceleration $\partial\bar{u}/\partial t$ and to be related to the master length scale L_m, defined in Section 6.1. Because of the density induced flow, at tidal slack $L_m < L_n$, where L_n is the length scale for non-stratified conditions. On the ebb tide and on the flood tide the damping functions have to describe mixing which is primarily external. On the ebb tide the damping functions may be related to the gradient Richardson number, Ri, as the production of turbulent energy is large. On the flood tide they are to be

related to the parameter E^* (Eq. 4.21), as the production of turbulent energy is small and the turbulent transport of turbulent energy is a factor to be considered. Damping functions, which account for the above effects explicitely, are not available in the literature and cannot be derived from higher order turbulence models. This limits the capabilities of zero-equation and one-equation turbulence models for salinity intrusion modelling.

The above issue is clearly illustrated by Smith and Takhar (1981,p. 32), who applied a one-equation turbulence model in salinity intrusion studies. In this application they found specifying L_m a major problem, which was solved by deriving L_m from experiments made in steady atmospheric flow. By doing so they in essence neglected the effect of longitudinal density gradients, because of which at low water slack $L_m \neq L_n$.

The above effect of the longitudinal density gradient is further neglected in the applications of zero-equation turbulendce models in salinity intrusion modelling made by Hamilton (1975), Blumberg (1977), Odd and Rodger (1978), Perrels and Karelse (1981,1986), Wang (1983) and Bloss (1985). These models use a variety of damping relations, each in agreement with a particular set of data. Some of these relations are given in Figs 7.1, 7.2 and 7.3. These figures give the relation between $\nu_t \nu_{to}^{-1}$, $K_t K_{to}^{-1}$, $\sigma_t \sigma_{to}^{-1}$ and Ri, as can be derived from the damping relations used, assuming that stratification does not influence the vertical gradient of the horizontal velocity component. The damping relations used by Blumberg show the unrealistic feature of $\nu_t \nu_{t.o}^{-1}$ increasing with increasing Ri.

In principle a two-equation turbulence model, such as the k-ε model, in combination with algebraic stress/flux relations are capable to describe the three regimes of turbulence distinguished at the end of Section 1.2. The algebraic stress/flux relations are to be used to express the effect of stratification on the model constants of the two-equation model. This leads to the type of turbulence model applied by Oey et al (1985). A factor to be considered in such models is whether the wall effect on the turbulence pressure field is included properly.

Two-equation turbulence models contain a partial differential equation to determine the length scale of turbulence. Hence, they give this length scale a function of time and spatial coordinates, not in terms of local parameters which characterize the local flow or the local turbulence. Therefore, the damping functions to be used in zero-equation or one-equation turbulence models cannot be derived using the algebraic stress/flux approach.

7.2 On boundary-induced entrainment

The limited information on boundary-induced entrainment, included in this review, is summarized in Section 3.3.

7.3 Recommendations for further research

This section gives some recommendations for the study of turbulence under stratified conditions, leaving aside subjects like the effect of three-dimensional topographic features either on the bottom or on the banks of a channel or the interaction between internal waves and turublence.

The effect of the longitudinal density gradient on the flow makes it necessary to distinguish the three regimes of turbulence, referred to at the end of section 1.2. Experimental studies on these regimes require this effect of the longitudinal density gradient to be reproduced. The DHL tidal flume satisfies this requirement.

A critical issue for a turbulence model to be applied in salinity intrusion modelling is whether or not it reproduces the internal mixing at low water slack correctly. The k-ε model using algebraic stress/flux relations seems to satisfy this requirement (Goussebaile and Viollet, 1982). Another option is the two-equation turbulence model using algebraic stress/flux relations, developed by Mellor and Yamada (1982), and applied in three-dimensional salinity intrusion modelling by Oey et al (1985).

Whether or not a given turbulence model reproduces mixing, which is primarily internal, can be studied performing experiments and collecting data on the development of the intermediate layer in steady stratified flow. In the ana-

lysis of the measurements, it is to be checked how well the above turbulence models reproduce this data, for practical reasons to begin with using the k-ε model. This procedure will give a first insight into the capabilities of these models at slack tide. This procedure is recommended as in steady flow turbulence measurements are less involved than in tidal flow.

Reproduction of the longitudinal density gradient and the effect of $\partial\bar{u}/\partial t$ on the variation of the flow over the depth is essential in the experiments to check whether or not a given turbulence model reproduces the internal slack tide turbulence regime and the external ebb tide and flood tide turbulence regimes. This requires tidal flume experiments to be performed either to measure turbulence characteristics or to determine the main flow. Whether under these circumstances the considered turbulence model works satisfactorily can be checked either on the turbulence level or on the main flow level, depending on the type of measurements made.

Turbulence ceases to exist because of the combined effect of buoyancy and viscosity when $L_R L_k^{-1} < C_1^{-1} C_2$ (Table 4.1, item 3), where the experimental value of $C_1^{-1}C_2$ is of the order 10.. In the tidal flume this situation may occur around tidal slack, when viscous effects are relatively important. If so, viscous effects are a factor to be considered in the calibration and verification of mathematical salinity intrusion models, using tidal flume experiments as a reference.

Whether or not the above situation occurs depends on whether or not at tidal slack local $L_R L_k^{-1}$-values are below the above limiting value. The $L_R L_k^{-1}$ - values can be determined from the local values of the buoyancy frequency, N, and the rate of dissipation of turbulent energy, ε. (Eqs. 4.6 and 4.8) In the tidal flume, the latter parameter is difficult to be measured. However, using the tidal flume experiments as a reference in the calibration and verification of mathematical models, the parameter ε can be derived from these models. If based on two-equation or higher order turbulence models, these models give ε directly. If based on zero-equation or one-equation turbulence models, a first estimate of ε can be obtained assuming turbulence to be in local equilibrium.

It is recommended to apply the above procedure in the calibration and verification of mathematical models to determine whether or not viscous effects play a role in the reference material derived from the tidal flume.

References

Abraham, G., Karelse, M. and van Os, A.G., 1979, On the magnitude of interfacial shear of subcritical stratified flows in relation to interfacial stability, Journal of Hydraulics Research, 17, note, 273-287

Abraham, G., 1980, On internally generated estuarine turbulence, Proceedings 2nd International Symposium on Stratified Flows, Trondheim, 1, 344-353

Alavian, V.A., 1986, Behaviour of density current on an incline, Proceedings American Society of Civil Engineers, Journal of Hydraulic Engineering, 112 (1), 27-42

Anwar, H.O. and Weller, J.A., 1981, An Experimental study of the structure of a freshwater-saltwater interfacial mixing, La Houille Blanche, 6, 450-412

Arya, S.P.S. and Plate, E., 1969, Modelling of the stably stratified atmospheric boundary layer, Journal of Atmospheric Sciences, 26, 656-665

Arya, S.P.S., 1972, The critical condition for the maintenance of turbulence in stratified flows, Quarterly Journal Royal Meteorological Society, 98, 264-273

Bloss, S. and Harleman, D.R.F., 1980, Effect of wind-induced mixing on the seasonal thermocline in lakes and reservoirs, Proceedings 2nd International Symposium on Stratified flows, Trondheim, 1, 291-300

Bloss, S., 1985, Parameterization of vertical eddy coefficients in stratified tidal flows, IUTAM Symposium on Mixing in Stratified Fluids, Martgaret River, Western Australia, Environmental Dynamics, Center for Water Research, University of Western Australia, Report 85-120, Topic IV

Blumberg, A.F., 1977, Numerical model of estuarine circulation, Proceedings of American Society of Civil Engineers, Journal of Hydraulics Division, 103 (3), 295-310

References (continued)

Bogliano, R., 1959, Turbulent spectra in a stably stratified atmosphere, Journal of Geophysical Research, 64, no 12, 2226-2229

Bowden, K.F. and Gilligan, R.M., 1971, Characteristic features of estuarine circulation as represented in the Mersey Estuary, Limnology and Oceanography 16, 490-502

Breusers, H.N.C., (ed), 1974, Momentum and mass transfer in stratified flows, Delft Hydraulics Laboratory, Report R 880

Businger J.A., Wijngaard, J.C., Izumi, Y. and Bradley, E.F., 1971, Flux-profile relationships in the atmospheric surface layer, Journal of Atmospheric Sciences, 28, 181-189

Christodoulou, G.C., 1986, Interfacial mixing in stratified flows, Journal of Hydraulic Research, 24, (2) 77-92

Chu, V.T. and Baddour, R.E., 1984, Turbulent gravity-stratified shear flows, Journal of Fluid Mechanics, 138, 353-378

Corcos, G.M. and Hopfinger, E.J., 1976, L'instabilité motrice de la turbulence en écoulements libres, Journal de Physique, Collogue C1, Supplément au n° 1, Tome 37, page C1-95

Corcos, G.M., 1979, The mixing layer: deterministic models of a turbulent flow, College of Engineering, University of California, Berkeley, Report No F.M.-79-2

Deardorff, J.W., 1967, Empirical dependence of the eddy coefficient for heat upon stability above the lowest 50 m., Journal Applied Meteorology, 6, 631-643

Delvigne, G.A.L., 1986, Model for vertical diffusion in stratified flows, Proceedings of American Society of Civil Engineers, Journal of Hydraulic Engineering, 112 (11), 1069-1086

References (continued)

Dickey, T.D. and Mellor, G.L., 1980, Decaying turbulence in neutral and stratified fluids, Journal of Fluid Mechanics, 99, 23-31

Dingemans, Mrs. M.P., 1972, Stability of three layer flow (Dutch text), Report S 57, Delft Hydraulics Laboratory

Dronkers, J.J., 1969, Some practical aspects of tidal computations, Proceedings of 13th Congress of International Association for Hydraulic Research, Kyoto, 3, paper C3, 11-20

Elder, J.W., 1959, The dispersion of marked fluid in turbulent shear flow, Journal of Fluid Mechanics, 5 (4), 544-560

Ellison, T.H. 1957, Turbulent transport of heat and momentum from an infinite rough plane, Journal of Fluid Mechanics, 2, 456-466

Ellison, T.H. and Turner, J.S., 1960, Mixing of dense fluid in a turbulent pipe flow, Part 2, Dependence of transfer coeficient on local stability, Journal of Fluid Mechanics, 8, 529,544

Fearnhead P.G., 1975, On the formation of fronts by tidal mixing around the British Isles, Deep Sea Research, 22, 311-322

Fischer, H.B. List, E.J., Koh, R.C.Y., Imberger, J. and Brooks, N.H., 1979, Mixing in inland and coastal waters, Accdemic Press, New York.

Gargett, A.E., Osborn, T.R. and Nasmyth, P.W., 1984, Local isotropy and the decay of turbulence in a stratified fluid, Journal of Fluid Mechanics, 144, 231-280

Garrett, G.J.R., Keyley, F.R. and Greenberg, D.A., 1978, The mixing versus thermal stratification in the Bay of Fundy and Gulf of Maine, Atmosphere-Ocean, 16 (4), 403-423

References (continued)

Gartrell, G. 1980, Vertical flux measurements in a density-stratified shear flow, Proceedings 2nd Symposium on Stratified Flows, Trondheim, 1, 301-314

Gibson, M.M. and Launder, B.E., 1978, Ground effects on pressure fluctuations in the atmospheric boundary layer, Journal of Fluid Mechanics, 86, 491-511

Gordon, C.M., 1975, Sediment entrainment and suspension in a turbulent tidal flow, Marine Geology, 18, M57-M64

Goussebaile, J. and Viollet, P.L., 1982, On the modelling of turbulent flows under strong buoyancy effects in cavities with curved boundaries, Symposium on Refined Modelling of Flows, Paris, Proceedings, 1, 165-174

Grigg, H.R. and Stewart, R.W., 1963, Turbulent diffusion in a stratified fluid, Journal of Fluid Mechanics, 15, 174-

Hamilton, P., 1975, A numerical model of the vertical circulation of tidal estuaries and its application to the Rotterdam Waterway, Geophysical Journal, Royal Astronomical Society, 40, 1-21

Harleman, D.R.F. and Ippen, A.T., 1967, Two-dimensional aspects of salinity intrusion in estuaries: analysis of salinity and velocity distributions, Committee on Tidal Hydraulics, Corps of Engineers, U.S. Army, Technical bulletin no. 13

Hazel, P, 1972, Numerical studies of the stability of inviscid stratified shear flows, Journal of Fluid Mechanics, 51, 39-61

Hinze, J.O., 1975, Turbulence, Mc Graw-Hill, New York

Hopfinger, E.J., 1985, Turbulence collapse in stratified fluids, IUTAM Symposium on Mixing in Stratified Fluids, Margeret River, Western Australia, Environmental Dynamics, Centre for Water Research, University of Western Australia, Report no. 85-120, Topic III

References (continued)

Howard, L.N., 1961, A note on a paper of John W. Miles, Journal of Fluid Mechanics, 10, 509-512

Imberger, J. and Spigel, R.H., 1980, Billowing and its influence on mixed layer deepening, Paper presented at Symposium on Surface Water Impoundments, Minneapolis, June 2

Imberger, J. and Hamblin, P.F., 1982, Dynamics of lakes, reservoirs and cooling ponds, Annual Review of Fluid Mechanics, 14, 153-187

Itsweire, E.C., Helland, K.N., van Atta, C.W., 1986, The evolution of grid-generated turbulence in a stably stratified fluid, Journal of Fluid Mechanics, 162, 299-338

Karelse, M., 1976, Dispersive transports in Rotterdam Waterway Estuary, Delft Hydraulics Laboratory Report M896-29 (Dutch text)

Kent, R.E. and Pritchard, D.W., 1959, A test of mixing length theories in a coastal plain estuary, Journal of Marine Research, 18, no 1, 62-72

Knight, D.W., Rodger, J.G., Shiono, K., Waters, C.B. and West, J.R., 1980, The measurement of vertical turbulent exchange in tidal flows, Proceedings 2nd International Symposuim on Stratified Flows. Trondheim, 1, 362-366

Komori, S., Ueda, H., Ogino, F. and Mizushina, T., 1982, Lateral and longitudinal turbulent diffusion of scalar quantities in thermally stratified flow in open channel, Heat Transfer 1982, Proceedings 7th International Heat Transfer Conference, München, 2, 431-436

Komori, S., Ueda, H., Ogino, F. and Mizushina, T., 1983, Turbulence structure in stably stratified open-channel flow, Journal of FLuid Mechanics, 130, 13-26

References (continued)

Kondo, J., Kanechika, O. and Yasuda, N., 1978, Heat and momentum transfers under strong stability in the atmosphere surface layer, Journal of the Atmospheric Sciences, 35, 1012-1021

Koop, C.G. and Browand, F.K., 1979, Instability and turbulence in a stratified fluid with shear, Journal of Fluid Mechanics, 93, 135-159

Kranenburg, C., 1985, A k-model for stably stratified nearly horizontal turbulent flows, Deparment of Civil Engineering, Delft University of Technology, Report No 4-85

Kranenburg, C., to be published, Boundary-induced entrainment in two-layer stratified flow, Journal of Geophysical Research, Special Issue on IUTAM on Mixing of stratified fluids,

Launder, B.E., 1975, On the effcts of a gravitational field on the turbulent transport of heat and momentum, Journal of Fluid Mechanics, 67 (3), 569-581

Lavelle, J.W., and Mofjeld, H.O., 1983, Effects of time-varying velocity on oscillatory turbulent channel flow, Journal of Geophysical Research, 86, C12, 7607-7616

Linden, P.F., 1979, Mixing in stratified fluids, Geophysical Astrophysical Fluid Dynamics, 13, 3-23

Lumley, J.L., 1964, The spectrum of nearly inertial turbulence in a stably stratified fluid, Journal of Atmospheric Sciences, 21, 99-102

McEwan, 1983, Internal Mixing in Stratieif Fluids, Journal of Fluid Mechanics, 128, 59-80

References (continued)

Mc Lean, S.R., 1983, Turbulence and sediment transport measurements in a North Sea tidal inlet (The Jade) in North Sea Dynamics, edited by Sündermann, C. and Lenz, W., Springer, Berlin, 436-452

Maxworthy, T. and Browand, F.K., 1975, Experiments in rotating and stratified flows: oceanographic application, Annual Review of Fluid Mechanics, 7, 273-305

Mellor, G.L. and Yamada, T., 1974, A hierarchy of turbulence closure models for planetary boundary layers, Journal of Atmospheric Sciences, 31, 1791-1806

Mellor, G.L. and Yamada, T., 1982, Development of a turbulence closure model for geophysical fluid problems, Review of Geophysics and Space Physics, 20, no4, 851-875

Miles, J.W., 1961, On the stability of heterogenous shear flows, Journal of Fluid Mechanics, 10, 496-508

Miles, J.W. and Howard, L.N., 1964, Note on heterogenous shear flow, Journal of Fluid Mechanics, 20, 3311-336

Mizushina, T., Ogino, F., Ueda, H. and Komori, S., 1978, Buoyancy effect on diffusivities in thermally stratified flow in open channel, Heat Transfer, Proceedings 6th International Heat Transfer Conference, Toronto 1, 91-98

Monin, A.S., 1959, Turbulence in shear flow with stability, Journal of Geophysical Research, 64, no. 12, 2224-2225

Odd, N.V.M. and Rodger, J.G., 1978, Vertical mixing in stratified tidal flows, Proceedings American Society of Civil Engineers, Journal of Hydraulics Division, 104, no HY 3, 337-351

References (continued)

Oey, L.Y., Mellor, G.L. and Hires, R.I., 1985, A three-dimensional simulation of the Hudson-Raritan Estuary, Part I: Description of the model and simulations; Part II: comparison with observation; Part III: Salt flux analysis, Journal of Physical Oceanography, 15, 1676-1692, 1693-1710, and 1711-1720

Ogino, F., Tominari, Y. and Mizushina, T., 1982, Heat transfer mechanism in a thermally stratified turbulent flow, Heat Transfer, Proceedings 7th International Heat Transfer Conference, München, 2, 443-448

Oke, T.R., 1970, Turbulent transport near the ground in stable conditions, Journal of Applied Meteorology, 9, 778-786

Ozmidov, R.V., 1965, On the turbulent exchange in a stably stratified ocean. Izv., Atmospheric and Oceanic Physics Series, 1, no. 8, pp 853-860

Perrels, P.A.J. and Karelse, M., 1981, A two-dimensional laterally averaged model for salt intrusion in estuaries, Chapter 13 of Transport models for inland and coastal waters, Fischer, H.B. (ed) Academic Press, New York

Perrels, P.A.J. and Karelse, M., 1986, Delft Hydraulics Laboratory, Report R 2208 (in Dutch)

Proudman, J., 1953, Dynamical oceanography, Methuen London

Pruitt W.O., Morgan, D.L. and Laurence, F.J., 1973, Momentum and mass transfers in the surface boundary layer, Quarterly Journal Royal Meteorological Society, 99, 370-386.

Reynolds, W.C., 1976, Computation of turublent flows, Annual Review of Fluid Mechanics, 8, 183-208

Rodi, W., 1976, A new algebraic relation for calculating the Reynolds stress, ZAMM, 56, T219-T221

References (continued)

Rodi, W., 1980, Turbulence mmodels and their application in hydraulics, International Association for Hydraulic Research, Delft

Rodi, W., 1985, Survey of calculation methods for flow and mixing in stratified fluids, IUTAM Symposium on Mixing in Stratified Fluids, Margeret River, Western Australia, Environmental Dynamics, Centre for Water Research, University of Western Australia, Report no. 85-120, Topic IV

Rohr, J.J., Itsweire, E.C. and van Atta, C.W., 1984, Mixing efficiency in stably-stratified decaying turbulence, Geophysical Astrophysical Fluid Dynamics, 29, 221-236

Rohr, J.J., Helland, K.N., Itsweire, E.C. and van Atta, C.W., 1985, Turbulence in a stably stratified shear flow: a progress report, Proceedings 5th Symposium on Turbulent Shear Flows, Cornell University, Ithaca, 22.1-22.6

Saffman, P.G., 1977, Problems and progress in the theory of turbulence, Proceedings of Structure and Mechanics of Turbulence II, Berlin, Springer, Berlin 273-306

Scheffers, M., 1984, Spectral distributions of turbulence in the stratified North Sea (dutch text), Institute for Meteorology and Oeanography, University of Utrecht, Report V84-17

Schumacher, J.D., Kinder, T.H., Paskinski, D.J. and Charnel, R.L., 1979, A structural front over the continental shelf of the Eastern Bering Sea, Journal of Physical Oceanography, 9, no 1, pp 79-87

Schijf, J.B. and Schönfeld, J.C., 1953, The motion of salt and fresh water, Proceedings Minnesota International Hydraulics Convention, Joint Meeting of International Association for Hydraulic Research and Hydraulics Division of American Society of Civil Engineers, 321-333

References (continued)

Sherman, F.S., Imberger, J. and Corcos, G.M., 1978, Turbulence and mixing in stably stratified waters, Annual Review of Fluid Mechanics, 10, 267-288

Simpson, J.H. and Hunter, J.R., 1974, Fronts in the Irish Sea, Nature (London), 250, 404-406

Simpson, J.H. and Bowers, D., 1981, Models of stratification and frontal movement in shelf seas, Deep Sea Research, 28A, 727-738

Smith, T.J. and Takhar, H.S., 1979, The effects of stratification on the turbulent transport of mass and momentum, Proceedings 18th Congress of International Association for Hydraulic Research, Cagliari, 3, 79-86

Smith, T.J. and Takhar, H.S., 1981, A mathematical model for partially mixed estuaries using the turbulent energy equation, Estuarine Coastal and Shelf Science, 13 (1), 27-45

Stigter, C. and Siemons, J., 1967, Calculation of longitudinal salt-distribution in estuaries as function of time, Delft Hydrauclics Laboratory Publication no 52

Stillinger, D.C., Helland, K.N. and van Atta, C.W., 1983, Experiments on the transition of homogenous turbulence to internal waves in a stratified fluid, Journal of Fluid Mechanics, 131, 91-122.

Talmon, A.M., Kunen, J.G.M. and Ooms, G., 1986, Simultaneous flow visualization and Reynolds-stress measurement in a turbulent boundary layer, Journal of Fluid Mechanics, 163, 459-478

Tennekes, H., and Lumley, T.L., 1972, A first course in turbulence M.I.T. Press, Cambridge

References (continued)

Tennekes, H. and Driedoncks, A.G.M., 1980, Basic entrainment equations for the atmospheric boundary layer, Proceedings 2nd International Symposium on Stratified Flows, Trondheim, 1, 205-238

Thatcher, M.L. and Harleman, D.R.F., 1981, Long-term salinity calculation in Delaware Estuary, Proceedings American Society of Civil Engineers, Journal of Environmental Engineering Division, 107, No EE1, 11-27

Thorpe, S.A., 1971, Experiments on the instability of stratified shear flows: miscible fluids, Journal of Fluid Mechanics, 46, 299-319

Thorpe S.A., 1973 a, Turbulence in stably stratified fluids: a review of laboratory experiments, Boundary Layer Meteorology, 5, 95-119

Thorpe S.A., 1973 b, Experiments on instabilities and turbulence in stratified shear Flow, Journal of Fluid Mechanics, 61, 731-751

Turner, J.S., 1973, Buoyancy effects in fluids, Cambridge University Press

Turner, J.S., 1981, Small-scale mixing processes, in Evolution of Physical Oceanography (eds Warren, B.A. and Wunsch, C.), M.I.T. Press, Cambridge

Ueda, H., Mitsumoto, S. and Komori, S., 1981, Buoyancy effects on the turbulent transport processes in the lower atmosphere, Quarterly Journal Royal Meteorological Society, 107, 561-578

van Aken, H.M., 1986, The onset of seasonal stratification in shelf seas due to differential advection in the presence of a salinity gradient, Continental Shelf Research, 5, (4), 475-485

van Rees A.J., 1975, Experimental results on exchange coeficient for non-homogeneous flow, Proceedings 16th Congress of International Association for Hydraulic Research, Sao Paulo, 3, 309-318

References (continued)

Wang, D.P., 1983, Two-dimensional branching salt intrusion model, American Society of Civil Engineers, Journal of Waterway, Port, Coastal and Ocean Engineering, 109 (1), 103-112

Webb, E.K., 1970, Profile relationships: the log-linear range, and extension to strong stability, Quarterly Journal Royal Meteorological Society, 96, 67-90

Webster, C.A.G., 1964, An experimental study of turbulence in a density stratified shear flow, Journal of Fluid Mechanics, 19, 221-245

Weinstock, J., 1978, On the theory of turbulence in the buoancy subrange of stably stratified flows, Journal of Atmospheric Sciences, 35, 634-649

Weinstock, J., 1985, On the theory of temperature spectra in stably stratified fluid, Journal of Physical Oceanography, 15, 475-477

West, J.R., Knight, D.W. and Shiono, K. 1986, Turbulence measurements in the Great Ouse Estuary, American Society of Civil Engineers, Journal of Hydraulic Engineering, 112 (3), 167-180

Yamada, T., 1975, The critical Richardson number and the ratio of the eddy coeficients obtained from a turbulence closure model, Journal of Atmospheric Sciences, 32, 926-933

Young, S.T.B., 1975, Turbulence measurements in a stably stratified turbulent shear flow, Queen Mary College, London, Report QMC-EP 6018 (quoted from Gibson and Launder (1978)).

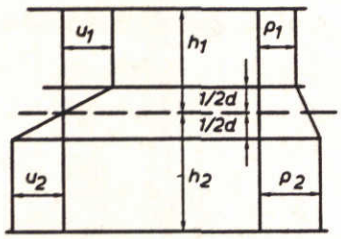

Fig. 2.1 Background flow for which the neutral stability curves represented in Fig. 2.2 were derived. ($h_1 = h_2$ and $|u_1| = |u_2|$)

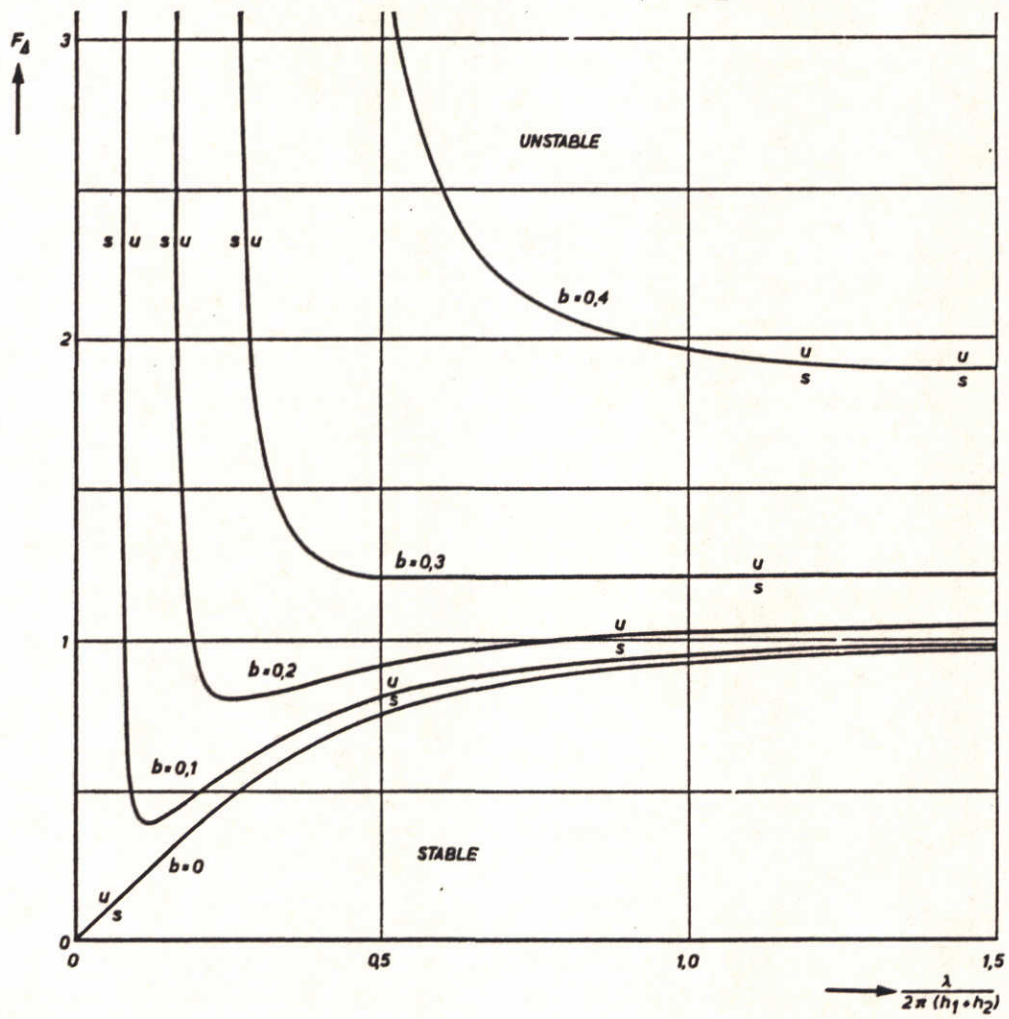

Fig. 2.2 Neutral stability curves derived for the background flow given by Fig. 2.1, the zone indicated by u being the zone of unstable conditions and the zone indicated by s being the one of stable conditions after Dingemans (1972)); ($h_1 = h_2$, $|u_1| = |u_2|$ and ($b = d\,(h_1 + h_2)^{-1}$); λ: wave length of disturbance

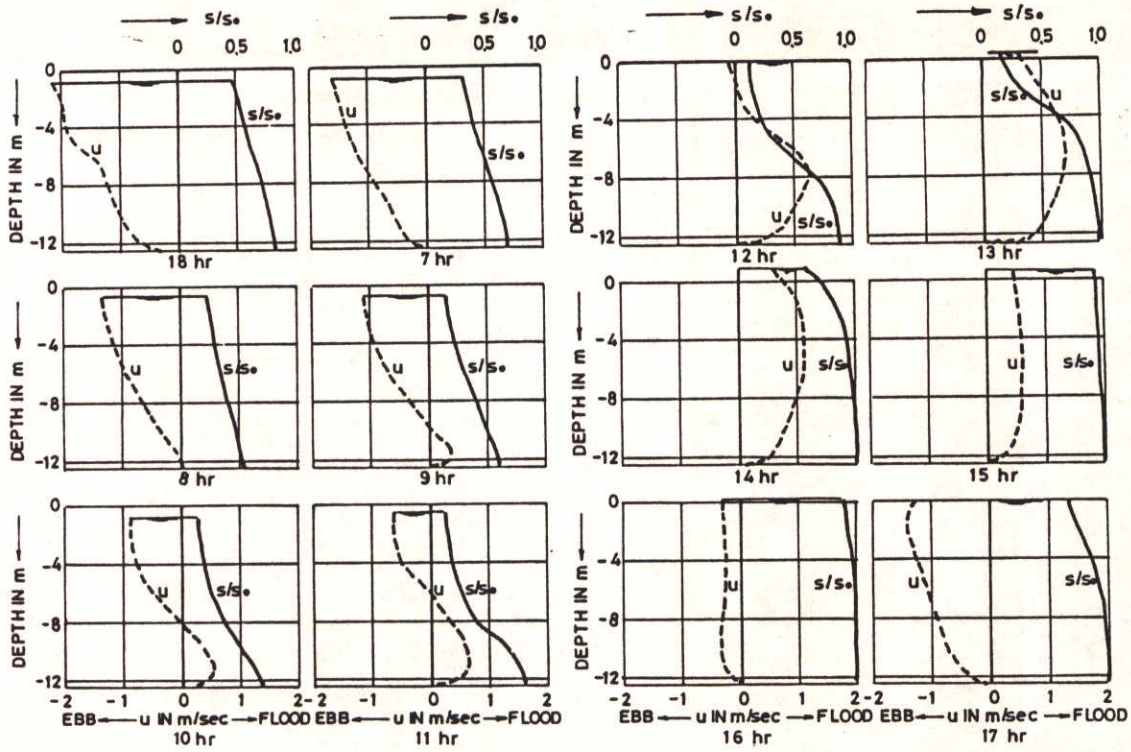

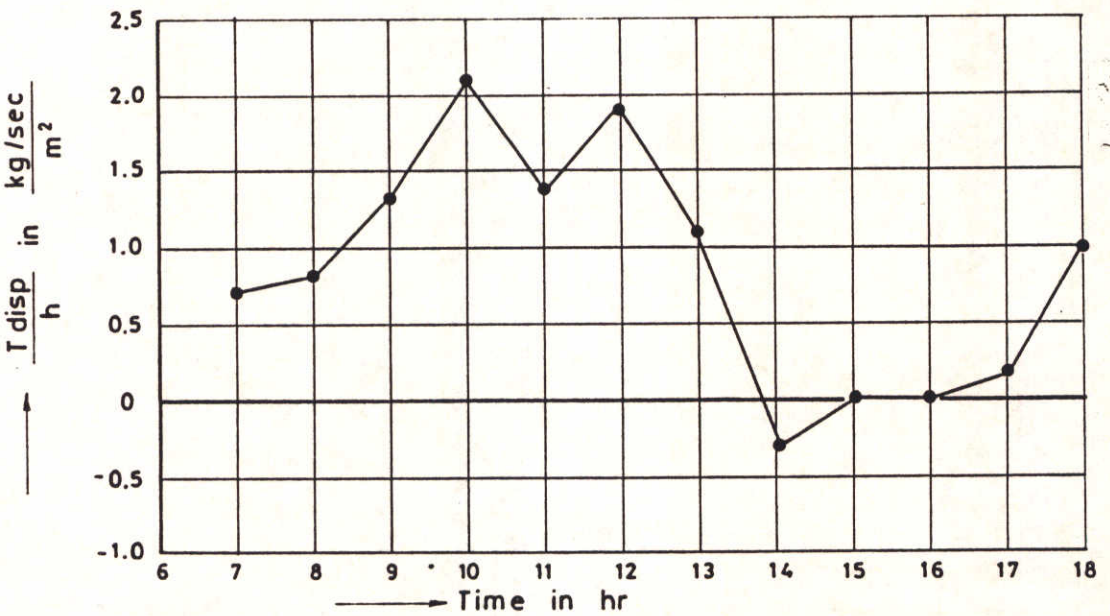

Fig. 2.3 Rotterdam Waterway Estuary, station 1030 km, June 1956; variation of velocity and salinity over depth (top) and associated dispersive transport (bottom).

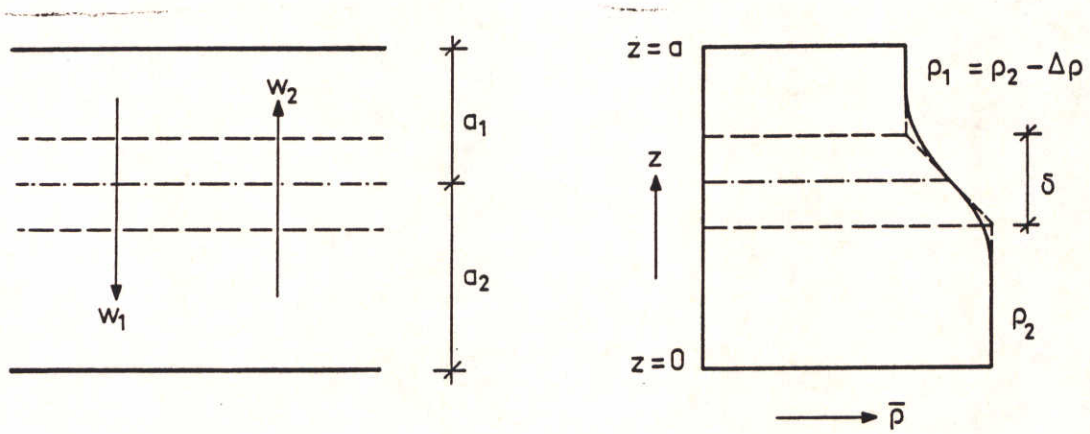

Fig. 3.1 Definition sketch showing entrainment rates and density distribution as observed in the experiments of Kranenburg (to be published). The horizontal dashed lines bound the transition layer; the dash-dot line defines the interface between upper and lower layers (after Kranenburg, to be published).

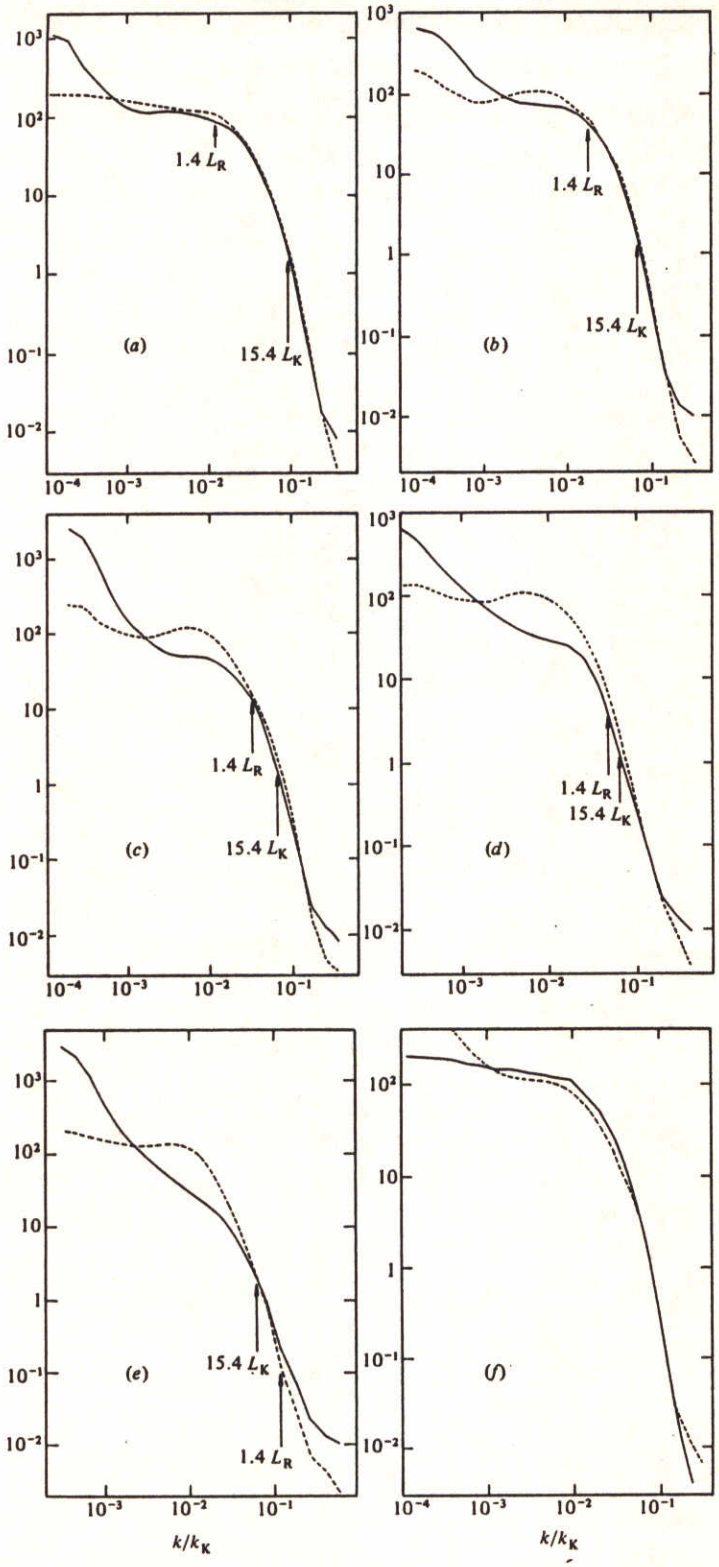

Fig. 4.1 Normalized vertical velocity spectra (after Stillinger et al, 1983). In Figs. (a)-(e): ——— N = 0.45 rad/s; - - - - N=0; Fig. f compares spectra measured at different stations, both for N=0.

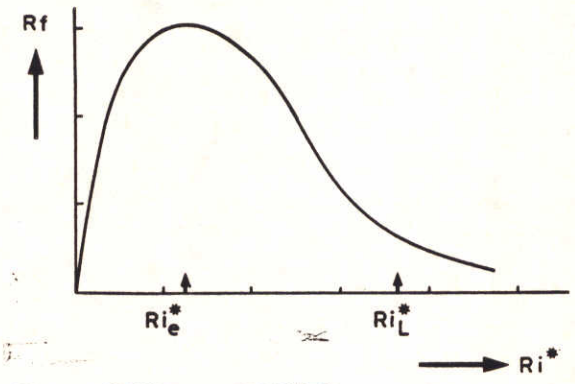

Fig. 4.2 Schematic relation between the flux Richardson number Rf (Eq. 4.16) and the overall Richardson number Ri^* (Eq. 2.1) for internal mixing (after Turner, 1981). The maximum of the curve corresponds to the equilibrium condition. Ri_L^* is the Ri^* value imposed by Kelvin-Helmholz instabilities (Section 2.2). External length scales are not relevant.

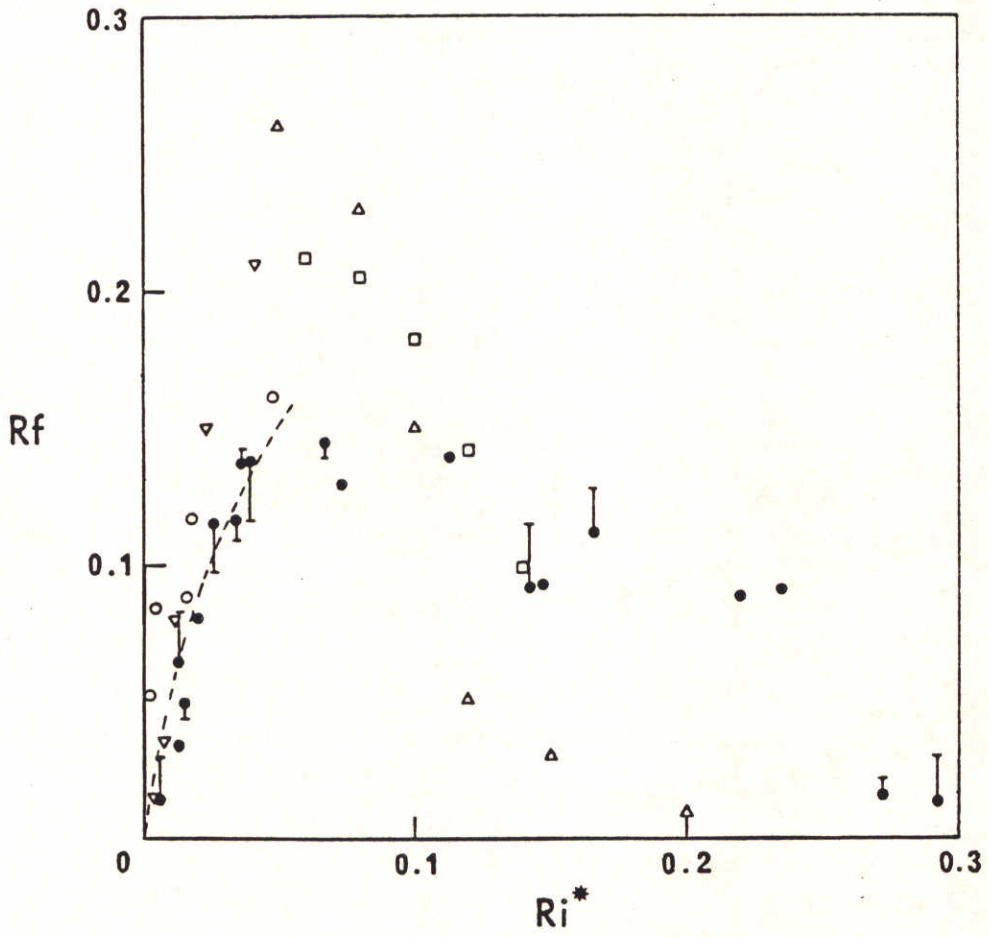

Fig. 4.3 The flux Richardson number Rf plotted against the overall Richardson number Ri^* for a number of different experiments. ● , data from mixing produced by dropping a grid of square bars through a density interface. ▽ , mixing induced by firing a number of vortex rings at an interface. ○ , values calculated from density profiles measured in the wake of a vertical plate □ , △ are values of Rf measured for mixing induced by shear instability at an interface. The broken line is an approximate representation of the data of Grigg and Stewart (1963). In the experiment external length scales are not relevant (after Linden, 1979).

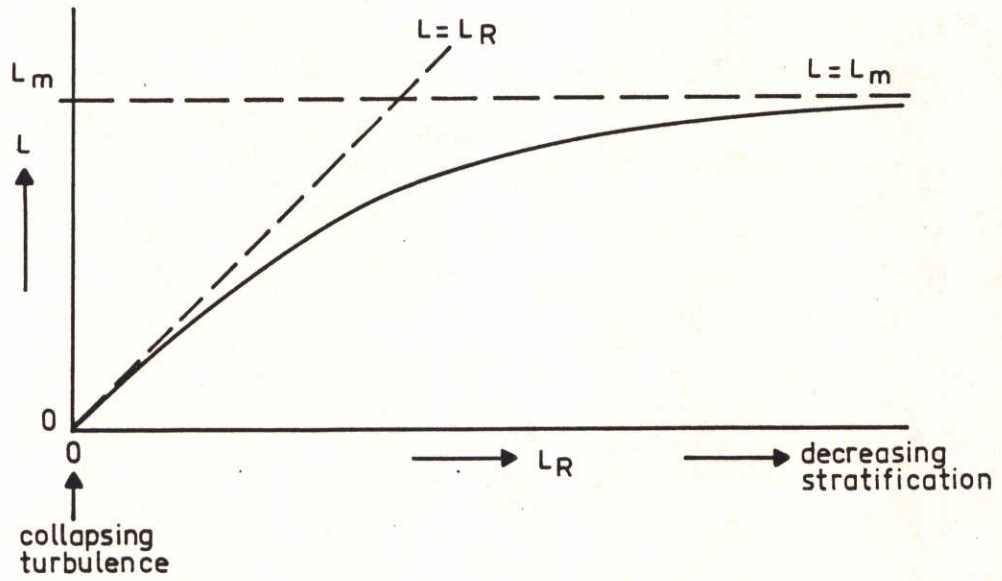

Fig. 6.1 Suggested relationship between length scales L and L_R defined by Eq. 6.3 for C_1= 1 (after Kranenburg, 1985).

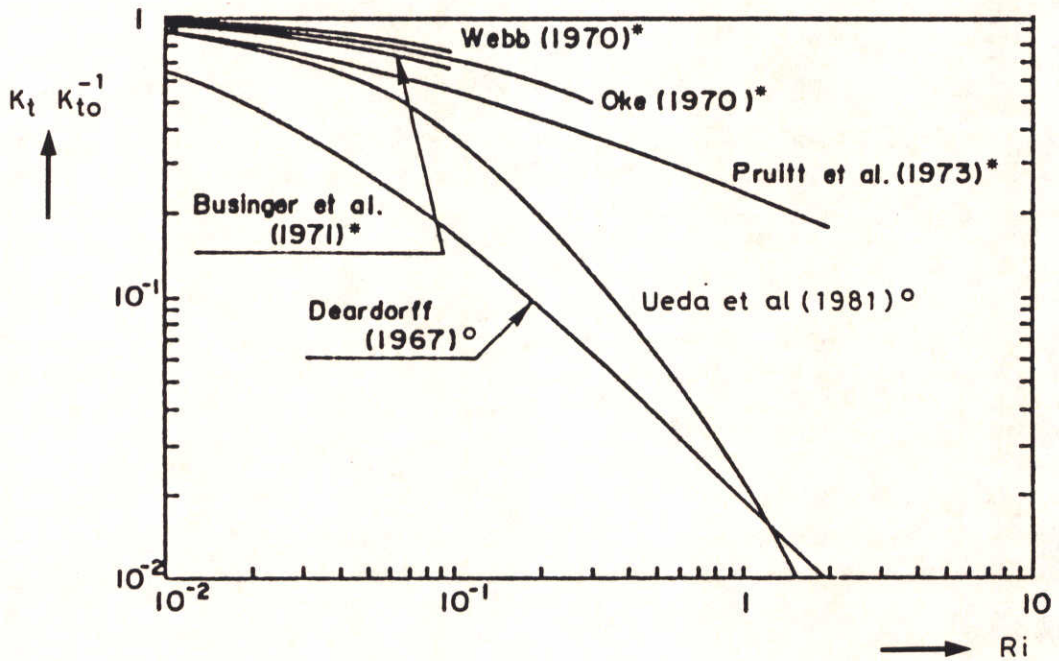

Fig. 6.2 Comparison of measurements in atmosphere (after Ueda et al, 1981)
* :measurements in surface layer, within a few meters adjacent to ground surface; o : measurements from 25 to 200 m from ground surface.

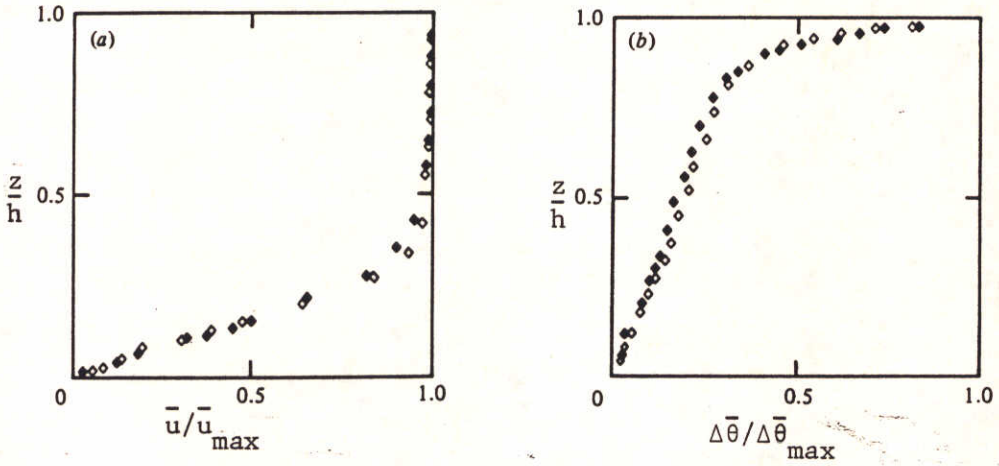

Fig. 6.3 Typical distributions of the mean velocity and temperature in a strongly stable flow (after Komori et al, 1983).

$\Delta\bar{\theta}$: temperature with respect to temperature at z = 0.

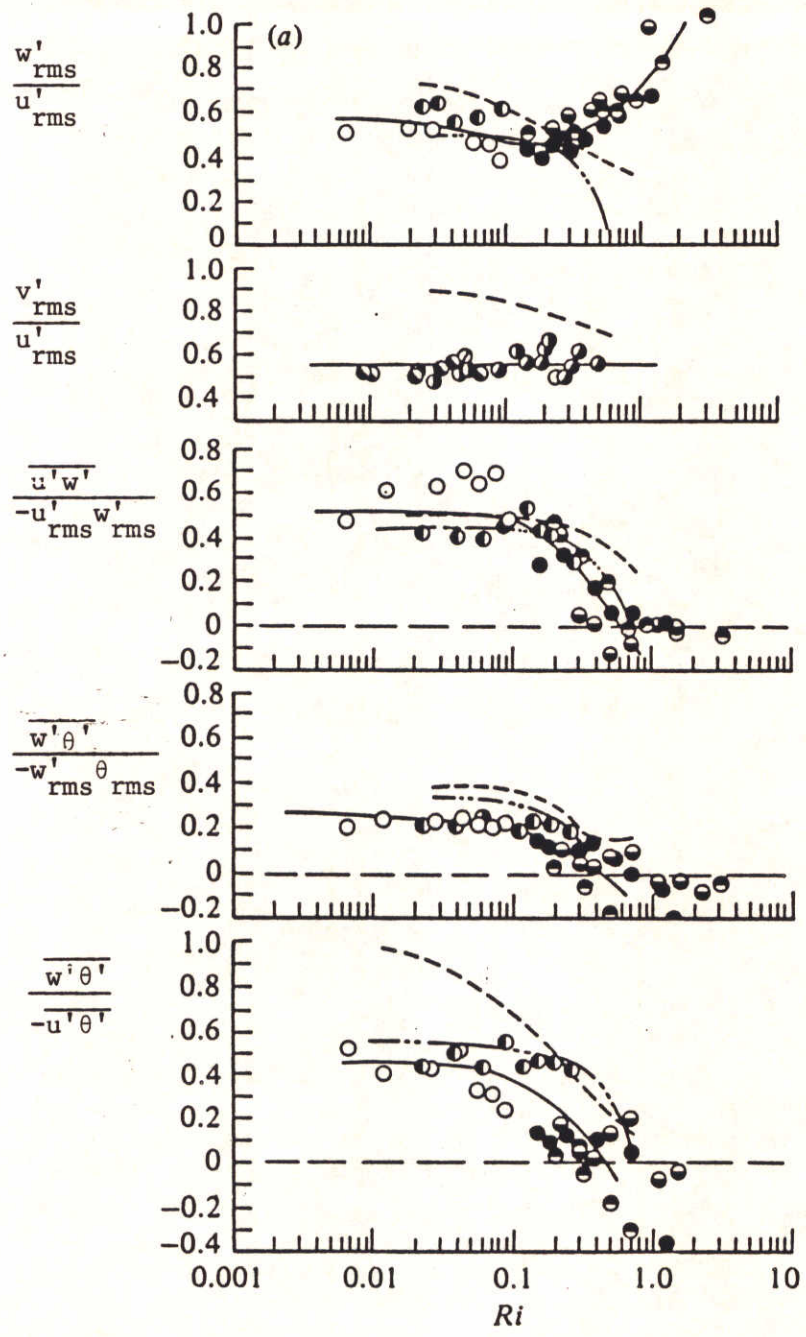

Fig. 6.4 Correlation of turbulence quantities with Ri for $0.4 < z/h < 0.75$; symbols refer to data of Komori et al (1983); ——: best fit of data of Komori et al (1983); - - - -: data of Webster (1964), —··— data of Young (1975) (after Komori et al).

θ : temperature

' : turbulent fluctuation of parameter underneath

$'_{rms}$: root mean square value of this turbulent fluctuation

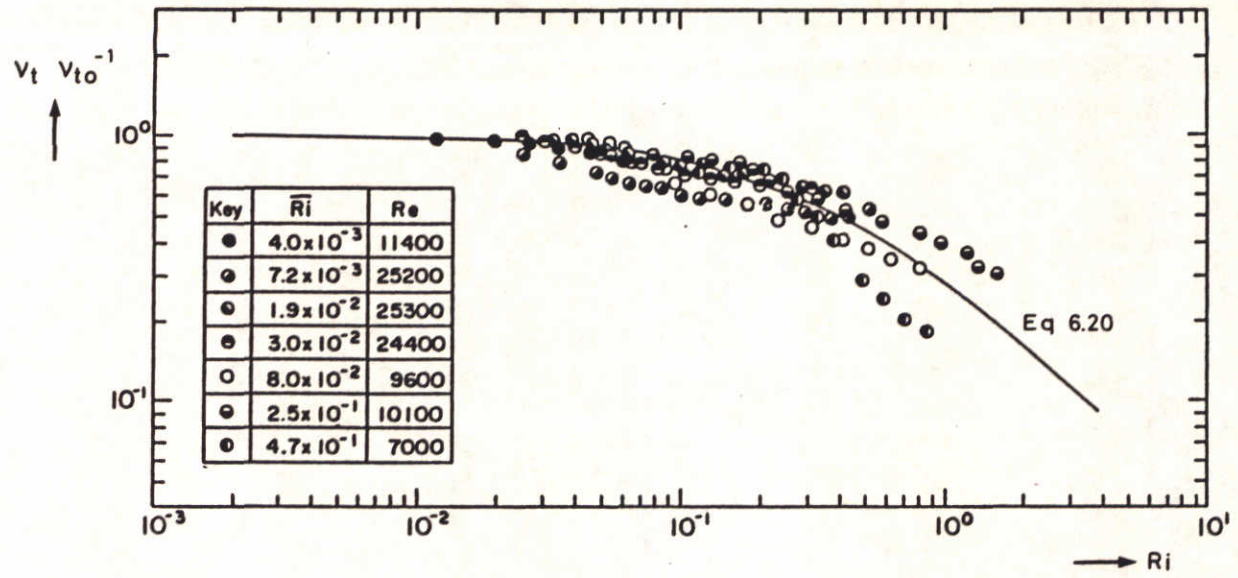

Fig. 6.5 $\nu_t \nu_{to}^{-1}$ versus Ri: experiments of Mizushina et al (1978) compared with empirical relationship proposed by Bloss (1985) (Eq. 6.20)

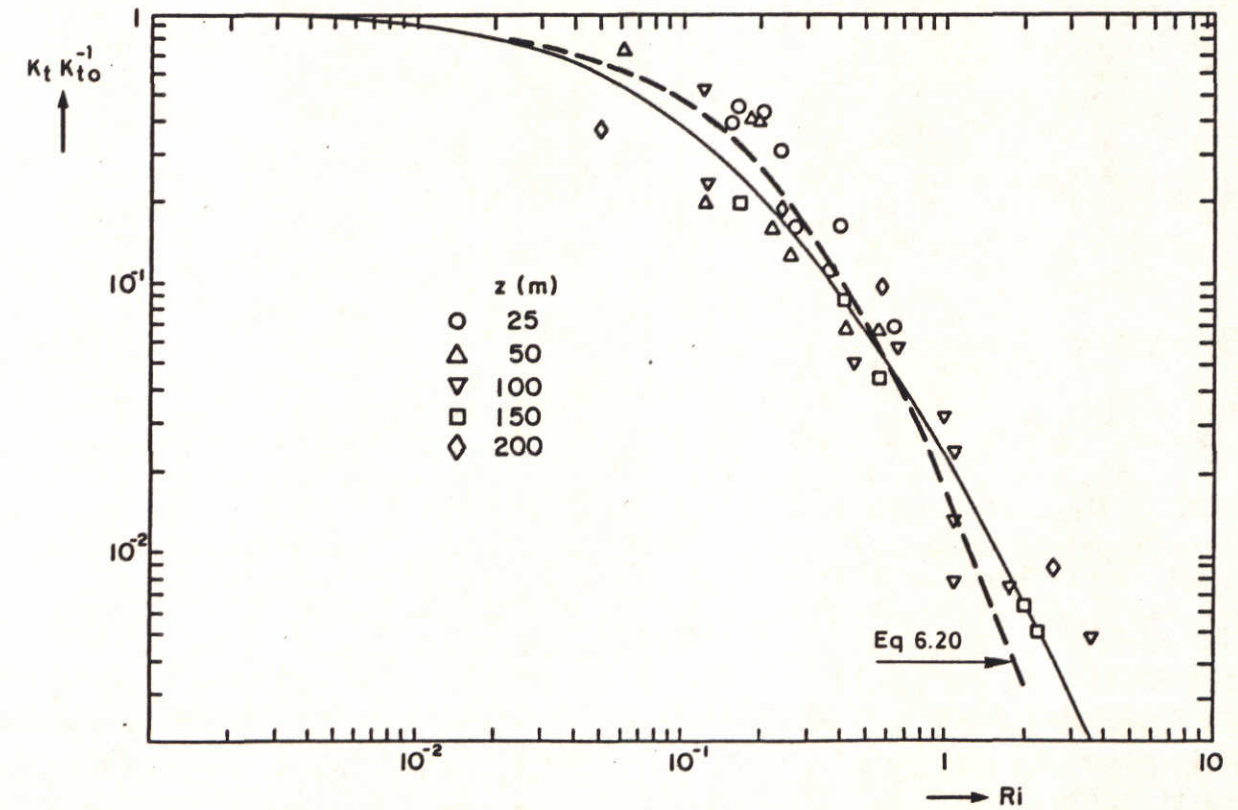

Fig. 6.6 $K_t K_{t.o}^{-1}$ versus Ri; experiments in atmospheric outer layer compared with Mizushina laboratory experiments (solid line) and empirical relationship proposed by Bloss (1985) (Eq. 6.20) (after Ueda et al, 1981).

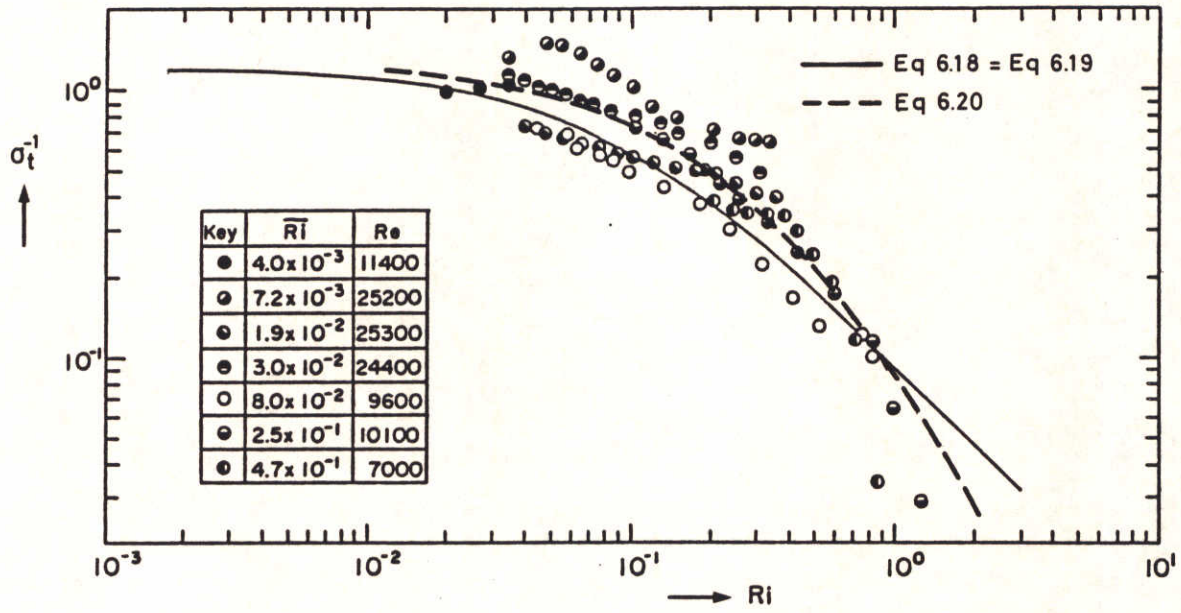

Fig. 6.7 σ_t^{-1} versus Ri; experiments of Mizushina et al (1978) compared with theoretical relationships proposed by Ellison (1957) (Eq. 6.19) and Launder (1975) (Eq. 6.18) both with $Rf_c = 0.1$ and $\sigma_{t.o} = 1.2^{-1}$ and empirical relationship proposed by Bloss (1985) (Eq. 6.20).

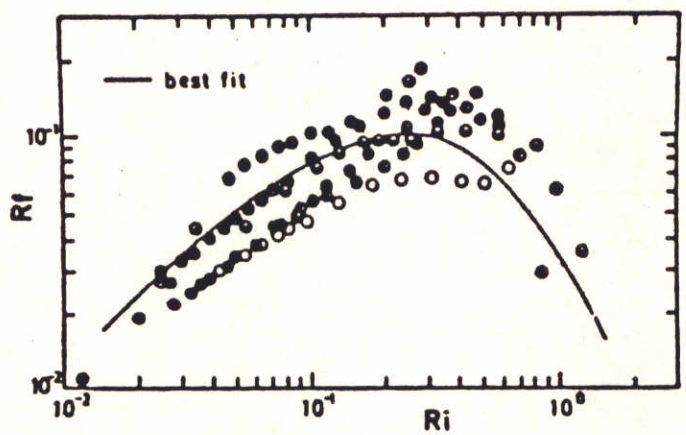

Fig. 6.8 Rf versus Ri, experiments of Mizushina et al (1978).

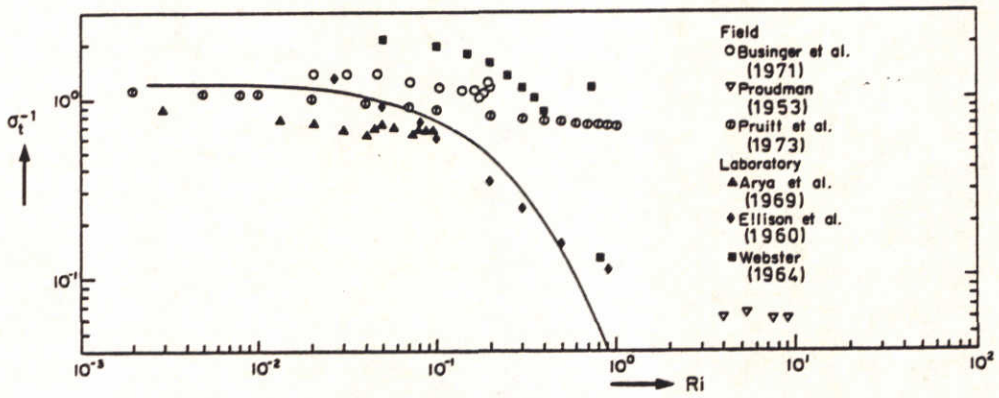

Fig. 6.9 Comparison of Mizushina experiments on σ_t^{-1} (solid line) with those of other investigators (after Ueda et al, 1981).

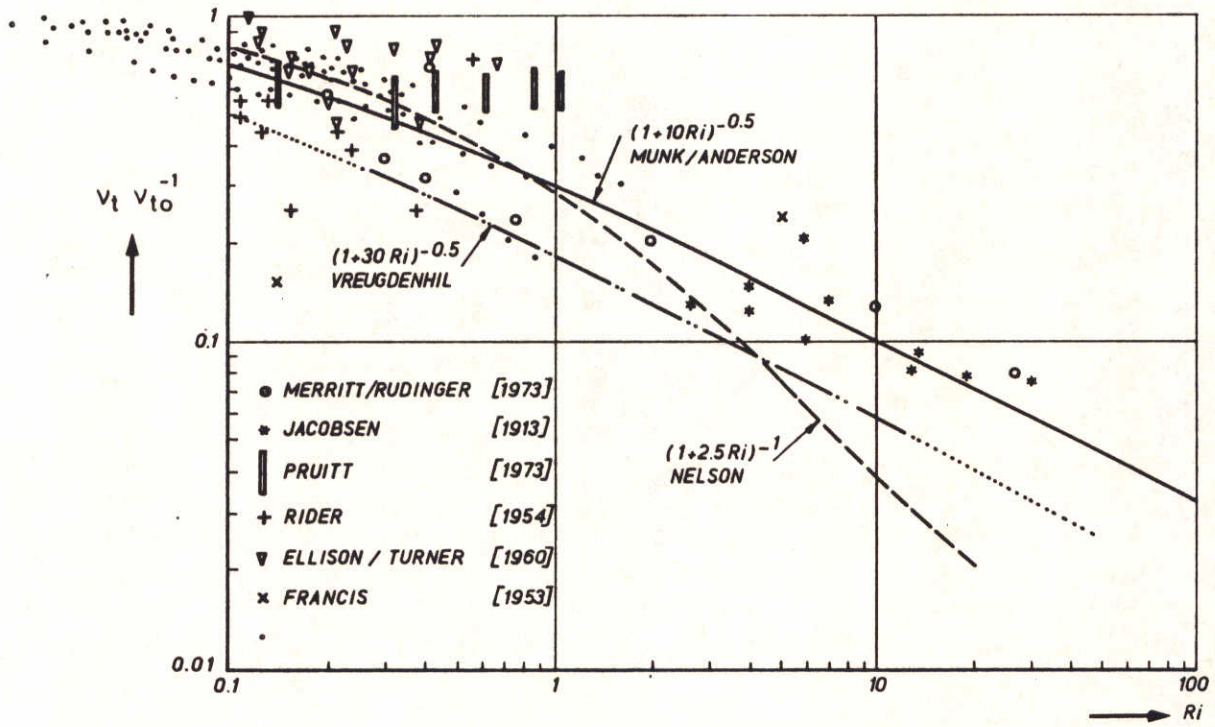

Fig. 6.10 $\nu_t\,\nu_{t.o}^{-1}$ versus Ri; Mizushina laboratory experiments (indicated by •) compared with data collected in 1974 study (Breusers, 1974)

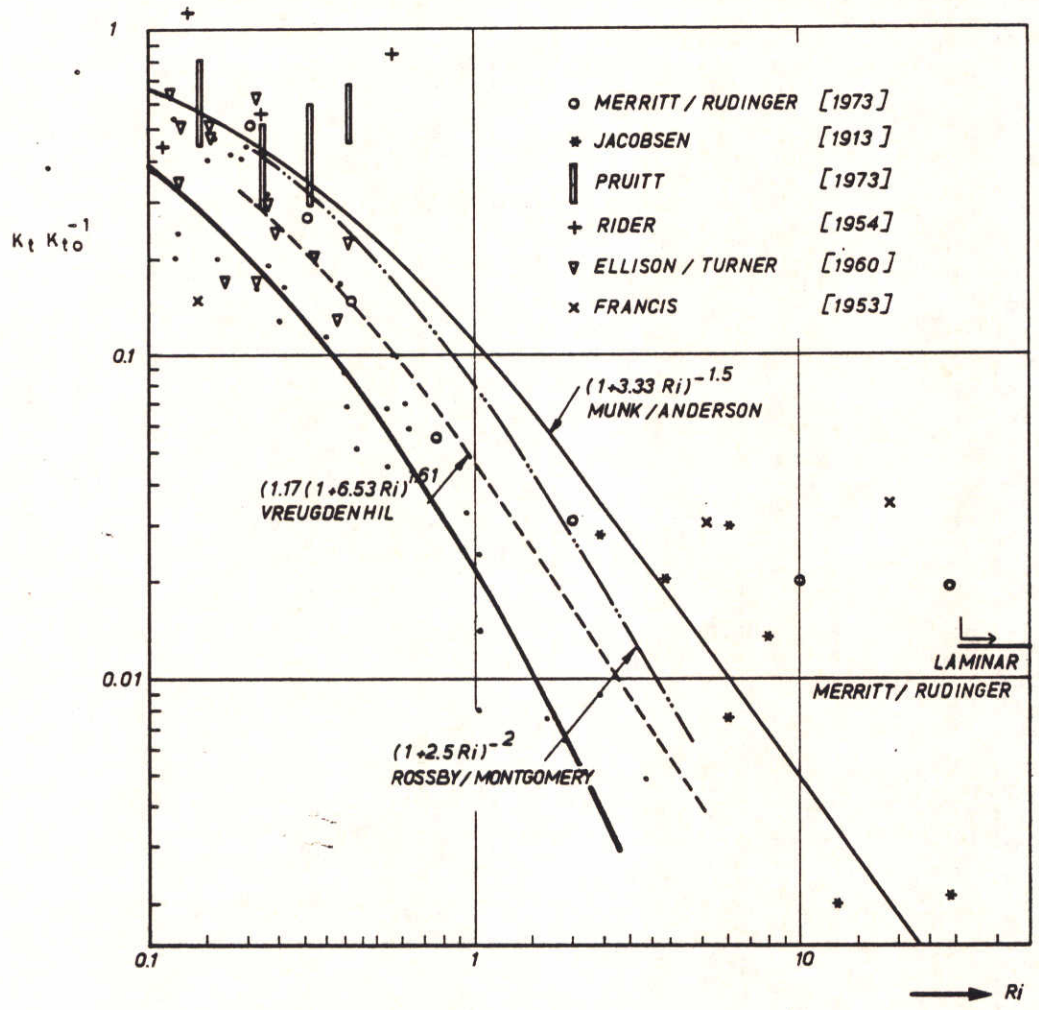

Fig. 6.11 $K_t K_{t.o}^{-1}$ versus Ri; Mizushina laboratory experiments compared with data collected in 1974 study (Breusers, 1974)

• Ueda et al (1981) experimental data collected in lower atmosphere

—— Mizushina laboratory data after Ueda et al (1981)

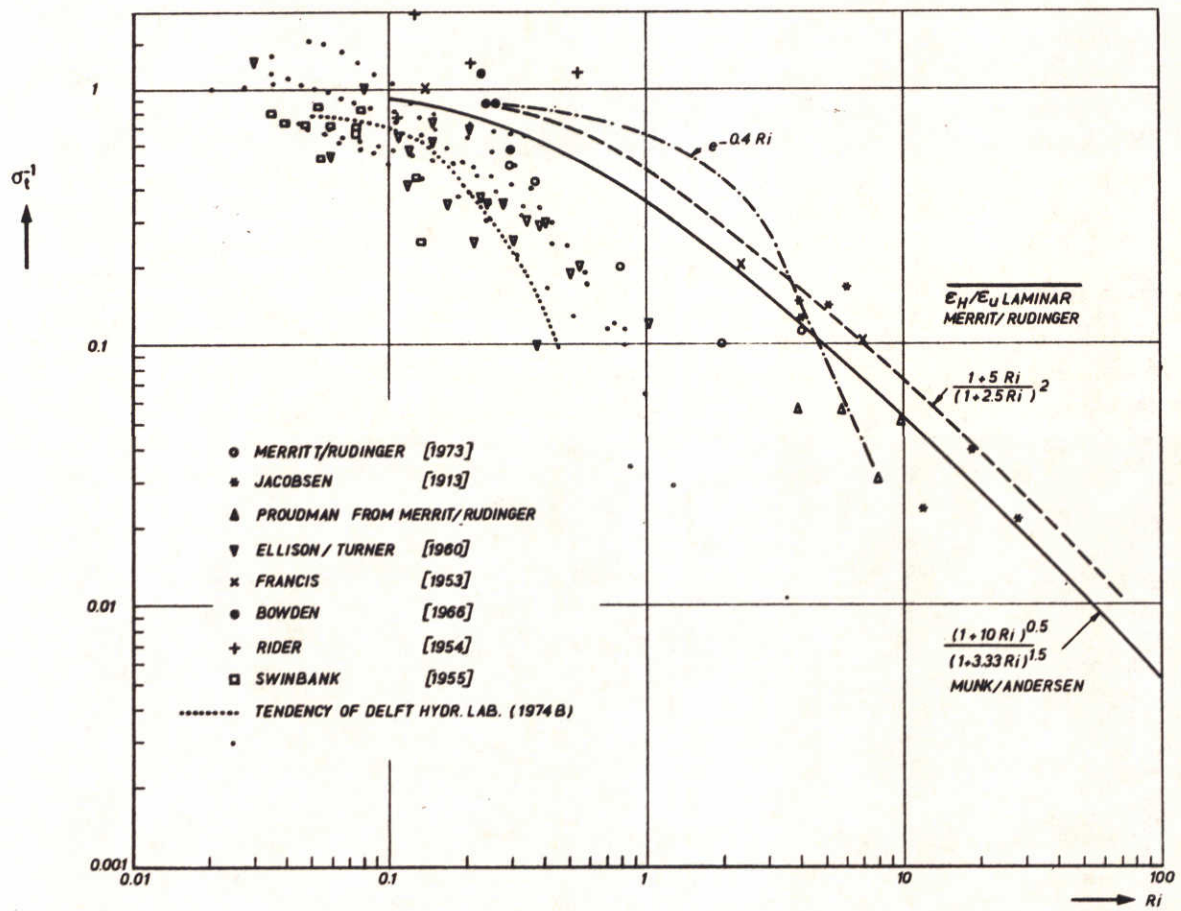

Fig. 6.12 σ_t^{-1} versus Ri; Mizushina laboratory experiments (indicated by ·) compared with data collected in 1974 study (Breusers, 1974)

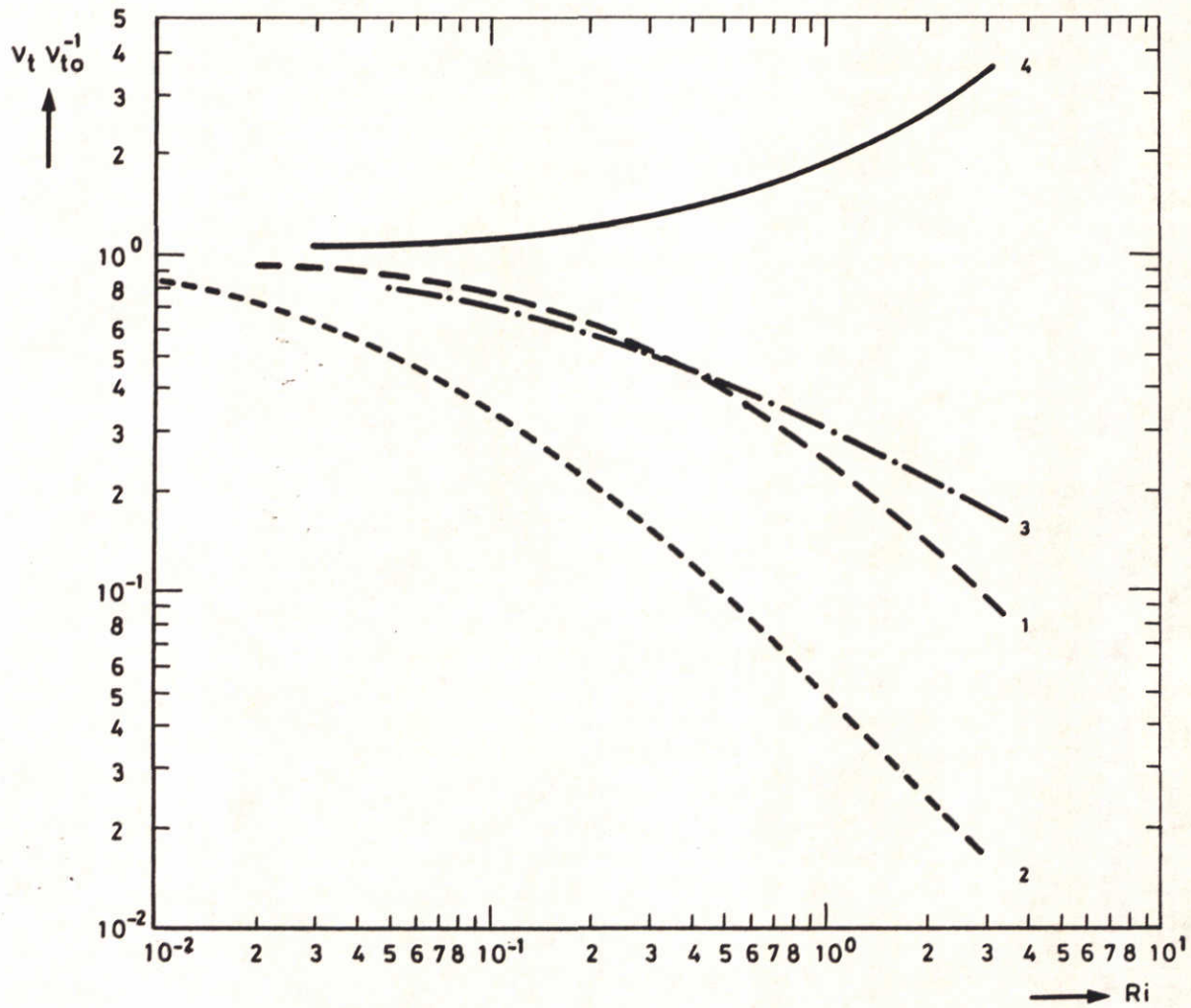

Fig. 7.1 $\nu_t \nu_{t.o}^{-1}$ versus Ri; according to damping relations used by (1) Bloss (1985), (2) Perrels and Karelse (1986), (3) Wang (1983) and Blumberg (1977)

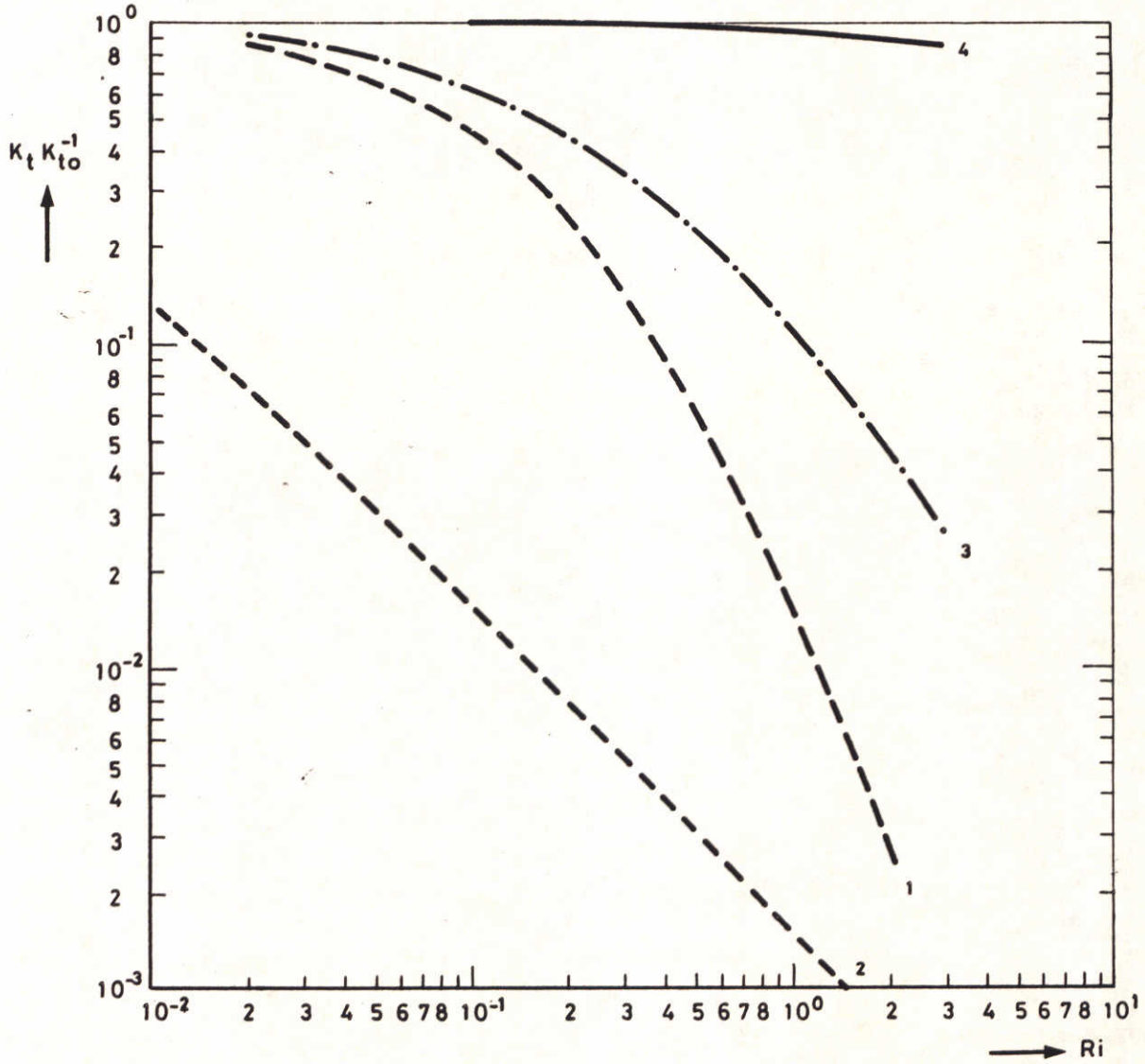

Fig. 7.2 $K_t K_{t.o}^{-1}$ versus Ri; according to damping relations used by (1) Bloss (1985), (2) Perrels and Karelse (1986), (3) Wang (1983) and Blumberg (1977)

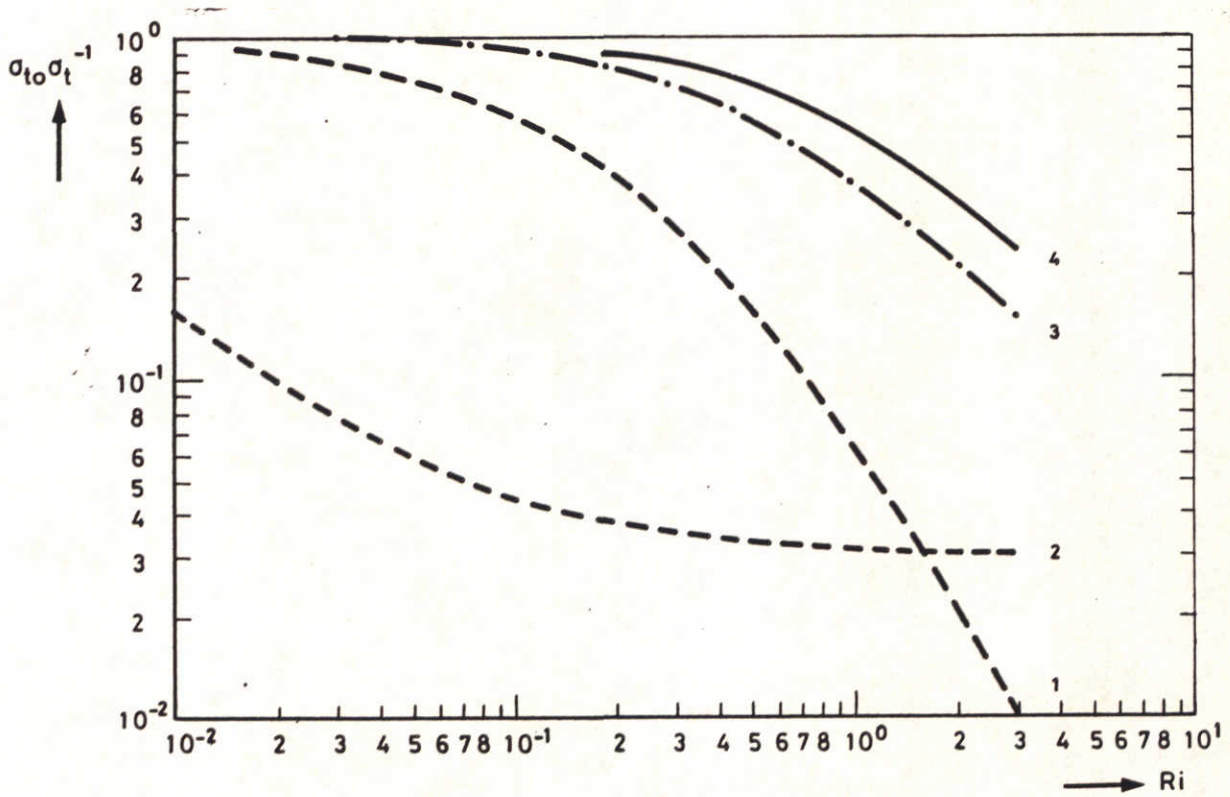

Fig. 7.3 $\sigma^{-1}\sigma_{t.o}$ versus Ri; according to damping relations used by (1) Bloss (1985), (2) Perrels and Karelse (1986), (3) Wang (1983) and Blumberg (1977)

Appendix A: Application of length scale classification to Rotterdam Waterway Estuary

1 Introduction

This appendix gives an analysis of the maximum ebb conditions observed in the Rotterdam Waterway Estuary in a station close to its mouth. For this station Fig. 2.3 gives the vertical distribution of velocity and salinity, 18 hours coinciding with maximum ebb. The maximum ebb profiles are represented separately in Fig. A.1.

Approximating the vertical variation of velocity as indicated in Fig. A.1, up to a depth of about 10 m, $\partial\bar{u}/\partial z \approx 0.13$ m s^{-1}, $\partial\bar{\rho}/\partial z \approx -0.94$ kg m^{-4}, Ri ≈ 0.56 (Eq. 4.14) and $N \approx 0.097$ s^{-1} (Eq. 4.3).

2 $L_R L_N^{-1}$ ratio

The vertical distribution of salinity of Fig. A.1 does not exibit an interface. Therefore

$$L_m \approx L_n \tag{A.1}$$

where L_m: master length scale, defined in Section 6.1

L_n: length scale for neutral conditions, defined in Section 6.1.

The length scale for neutral conditions can be derived from (Perrels and Karelse, 1981).

$$\begin{aligned} L_n &\approx \kappa z && z \leq \tfrac{1}{4} h \\ L_n &\approx \tfrac{1}{4} \kappa h && z \geq \tfrac{1}{4} h \end{aligned} \tag{A.2}$$

where z: vertical distance from bottom

h: depth

κ: von Karmann constant.

As shown in Appendix B, production of turbulent energy is influenced by both bottom shear and longitudinal density gradients. From this appendix, for conditions of maximum ebb velocity

$$\beta = [1 + \frac{1}{2} g z \left|\frac{\partial \bar{\rho}}{\partial x}\right| \frac{h}{|\tau_b|}]^2 \qquad (A.3)$$

where β : ratio between total production rate of turbulent energy and that due to bottom shear (Appendix B)

$\partial\bar{\rho}/\partial x$: longitudinal gradient of depth mean density

τ_b : bottom shear stress.

In first approximation the dissipation rate of turbulent energy per unit mass of fluid may be estimated as that pertaining under neutral conditions, the depth averaged velocity being the same, multiplied by the ratio β. Therefore

$$\varepsilon = \beta \gamma \frac{u_*^3}{h} \qquad (A.4)$$

where ε : disspation rate of turbulent energy per unit mass of fluid

u_*: shear stress velocity

γ : ratio between ε and $u_*^3 h^{-1}$.

The ratio γ varies with z. It can be derived from experimental data as presented by Hinze (1975, Fig. 7.67).

Eq. 4.6 and Eqs. A.1 - A.4 can be used to determine the ratio $L_n L_R^{-1}$. This procedure gives the results which are listed in Tables A.1 and A.2, for values of the Chezy coefficient of 80 $m^{1/2}s^{-1}$ and 60 $m^{1/2}s^{-1}$ respectively. The former value applies to the 1956 stratified maximum ebb conditions (Dronkers, 1969). The latter value applies to neutral conditions. For $z\, h^{-1} > 0.2$ both tables give values of the ratio $L_n L_R^{-1}$ which are substantially larger than the parameter C_1, defined in Table 4.1, which according to the experiments described in Section 4.2 C_1 ranges from 1.4 to 2.0. This means that for the conditions represented in Fig. 4.1 turbulence is influenced by stratififcation. Given the Ri-value of 0.56 this was to be expected (Figs. 6.5 - 6.7).

3 F_o - value

From Eq. 6.3, for $L_n >> L_R$ it may be expected that

$$L = C_1 L_R \tag{A.5}$$

where L : length scale of energy containing eddies
C_1 : dimensionless parameter defined in Table 4.1
L_R : Ozmidov length scale (Eq. 4.16).

Hence from Eqs. 6.10, A.1 and A.5

$$F_o(Ri) = (C_1 \frac{L_R}{L_n})^2 (1 - \frac{Ri}{\sigma_t})^{\frac{1}{2}} \tag{A.6}$$

where F_o: damping function, defined by Eq. 6.8
Ri: gradient Richardson number, defined by Eq. 4.16
σ_t : turbulent Prandtl number, $\sigma_t = \nu_t K_t^{-1}$ (ν_t: eddy viscosity, K_t: eddy diffusivity).

Figs. 6.5 - 6.7, derived from the Mizushina experiments, apply to steady open channel flow, where the effect of longitudinal density gradients on the variation of the horizontal velocity over the depth is small. Hence, from these figures which apply to $0.4 < z\, h^{-1} < 0.75$, $\sigma_t^{-1} = 0.2$ and $F_o = 0.4$ for Ri = 0.56.

Substituting Ri = 0.56, $\sigma_t^{-1} = 0.2$ and $L_n L_R^{-1}$-values from Tables A.1 en A.2 into Eq. A.6 gives F_o values which are listed in these tables.

The F_o-values derived from Eq. A.6 are of the same order of magnitude as the value derived from the Mizushina experiments for the same Ri-value. This illustrates that the length scale considerations of Chapters 4 and 6 are consistent. Perfect agreement between the F_o-values is too much to be expected since turbulence in the three-dimensional Rotterdam Waterway Estuary must have features which are different from that pertaining in the experiments from which experimental C_1-values and the experimental F_o-value where derived. In

addition, the calculated F_o-values are quite sensitive for the approximations made in the derivation. With respect to the effect of the Chezy-coefficient this is illustrated by the difference in F_o-values between Tables A.1 and A.2.

Table A.1: Length scales for Rotterdam Waterway
1956 maximum ebb conditions ($C = 80\ m^{½}s^{-1}$)

$z\ h^{-1}$	β Eq.A.3	γ 1)	L_R Eq.4.6	L_n Eq.A.2	$L_n L_R^{-1}$	F_o(Eq.A.6) $C_1=1.4$	$C_1=1.7$	$C_1=2.0$	F_o (Fig.6.5)
0.1	1.05	22.5	0.73 m	0.48 m	0.7				
0.2	1.09	12.3	0.51	0.96	1.9				
0.3	1.14	8.5	0.43	1.20	2.8				
0.4	1.19	6.1	0.37	1.20	3.2	0.18	0.26	0.36	0.40
0.5	1.24	4.7	0.33	1.20	3.6	0.14	0.21	0.29	0.40
0.6	1.29	3.8	0.31	1.20	3.9	0.12	0.18	0.25	0.40
0.7	1.36	3.1	0.28	1.20	4.3	0.10	0.15	0.21	0.40
0.8	1.39	2.6	0.26	1.20	4.6				
0.9	1.45	2.1	0.24	1.20	5.0				
1.0	1.50	1.9	0.23	1.20	5.2				

characteristic parameter values

h = 12 m
$\bar{u}$ = 1.5 m s^{-1}
C = 80 $m^{½}s^{-1}$ (Dronkers, 1969)
$\partial\bar{\rho}/\partial x = 1.1\ 10^{-3}$ kg m^{-4}
$\partial\bar{u}/\partial z = 0.13\ s^{-1}$ (Fig. A.1)
$\partial\bar{\rho}/\partial z = 0.94$ kg m^{-4} (Fig. A.1)
$Ri = 0.56$
$\sigma_t^{-1} = 0.2$ (Fig. 6.7)

1) after Hinze (1975, Fig. 7.67)

Table A.2: Length scales for Rotterdam Waterway
1956 maximum ebb conditions ($C = 60\ m^{½}s^{-1}$)

$z\ h^{-1}$	β Eq.A.3	γ 1)	L_R Eq.4.6	L_n Eq.A.2	$L_n L_R^{-1}$	F_o (Eq.A.6) $C_1=1.4$	$C_1=1.7$	$C_1=2.0$	F_o (Fig.6.5)
0.1	1.03	22.5	1.02 m	0.48 m	0.5				
0.2	1.05	12.3	0.76	0.96	1.3				
0.3	1.08	8.5	0.64	1.20	1.9				
0.4	1.10	6.1	0.55	1.20	2.2	0.39	0.57	0.79	0.40
0.5	1.13	4.7	0.49	1.20	2.4	0.31	0.45	0.63	0.40
0.6	1.16	3.8	0.45	1.20	2.7	0.26	0.38	0.53	0.40
0.7	1.19	3.1	0.41	1.20	2.9	0.22	0.32	0.44	0.40
0.8	1.21	2.6	0.38	1.20	3.2				
0.9	1.24	2.1	0.34	1.20	3.5				
1.0	1.27	1.9	0.33	1.20	3.6				

characteristic parameter values

h	$= 12$ m	$\partial\bar{u}/\partial z = 0.13\ s^{-1}$	(Fig.A.1)
$\bar{\bar{u}}$	$= 1.5\ m\ s^{-1}$	$\partial\bar{\rho}/\partial z = 0.94\ kg\ m^{-4}$	(Fig.A.1)
C	$= 60\ m^{½}\ s^{-1}$	$Ri = 0.56$	
$\partial\bar{\bar{\rho}}/\partial x$	$= 1.1\ 10^{-3}\ kg\ m^{-4}$	$\sigma_t^{-1} \simeq 0.2$	(Fig.6.7)

1) after Hinze (1975, Fig. 7.67)

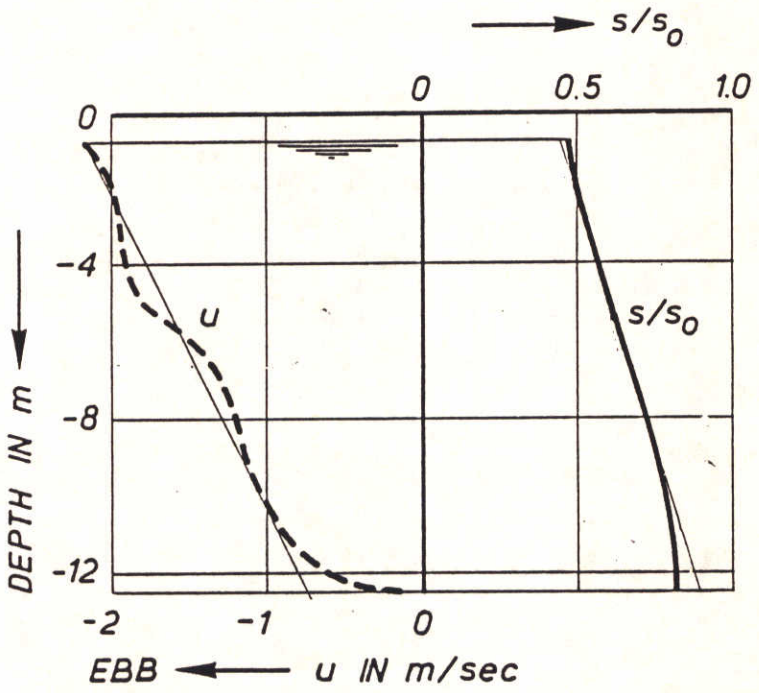

Fig. A.1 Rotterdam Waterway Estuary, station 1030 km, June 1956; variation of velocity and salinity over depth at 18 hrs (maximum ebb velocity).

Appendix B: Effect of longitudinal density gradient on turbulence in stratified tidal flow

1 Introduction

In stratified tidal estuaries, the flow has the same direction over the whole depth, except at tidal slack, and the density varies in the longitudinal direction. In steady stratified open-channel flow with the same direction of flow over the whole depth, the density varies primarily over the depth, while the variation of the density in the longitudinal direction is small. Within this context, this appendix addresses the question whether or not there is a difference in turbulence between flows with and without a longitudinal density gradient.

The appendix expands previous considerations on this matter (Abraham, 1980).

2 Effect of longitudinal density gradient on production of turbulent kinetic energy

With a variation of density in the longitudinal direction, the variation of velocity and turbulent shear - and hence that of the production of turbulent energy - over the depth is different from as it is without. The longtidudinal density gradient may be expected to influence turbulence, when there is a significant difference in the production of turbulent energy with and without such gradients.

Neglecting the variation in the lateral direction of salt concentration, velocity and water depth, neglecting advective accelerations, and finally neglecting the variation of $\partial\rho/\partial x$ en $\partial u/\partial t$ over the depth ($\partial\rho/\partial x \approx \partial\bar{\rho}/\partial x$, $\partial u/\partial t \approx \partial\bar{u}/\partial t$), for a stratified flow over a horizontal bottom the equation of motion may be written as

$$\frac{\partial \bar{u}}{\partial t} + g\,\frac{\partial h}{\partial x} + \frac{1}{\bar{\rho}}\,g\,(h - z)\,\frac{\partial \bar{\rho}}{\partial x} - \frac{1}{\bar{\rho}}\,\frac{\partial \tau}{\partial z} = 0 \qquad \text{(B.1)}$$

where x: longitudinal coordinate, positive when directed landinward

z: vertical coordinate, positive when directed upward and measured

from the botton (z = 0)

t: time

u: velocity in x-direction

h: water depth

g: gravitational acceleration

τ: turbulent shear stress, positive when deceratating fluid above flowing in positive direction

ρ: density

$\bar{}$: depth mean value of quantity

$$\tau = \tau_b \quad \text{for } z = 0 \quad ; \quad \tau = 0 \quad \text{for} \quad z = h \tag{B.2}$$

where τ_b: bottom shear stress

Integrating Eq B.1 with respect to z gives (Abraham, 1980)

$$\tau = \tau_b \frac{(h - z)}{h} + \frac{1}{2} z (h - z) g \frac{\partial \bar{\rho}}{\partial x} \tag{B.3}$$

with on the flood tide $\tau_b > 0$, $\partial\bar{\rho}/\partial x < 0$, and on the ebb tide $\tau_b < 0$, $\partial\bar{\rho}/\partial x < 0$.

When damping of turbulence by stratification may be neglected

$$\tau = \rho \nu_t \frac{\partial u}{\partial z} \quad \text{with } \nu_t = \kappa |u_*| \frac{h - z}{h} z \tag{B.4}$$

where u_*: bottom shear stress velocity; $u_* = (\tau_b \rho^{-1})^{1/2}$

ν_t: eddy viscosity

κ: von Karmann constant.

Eqs B.3 and B.4 give an expression for $\partial u/\partial z$. Multiplying this expression with τ gives

$$\tau \frac{\partial u}{\partial z} = \frac{(h - z) h}{\bar{\rho} \kappa |u_*| z} \left[\frac{\tau_b}{h} + \frac{1}{2} z g \frac{\partial \bar{\rho}}{\partial x}\right]^2 \tag{B.5}$$

and

$$\int_{z_0}^{h} \tau \frac{\partial u}{\partial z}\, dz = \frac{1}{\bar{\bar{\rho}}\kappa|u_*|}\left[-\left(1 + \ln\frac{z_0}{h}\right)\tau_b^{\,2} + \frac{1}{2}\,h^{\,2} g \frac{\partial \bar{\bar{\rho}}}{\partial x}\tau_b + \frac{1}{24}\,g^2 h^4 \left(\frac{\partial \bar{\bar{\rho}}}{\partial x}\right)^2\right] \qquad (B.6)$$

where z_0: small value of z; u=0 for $z=z_0$; $z_0 \ll h$.

Intergrating $\partial u/\partial z$ from Eqs B.3 and B.4 with respect to z gives

$$(u - \bar{\bar{u}}) = \frac{1}{\kappa}\frac{\tau_b}{\bar{\bar{\rho}}|u_*|}\left(1 + \ln\frac{z_0}{h}\right) + \frac{1}{4\kappa}\frac{gh^2}{\bar{\bar{\rho}}|u_*|}\frac{\partial \bar{\bar{\rho}}}{\partial x}\left(2\,\frac{z}{h} - 1\right) \qquad (B.7)$$

Substituting $u(z_0) = 0$ into Eq B.7 yields

$$|u_*| = -\frac{1}{\kappa}\quad\frac{\tau_b}{\bar{\bar{\rho}}\,\bar{\bar{u}}}\left(1 + \ln\frac{z_0}{h}\right) + \frac{1}{4\kappa}\frac{g\,h^2}{\bar{\bar{\rho}}\,\bar{\bar{u}}}\frac{\partial \bar{\bar{\rho}}}{\partial x} \qquad (B.8)$$

For $\partial\bar{\bar{\rho}}/\partial x = 0$

$$\frac{|u_*|}{|\bar{\bar{u}}|} = \frac{g^{1/2}}{C} \qquad (B.9)$$

where C : Chezy coefficient.

Assuming that in first approximation Eq B.9 may be applied for $\partial\bar{\bar{\rho}}/\partial x \neq 0$, Eqs B.8 and B.9 imply

$$\left(1 + \ln\frac{z_0}{h}\right) = -\kappa\frac{C}{g^{1/2}} \qquad (B.10)$$

Eq B.5 gives the variation over the depth of the production of turbulent energy. Eqs B.6 and B.10 give the depth integrated production. The contribution of $\partial\bar{\bar{\rho}}/\partial x$ to the production of turbulent energy can be derived from these equations, assuming τ_b to be the same for $\partial\bar{\bar{\rho}}/\partial x = 0$ and $\partial\bar{\bar{\rho}}/\partial x \neq 0$.

In connection with the above derivation the following points are to be raised.

(1) At tidal slack τ_b, u_* and ν_t are small. Then the approximation $\partial u/\partial t \sim \partial \bar{\bar{u}}/\partial t$, which is introduced in Eq B.1, is not satisfied. Nevertheless it may be concluded form Eq B.5 that by then the contrubution of $\partial \bar{\bar{\rho}}/\partial x$ to the production of turbulent energy is relatively large.

(2) When there is a significant variation of $\partial\rho/\partial x$ over the depth Eq B.1 must be written as

$$\frac{\partial \bar{\bar{u}}}{\partial t} + g\frac{\partial h}{\partial x} + \frac{1}{\bar{\bar{\rho}}} g(h - z)\frac{\partial \bar{\rho}}{\partial x} - \frac{1}{\bar{\bar{\rho}}}\frac{\partial \tau}{\partial z} = 0 \qquad \text{(B.11)}$$

where $\bar{\rho}$: density averaged form z = z to z = h.

When $\partial\rho/\partial x$ decreases with increasing z, only at the bottom $\bar{\bar{\rho}} = \bar{\rho}$, while elsewhere over the death ($z > 0$) $\bar{\bar{\rho}} < \bar{\rho}$. By then Eqs B.5 and B.6 overestimate the effect of $\partial\rho/\partial x$. The opposite applies when $\partial\rho/\partial x$ increases with increasing z.

(3) Damping of turbulence by density stratification implies

$$\nu_t = \alpha|Ri|\ \kappa\ |u_*|\ \frac{h - z}{h}\ z \qquad \alpha \leq 1 \qquad \text{(B.12)}$$

where α: damping factor, which depends on Ri.

Damping implies that in Eq B.5 the factor κ has to be replaced by the factor $\alpha\kappa$. This has no effect on the ratio of the terms between the brackets, which determines the relative contribution of $\partial \bar{\bar{\rho}}/\partial x$ to $\tau\ \partial u/\partial z$. In Eq B.6 the effect of α varying with z must be taken into account when performing the integration.

3 Application to Rotterdam Waterway estuary

Abraham (1980) separates the turbulent shear stress into the following parts

$$\tau = \tau_{ex} + \tau_{in} \qquad \text{(B.13)}$$

with

$$\tau_{ex} = \tau_b \frac{(h - z)}{h} \qquad \tau_{in} = \frac{1}{2} z (h - z) g \frac{\partial \bar{\rho}}{\partial x} \qquad \text{(B.14)}$$

where τ_{ex}: fraction of τ which is related to bottom shear stress (an external effect)

τ_{in}: fraction of τ which is related to longitudinal density gradient $\partial\bar{\rho}/\partial x$ (an internal effect)

From an analysis of field data, which were collected in the Rotterdam Waterway estuary in April 1971 (Abraham, 1980, Table 1).

$\tau_{in}/\tau_{ex} > \frac{1}{2}$ throughout the ebb tide

> 1 for half of the ebb tide

$|\tau_{in}/\tau_{ex}| > 1/5$ throughout the flood tide

> 1 for one third of the flood tide

These paramtere values imply that $\partial\bar{\rho}/\partial x$ may be expected to have a significant effect on $\partial u/\partial z$.

Table B.1 gives characteristics of the conditions of the Rotterdam Waterway April 1971 measurements. Table B.2 gives the $\partial\bar{\rho}/\partial x$ contribution to the depth integrated production of turbulent energy. Table B.3 gives the $\partial\bar{\rho}/\partial x$ contribution to the production of turbulent energy at level $z = \frac{1}{2} h$, where τ_{in} has a maximum value (Eq B.14).

Table B.2 gives the relative magnitude of the terms between brachets of Eq. B.6. Table B.3 gives the relative magnitude of the terms obtained by taking the square of the terms between brackets of Eq B.5. The relative magnitude of the above terms is given for different ebb velocities ($\bar{u} = \bar{u}_{m.e}$ and $1/2\ \bar{u}_{m.e}$) and flood velocities ($\bar{u} = \bar{u}_{m.f}$, $\bar{u} = 1/2\ \bar{u}_{m.f}$, $\bar{u} = 1/3\ \bar{u}_{m.f}$ and $\bar{u} = 1/4\ \bar{u}_{m.f}$) where $\bar{u}_{m.e}$ and $\bar{u}_{m.f}$ are respectively the extreme value of $\bar{u}$ during the ebb tide and the flood tide.

Depth integrated the $\partial\bar{\rho}/\partial x$ contribution to $\tau\ \partial u/\partial z$ is of the same order as the τ_b contribution or larger when

$|\bar{\bar{u}}| < 1/2\ |\bar{\bar{u}}_{m.e}|$ on the ebb tide

$|\bar{\bar{u}}| < 1/4\ |\bar{\bar{u}}_{m.f}|$ on the flood tide.

For $z = 1/2h$ thoughout the tidal cycle the $\partial\bar{\bar{\rho}}/\partial x$ contribution to $\tau\ \partial u/\partial z$ is of the same order as the τ_b contribution, except during that fraction of the flood tide with $1/2\ \bar{\bar{u}}_{m.f} > \bar{\bar{u}} > 1/3\ \bar{\bar{u}}_{m.f}$.

Tables B.2 and B.3 are obtained for a chlorinity distrubution in the Rotterdam Waterway estuary as represented in Fig. B.1. There are locations along the estuary where $|\partial\rho/\partial x|$ increases with increasing z, as well as zones where $|\partial\rho/\partial x|$ decreases with uncreasing z. Given point (2) raised at the end of Section 2, this implies that a first estimate of the effect of $\partial\bar{\bar{\rho}}/\partial x$ on $\tau\ \partial u/\partial z$ may be derived from Tables B.2 and B.3. The parameter values given in these tables show that the effect of $\partial\bar{\bar{\rho}}/\partial x$ on $\tau\ \partial u/\partial z$ is significant.

4 Conclusion

For the Rotterdam Waterway April 1971 conditions the above observations lead to the conclusion that because of the longitudinal density gradients turbulence is different than it would be without. For zero-equation and one-equation turbulence models this means that the effect of longitudinal density gradients on the length scale of turbulence has to be specified.

Table B.1: Characteristics of the conditions of the Rotterdam Waterway April 1971 measurements (Abraham, 1980).

$h = 15$ m	
$\partial\bar{\rho}/\partial x = 1.2\ 10^{-3}$ kg m^{-4}	
$\bar{u}_{m.e} = 1.05$ ms^{-1}	$\bar{u}_{m.e}$: maximum ebb velocity
$\bar{u}_{m.f} = 1.05$ ms^{-1}	$\bar{u}_{m.f}$: maximum flood velocity
$C = 70$ $m^{\frac{1}{2}}s^{-1}$	

Table B.2: $\partial\bar{\bar{\rho}}/\partial x$ contribution to depth averaged production of turbulent energy (Eq A.6); Rotterdam Waterway Estuary. April 1971.

	$-(1+\ln\frac{z_0}{h})\frac{\tau_b^2}{h}$: $\frac{1}{2}h^2 g\frac{\partial\bar{\bar{\rho}}}{\partial x}\tau_b$: $\frac{1}{24}g^2h^4(\frac{\partial\bar{\bar{\rho}}}{\partial x})^2$
ebb $\bar{\bar{u}} = \bar{\bar{u}}_{m.e}$	1 : 0.08 : 0.01
	0.09
$\bar{\bar{u}} = \frac{1}{2}\bar{\bar{u}}_{m.e}$	1 : 0.31 : 0.14
	0.45
flood $\bar{\bar{u}} = \bar{\bar{u}}_{m.f}$	1 : -0.08 : 0.01
	-0.07
$\bar{\bar{u}} = \frac{1}{2}\bar{\bar{u}}_{m.f}$	1 : -0.31 : 0.14
	-0.17
$\bar{\bar{u}} = \frac{1}{3}\bar{\bar{u}}_{m.f}$	1 : -0.69 : 0.70
	0.01
$\bar{\bar{u}} = \frac{1}{4}\bar{\bar{u}}_{m.f}$	1 : -1.23 : 2.24
	1.0

Table B.3: $\partial\bar{\bar{\rho}}/\partial x$ contribution to production of turbulent energy at half depth (z = 1/2 h) (Eq A.5); Rotterdam Waterway Estuary, April 1971.

	$\frac{\tau_b^2}{h^2}$	: $\frac{1}{2} g \frac{\partial\bar{\bar{\rho}}}{\partial x} \tau_b$	: $\frac{1}{16} g^2 h^2 (\frac{\partial\bar{\bar{\rho}}}{\partial x})^2$
ebb $\bar{\bar{u}} = \bar{\bar{u}}_{m.e}$	1	: 0.7	: 0.1
		0.8	
$\bar{\bar{u}} = \frac{1}{2} \bar{\bar{u}}_{m.e}$	1	: 2.7	: 1.9
		4.6	
flood $\bar{\bar{u}} = \bar{\bar{u}}_{m.f}$	1	: -0.7	: 0.1
		-0.6	
$\bar{\bar{u}} = \frac{1}{2} \bar{\bar{u}}_{m.f}$	1	: -2.7	: 1.9
		-0.8	
$\bar{\bar{u}} = \frac{1}{3} \bar{\bar{u}}_{m.f}$	1	: -6.1	: 9.7
		-3.6	

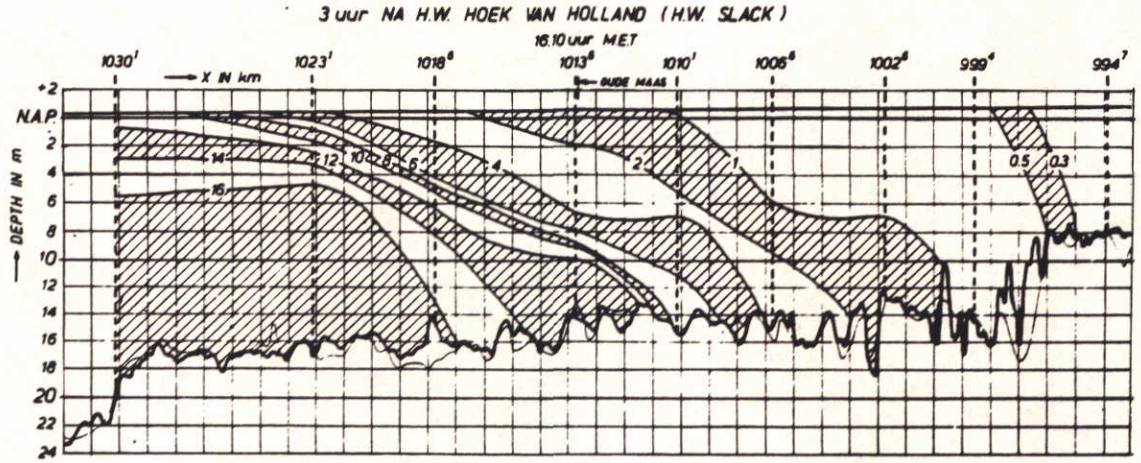

Fig. B.1 Rotterdam Waterway, 1971, chlorinity data (Rijkswaterstaat, 1971); number refer to chlorinity in gr/l.

Appendix C: Ratio of terms at right hand side of Eq. 6.13 for Rotterdam Waterway conditions

For homogeneous flows the velocity profile may be approximated as being logarithmic when

$$\left| \int_0^z \frac{\partial(\bar{u}-\bar{\bar{u}})}{\partial t} \, \partial z \right| << \left| \frac{1}{\rho} \left(1 - \frac{z}{h}\right) \tau_b \right| \qquad (C.1)$$

where $\bar{u}$: velocity in x-direction, after turbulent fluctuations are filtered out

$\bar{\bar{u}}$: depth mean value of $\bar{u}$

t : time

z : vertical coordinate ($z = 0$: bottom, $z = h$: water surface)

h : water depth

ρ : density

τ_b : bottom shear

By then (Elder, 1959)

$$(u-\bar{\bar{u}}) = \frac{u_*}{\kappa} \left(1 - \ln \frac{z}{h}\right) \qquad (C.2)$$

where u_* : shear velocity ($u_*^2 = \tau_b \rho^{-1}$)

κ : von Karman coefficient.

Assuming a sinusoidal variation of velocity with time

$$\bar{\bar{u}} = \bar{\bar{u}}_o \sin 2\pi \frac{t}{T} \qquad (C.3)$$

where $\bar{\bar{u}}_o$: amplitude of $\bar{\bar{u}}_o$

T : duration of tidal cycle

Eqs. C.2 and C.3 imply

$$\frac{\int_0^z \frac{\partial(\bar{u}-\bar{\bar{u}})}{\partial t} \, dz}{\tau_b\left(1 - \frac{z}{h}\right)} = \frac{C}{g^{1/2}\kappa} \frac{2\pi}{T} \frac{h}{\bar{\bar{u}}_o} \frac{\frac{z}{h} \ln \frac{z}{h}}{1 - \frac{z}{h}} \frac{\cos 2\pi \frac{t}{T}}{\sin^2 2\pi \frac{t}{T}} = n \qquad (C.4)$$

where C : Chezy coefficient

n : dimensionless parameter, defined by Eq. C.4.

The approximations behind Eq. C.4 are satisfied for $|n| << 1$.

Table C.1 gives $|n|$-values for homogeneous flow with h, $\bar{u}$ and C as for the Rotterdam Waterway 1956 conditions. For velocities $\bar{u}$, ranging from 1.50 m s^{-1} (the maximum value) to about 1.34 m s^{-1}, the $|n|$-value ranges from zero to about 4%, meaning that the approximations behind Eq. C.4 are satisfied. For velocities in this range, and accelerating flow the shear stress τ is about n% smaller than it is for steady homogeneous flow, deriving n from Table C.1, while in decelerating homogeneous flow the shear stress is about n% larger.

The largest $|n|$-values occur at tidal slack, but cannot be derived from Eq. C.4, as by then the velocity profile is no longer logarithmic because of inertia-effects. What can be learned for the whole velocity range from maximum flow to slack is that $|n|$-values are likely to be of the order of at least 5%. Whether or not larger $|n|$-values occur can be studied from homogeneous tidal flow computations using the Distro-model.

Table C.1: n-values for homogeneous flow with h, $\bar{\bar{u}}$ and C as for Rotterdam Waterway 1956 conditions

	4 t/T										
	0	0.1	0.2	0.3	0.4	0.5	0.6	0.7	0.8	0.9	1.0
	$\bar{\bar{u}}$ in m s^{-1} (Eq. C.3)										
	0	0.23	0.46	0.68	0.88	1.06	1.21	1.34	1.43	1.48	1.50
z/h[1]	|n|- values in % (Eq. C.4)[2]										
0	∞	0	0	0	0	0	0	0	0	0	0
0.1	∞	68	16.9	7.4	4.0	2.4	1.5	1.0	0.6	0.3	0
0.2	∞	108	26.5	11.5	6.2	3.8	2.4	1.5	1.2	0.4	0
0.3	∞	138	34.0	14.8	8.0	4.8	3.1	2.0	1.4	0.5	0
0.4	∞	163	40.3	17.5	9.5	5.7	3.6	2.3	1.6	0.6	0
0.5	∞	185	45.7	19.8	10.7	6.5	4.1	2.6	2.3	0.7	0
0.6	∞	205	50.5	21.9	11.9	7.2	4.6	2.9	1.7	0.8	0
0.7	∞	222	54.9	23.8	12.9	7.8	4.9	3.2	1.9	0.9	0
0.8	∞	238	58.8	25.5	13.8	8.4	5.3	3.4	2.0	0.9	0
0.9	∞	253	62.5	27.1	14.7	8.9	5.6	3.6	2.1	1.0	0
1.0	∞	267	65.9	28.6	15.5	9.4	5.9	3.8	2.3	1.1	0

characteristic parameter values
h = 15 m $\quad \bar{\bar{u}}_o$ = 1.5 m s^{-1} $\quad$ C = 60 $m^{\frac{1}{2}}s^{-1}$

1) z = 0: bottom; z = h: water surface.

2) approximations behind Eq. C.4 are satisfied for $\bar{\bar{u}} \geq 1.34$ m s^{-1}.